CONTENTS

SOUTHAMPTON OCEANOGRAPHY CENTRE

CRUISE REPORT No. 33

RRS *JAMES CLARK ROSS* CRUISE 44
23 JUL - 31 AUG 1999

Circulation And Thermohaline Structure
- Mixing, Ice And Ocean Weather
CATS-MIAOW

Principal Scientists
S Bacon & M J Yelland

2000

James Rennell Division for Ocean Circulation and Climate
Southampton Oceanography Centre
University of Southampton
Waterfront Campus
European Way
Southampton
Hants SO14 3ZH
UK

Tel: +44 (0)23 8059 6441
Fax: +44 (0)23 8059 6204
Email: S.Bacon@soc.soton.ac.uk, M.J.Yelland@soc.soton.ac.uk

CONTENTS

DOCUMENT DATA SHEET

AUTHOR	*PUBLICATION DATE*
BACON, S & YELLAND, M J et al	2000

TITLE

RRS *James Clark Ross* Cruise 44, 23 Jul-31 Aug 1999. Circulation And Thermohaline Structure - Mixing, Ice And Ocean Weather: CATS-MIAOW.

REFERENCE

Southampton Oceanography Centre Cruise Report, No. 33, 140pp.

ABSTRACT

This report describes *RRS James Clark Ross* Cruise 44, called CATS-MIAOW (Circulation And Thermohaline Structure - Mixing, Ice And Ocean Weather). It was funded by the UK Natural Environment Research Council as part of its Arctic Ice and Climate Variability (ARCICE) Thematic Research Programme. The cruise supported projects in hydrography, meteorology and geophysics. The cruise divided into two parts, one hydrographic and one meteorological. The hydrographic work comprised sections under ERS-2 satellite overpasses: two long sections with CTD and lowered ADCP, from Norway to Greenland and from Svalbard to Iceland; and a shorter section across northern Denmark Strait, which was repeated. There was also a near-zonal section in Fram Strait. Bottle samples were taken throughout for salinity, dissolved oxygen and SF6.

The meteorological work took place in the marginal ice zone (MIZ) during a 10 day period in the middle of the cruise. While in the MIZ atmospheric profiles were obtained using GPS radiosondes and a tethered balloon system. The AUTOFLUX ship mounted surface fluxes system was also used to measure the surface fluxes of heat, momentum and moisture in addition to the usual mean meteorological variables. A suite of short-wave and long-wave sensors were also employed to measure both up- and down-welling radiation. The AUTOFLUX system operated throughout the cruise, providing surface flux and mean meteorological data in support of the hydrographic work.

KEYWORDS

ACRONYM, ARCICE, AUTOFLUX, CATS-MIAOW, CRUISE 44 1999, CTD OBSERVATIONS, DENMARK STRAIT, ERS-2, FRAM STRAIT, GREENLAND SEA, HYDROGRAPHY, *JAMES CLARK ROSS*, LADCP, MARGINAL ICE ZONE, METEOROLOGY, NORDIC SEAS, NORWEGIAN SEA, SF6

ISSUING ORGANISATION

Southampton Oceanography Centre
Empress Dock
European Way
Southampton SO14 3ZH UK

Copies of this report are available from: **National Oceanographic Library, SOC** *PRICE*: £29.00
Tel: +44 (0)23 80596116 Fax: +44 (0)23 80596115 Email: nol@soc.soton.ac.uk

CONTENTS

SCIENTIFIC PERSONNEL

Name:		From:	Role:
BACON	Sheldon	SOC	Principal Scientist (Hydrography)
YELLAND	Margaret	SOC	Principal Scientist (Meteorology)
ANDREWS	Paul	Newcastle University	Underway biology
BARLOW	Michelle		General assistant
CENTURIONI	Luca	SOC	Navigation & computing
COALS	Alison	Leeds University	Meteorology
COOPER	Pat	BAS	Scientific engineering
GOY	Keith	SOC	LADCP engineering
HEATH	Phil	BAS	Meteorology
HOPKINS	Jim	Leeds University	Atmospheric chemistry
HUGHES	Nick	SPRI	Ice + hydrography
HUTCHINGS	Jenny	UCL	Hydrography + VM-ADCP
JONES	Ian	Leeds University	Meteorology
KALETZKY	Arthur	SPRI	Ice + hydrography
LEE	Gareth	UEA	SF6
MEDONOS	Simone	Edinburgh University	Sample oxygens
MESSIAS	Marie–Jose	UEA	SF6 (PI)
OLIVER	Kevin	UEA	SF6 + hydrography
PASCAL	Robin	SOC	Meteorology
RUBYTHON	Katie	UEA	LADCP data
SMITHERS	John	SOC	CTD / Electronic engineering
STEWART	Mark	BAS	Shipboard computing
THORNTON	Hazel	UEA	Hydrography
TSIMPLIS	Mikis	SOC	CTD (PI)
WRIGHT	Adrian	SOC	Sample oxygens (PI)

Key

BAS:	British Antarctic Survey
SOC:	Southampton Oceanography Centre
SPRI:	Scott Polar Research Institute
UCL:	University College, London
UEA:	University of East Anglia

SHIP'S PERSONNEL

Name:		**Rank / Rating:**
BURGAN	Jerry	Master
CHAPMAN	Graham	Chief Officer
KILROY	Robin	Second Officer
McCARTHY	Justin	Third Officer
SUMMERS	John	Deck Officer
MEE	Stephen	Radio Officer
ANDERSON	Duncan	Chief Engineer
SMITH	Colin	Second Engineer
MACASKILL	Robert	Third Engineer
JONES	Michael	Fourth Engineer
TREVETT	Douglas	Deck Engineer
ROWE	Anthony	Electrician
GIBSON	James	Catering Officer
LANG	Colin	Bosun
PECK	David	Bosun's Mate
BOWEN	Albert	SG1
LITTLEHALES	Noel	SG1
TAYLOR	David	SG1
DALE	George	SG1
TRUSSLER	Luke	SG1
ALLAN	Erwin	MG1
PARSLEY	Richard	MG1
MCMANAMY	Daniel	Chief Cook
MACASKILL	Tracey	Second Cook
HEENEY	Robert	Second Steward
JONES	Lee	Assistant Steward
HADGRAFT	Simon	Steward
WEIRS	Michael	Steward
POLLARD	John	BAS Medic

LIST OF TABLES

LIST OF FIGURES and PLATES

ACKNOWLEDGEMENTS

The PSOs wish to thank the officers and crew of the JCR for their contribution to a successful cruise. We are also grateful to Steve Groom (PML) and Helen Snaith (SOC) for supplying AVHRR images, and to Ben Moat (SOC) for supplying SSMI images and egg charts. We also thank Uwe Meyer and Joerg Hartmann (Alfred-Wegener-Institut, Germany) for their kindness in arranging and performing a laser altimeter section using the aircraft *Polar2*.

We are also grateful to the responsible authorities for granting permission to work in territorial waters: Greenland (Denmark), Norway and Iceland.

Sheldon Bacon and Margaret Yelland

1. THE CRUISE

1.1 SCIENTIFIC OBJECTIVES

RRS *James Clark Ross* cruise 44 (*Cats–Miaow*) was funded by the U. K. Natural Environment Research Council under the Arctic Ice and Environmental Variability (ARCICE) thematic programme. The cruise supported several projects under this programme, in particular:

Bacon, S. and P. Wadhams, ***Sea ice and oceanic vertical circulation***;

Dowdeswell, J. A., N. H. Kenyon and A. Rossell-Mélé, ***Geophysical and geological investigations of sedimentation and ice-ocean variability on Arctic continental margins***;

Lewis, A., ***Non-Methane Hydrocarbons and Dimethyl Sulphide in the Arctic Troposphere***;

Mobbs, S. D., I. Jones, M. J. Yelland, J. King and P. S. Anderson, ***Measuring and Modelling Surface Fluxes in the Marginal Ice Zone***;

Watson, A., K. Heywood and P. Dennis, ***The influence of ice and fresh water on the Nordic Seas thermohaline circulation.***

The main work of the cruise was hydrographic and meteorological, concentrating on the first, fourth and fifth of the above. Further information is available on the ARCICE website: http://www.arcice.cecs.ed.ac.uk/. We briefly summarise here the scientific objectives of the three main projects on the cruise.

1.1.1 Bacon and Wadhams

We will study the effect of sea ice on oceanic vertical circulation, meaning the local exchange of water properties in the Greenland Sea by convection, both to greater and lesser depths; the transfer of intermediate waters in the Nordic Seas to great depth in the North Atlantic via overflows between Greenland and Scotland; and the Atlantic thermohaline circulation as a whole. Three essential areas of this study will be the role of ice-ocean interaction in the Greenland Sea in triggering deep water convection, determination of the effect of ice on the convective processes in both shallow water and thermohaline processes in the North Atlantic, and the role of seasonality as it affects shallow and deep convection. We will carry out one summer and one winter expedition to the Nordic Seas to measure absolute circulation, winter ice formation and melt, deep and shallow convective intensity, and the effects of seasonality on local preconditioning and overflows. Satellite altimetry, and passive microwave and SAR measurements will link between and extrapolate from our measurements.

1.1.2 Mobbs, Jones, Yelland, King and Anderson

Fluxes of heat, moisture, radiation and momentum vary considerably between ice/atmosphere and ocean/atmosphere interfaces. The intermingling of ice and ocean surfaces in the Marginal Ice Zones causes highly complex behaviour of surface fluxes in this region. Determining air-sea interactions over the polar regions is an essential part of understanding the global climate system. This project will measure radiative and turbulent fluxes in the Marginal Ice Zone (MIZ). The inhomogeneous nature of the MIZ makes the air-sea interaction there more difficult to predict than that over pack ice or open ocean. Large Eddy Simulation (LES) will be used to model the turbulence above the MIZ. The difference in roughness length, surface temperature and albedo between areas of sea-ice and areas of open water is often great, leading to large variations in heat, moisture, momentum and radiative fluxes. LES modelling can capture the atmospheric response to spatially varying surface conditions on these fine scales more realistically than using parametrisations for all scales of turbulence. Parametrisations of the aggregate (i.e. on scales larger than the leads in the ice) fluxes will be derived from the LES modelling for use in larger scale models. Such parametrisations are necessary in order for global circulation models to simulate and predict climate with more accuracy. Shipboard measurements of heat, moisture, momentum and radiative fluxes will be taken. Atmospheric profiles will be measured using tethered balloon and radiosonde launches. These measurements will be used for initialisation and validation of the modelling.

1.1.3 Watson, Heywood and Dennis

New tracer techniques will be used to investigate the origin of ice-melt input to, and inter-mixing with, the water masses around the Greenland Sea. The role of ice and freshwater inputs in both limiting and promoting deep convection, and the formation of the dense water overflow at the Denmark Strait will be quantified. Our tools will be SF6 and d18O tracer techniques plus Acoustic Doppler Current Profilers, hydrography and remote sensing measurements. ARCICE is ideally timed to take advantage of a SF6 release experiment begun in 1996 in the Greenland Sea. This will be producing its most informative data on water mass transport during ARCICE. d18O provides unique information on the source of ice-melt, while hydrographic measurements will enable us to measure oceanic heat, mass and salt transport into the Arctic. Primary data will be collected on the *James Clark Ross*, and augmented with data from other vessels and stationary moorings in the Denmark Strait.

1.2 OVERVIEW

The work of the cruise began with two test stations at 64 °N, 4 °E on the morning of 26 July 1999. We then moved to station 3, the start of the first section, Cat's Leg 1, off the coast of Norway later the same evening. See figures 1.1, 1.2 and 1.3 for cruise track and station positions. With stations 29-30 on 31 July we crossed the Mohns Ridge from the Norwegian Sea into the Greenland Sea. Leg 1 was oriented to lie under an ascending (south-east to north-west) ERS-2 overpass timed for 3 August, on which day we expected to be in the vicinity of the East Greenland Current – and we were. Leg 1 ended with station 54 late on 4 August, deep in the ice over the north-east Greenland shelf.

The Meteorology phase (or Cat's Whiskers) took place from 4 to 14 August, and was split into two geographic areas. Four stations were performed between 77 °N, 14 °W and 77 °N, 6 °W between 4 and 7 August as the ship headed east across the MIZ towards open water. After travelling north in open water for 30 hours the ship re-entered the MIZ on 9 August at 80.5 °N, 8 °E and performed a further 17 stations following the ice margin south west, finishing with station 74 at 79.9 °N, 1 °E late on 14 August. During station 68 the *Polar2* aircraft performed a laser altimeter section across the ice in the vicinity of the ship. Each station contained two parts:

1) two or more hours of continuous measurement of the surface fluxes with the ship held head to wind. A CTD cast was also carried out if ice conditions permitted

2) a period of two or more hours with the wind on the port beam during which surface profiles of the atmosphere were obtained using the tethered balloon (Section 5.2).

The duration of the stations varied, with the longest stations usually taking place between 20:00 of one day to 04:00 of the next, since the ship was not permitted to manoeuvre in the ice during these hours. Surface flux measurements were performed continuously throughout the cruise. The Meteorology phase is described in more detail in Section 5.

Cat's Leg 2 ran across Fram Strait following the line of an array of moorings deployed by the Alfred Wegener Institute, Bremerhaven, on about 78° 50' N. It began with station 75 on 15 August just off the ice edge in the west side of Fram Strait and ended with station 84 off the west coast of Svalbard on 16 August. We then had a few hours' entertainment break when we headed closer in to the coast in the direction of Ny Ålesund to admire the scenery.

By later the same evening, we had steamed south down the coast of Svalbard to start Cat's Leg 3 with station 85. Leg 3 lay under an ERS-2 descending (north-east to south-west) pass, timed for 18 August. Station 103 was a repeat of station 37 in the middle of the Greenland Sea and marked the junction of Legs 1 and 3. Stations 110, 111 and 112 passed over the Jan Mayen Fracture

Zone and gave us a close approach to the west of Jan Mayen Island itself, shrouded in fog. Now in the Iceland Basin, the leg ended with station 124 on 23 August.

The start of Cat's Leg 4 lay about half a day's steaming away. It began with station 125 later the same day on the Iceland side of northern Denmark Strait. This section lay under an ERS-2 ascending pass timed for 28 August. The section was executed at high horizontal resolution with nominal station spacing of 8 nm, and ended with station 150 about 2 nm from the Greenland coast in the early evening of 25 August. We had a pause of an hour or so to admire the scenery.

Time permitted a reduced-resolution repeat of Leg 4, so to end the cruise we had Cat's Tail, nominally repeating alternate stations from Leg 4. The Tail began with station 151, and ended with station 165 in the position of station 125 early in the morning of 27 August.

At the end of this report, we show three plates depicting (respectively) the sea ice over Belgica Bank (off north-east Greenland), the JCR (taken from the rubber boat), and the polar bears which wandered by one fine day in the MIZ.

2. HYDROGRAPHIC STATION MEASUREMENTS

All stations, hydrographic and meteorological, were numbered sequentially. Station numbering for each section is described in section 1.2. During the meteorology phase of the cruise, some stations were met.-only, some included hydrographic casts. Bottle depths for all hydrographic stations are shown in figure 2.1, and station information (times, depths, positions etc) is summarised in table 2.1.

2.1 CTD

2.1.1 Equipment

John Smithers, Keith Goy and Pat Cooper.

Neil Brown / General Oceanics (GO) Mk. IIIc CTD	S/N DEEP03
Rosette Pylon, Falmouth Scientific Instruments (FSI) 24 Bottle	S/N 02
Fluorimeter, Chelsea Instruments	S/N 88/2960/163
Transmissometer, Chelsea Instruments	S/N 161/2642/002
Altimeter, Simrad 200 metre	S/N 9309055
10 Litre Niskin Bottles, mixture of GO and FSI.	
Lowered Acoustic Doppler Current Profiler, RD Instruments, and rechargeable battery pack.	
Reversing Pressure Meters	P6534, P6394H
Reversing Thermometers	T1545, T995

A total of 165 stations were occupied during the cruise of which 151 were CTD casts. The depth range was 100-3500 metres and were mostly carried out without fault. The CTD conducting cable was terminated at the beginning of the cruise and a further 2 terminations were required after stations 8 and 74. Both were required after the cable had been severely kinked. A number of Niskin bottles were replaced because of leaking or very stiff taps. These were bottles 10 and 5 with 10 replaced a second time after a crack developed. A pair or reversing pressure meter and thermometers were fitted to bottles 1 and 4. These worked well with the exception of thermometer T995 which would fail to remain in the HOLD mode after reversing on all occasions.

The electrical connectors joining the sea cable and instrument package was also replaced on 2 occasions due to ingress of seawater. A new Dissolved Oxygen sensor had been fitted to CTD DEEP03 before the cruise but its performance was not monitored and in fact was intermittent in operation until Station 103. The type fitted did not have a thermistor fitted so a lagged value of CTD temperature was used for calculating Oxygen content. The Deck Units and power supplies running the CTD and Rosette worked without fault.

2.1.2 Calibration

Sheldon Bacon and Mikis Tsimplis

Introduction

Throughout the cruise, there was an unusual problem of high noise and bias in the downcast conductivity data. The nature of the problem, which obtained over a few cruises, and its cure, is described in Holliday (2000). In brief, a change in the type and configuration of instruments on a new CTD/LADCP frame caused eddies to flow over the conductivity sensor on the downcast. Upcast data were unaffected, so that at-sea calibrations appeared fine, while their match with the downcast profiles was poor. Therefore we describe here the calibrations as derived after the cruise and as applied to the upcast data.

Pre-cruise calibrations as described below for CTD pressure and temperature were provided by Ocean Scientific International Ltd. (OSIL) of Petersfield, Hampshire, U. K.

Data acquisition

The primary CTD data acquisition route on this cruise was via the SOC DAPS system. DAPS runs on a SUN Ultra-Sparc workstation with an expansion box giving 16 extra serial ports. It captures the CTD profile and firing data directly from the CTD console and stores the data as individual ASCII files for each cast. DAPS checks the data for pressure jumps, averages the 25 Hz data to 1 Hz and calculates the temperature gradient over the 1 second samples. The first column of the ASCII files is decimal Julian day with 1 ms resolution.

CTD Temperature

Temperature raw counts (T_{raw}) were calibrated (T) using (2.1). The calibration was provided by OSIL using a 5-point fit between 0.9°C and 29.1°C whose accuracy is ±2 m°C.

$$T = -2.144346 + 4.956295E \pm 04 \times T_{raw} \qquad (2.1)$$

To correct the mismatch in the temperature and conductivity measurements temperature is 'speeded up' by (2.2)

$$T = T + \tau \frac{dT}{dt} \qquad (2.2)$$

where the time rate of change of temperature is determined over a one second interval. The time constant chosen to minimise salinity spikes was $\tau = 0.25$ s. Temperatures are reported using the ITS-90 scale. ITS-68 is used for computing derived quantities. Temperatures are converted to ITS-68 by (2.3), as suggested by Saunders (1990).

$$T_{68} = 1.00024 \times T_{90} \tag{2.3}$$

CTD Pressure

Raw pressure counts (P_{raw}) were calibrated (P) using (2.4). The calibration was provided by OSIL using a 10-point fit between 0 and 6000 dbar whose accuracy is better than ±0.1 dbar.

$$P = \pm 38.4600 + 0.107489 \times P_{raw} \tag{2.4}$$

To account for the temperature dependence of the pressure sensor, the correction (2.5) is applied:

$$P = P + 0.14(\text{ptlag} - 25.4) \tag{2.5}$$

where ptlag is a lagged version of the CTD temperature, and is constructed by (2.6) and (2.7):

$$W = \exp(-\text{tdel}/\text{tconst}) \tag{2.6}$$

$$\text{ptlag}(t_0 + \text{tdel}) = W \times \text{ptlag}(t_0) + (1 - W) \times T(t_0 + \text{tdel}) \tag{2.7}$$

where T is the CTD temperature, tdel is the time interval in seconds over which ptlag is updated with tconst = 400 s.

Laboratory measurements have shown that the CTD Deep03 suffers from no significant pressure hysteresis effect.

CTD deck pressure was non-zero and exhibited trends over the cruise; see figure 2.2. It rose from ~3 dbar at the start of the cruise to ~7 dbar around station 54, then drifted back to ~5 dbar by the end of the cruise. These non-zero deck pressures were treated as offsets on a station-by-station basis. The offsets were determined by fitting a straight line to deck pressure as a function of station number for (a) stations 3 to 54, and (b) stations 56 to 165. The results of the fit for (a) were: intercept 3.32 (se 0.05), slope 6.95E–02 (se 0.30E-02), and for (b): intercept 7.00 (se 0.06), slope –0.97E–02 (se 0.19E–02). Application of these corrections produced a mean deck pressure for the cruise of 0.01 (sd 0.45) dbar; see figure 2.3 for corrected deck pressures.

A check on pressure calibration is provided by comparing the sum of the CTD pressure at the bottom of the cast (converted to depth in metres) and the closest approach of the CTD to the bottom as determined by the altimeter (see below) with the depth as measured by the echo sounder (see section 3.6). The quantities are termed estimated and measured water depth (ewd and mwd). For 151 stations, the mean of mwd minus ewd is –8.6 (sd 26.0) m. This negative bias is normal overall because in steeply sloping topography, side echoes from features above the bottom reduce the measured water depth. Excluding such outliers, for 131 stations, the mean difference is –2.8 (sd 3.2) m. This is less than 0.1% of the maximum water depth. Figure 2.4 shows measured minus estimated water depth plotted as a function of measured water depth. There is a structure to the data viewed in this way which resembles the major water mass features in the Nordic Seas: there is an offset between shallow points (less than 600 m) and deep points. It may be that the sound speed correction function (Carter's Tables: Carter, 1980) for the echo sounder data needs to be updated for the area. Further work is needed to resolve this small discrepancy.

CTD Conductivity

We describe here the final empirical calibration derived after the cruise. The raw conductivities (C_{raw}) are first scaled by 2.9:

$$C_{raw} = 0.001 \times C_{raw} \qquad (2.9)$$

Next an approximate calibration is generated which covers the whole cruise by comparison between sample and CTD conductivities, where sample values are derived from sample salinities. After removal of outliers, fitting bottle conductivity (C_{bot}) as a function of C_{raw} (actually fitting C_{bot}–C_{raw} as a function of C_{raw}) gave 2.10:

$$C_{bot} = 2.3626E-03 + 0.945878C_{raw} \qquad (2.10)$$

with coefficient se's 1.245E-03 and 4.768E-04 respectively, and using 2507 samples. This function was applied to C_{raw} as an initial calibration to give C_{init}. To obtain the final calibration, the conductivity difference C_{bot}–C_{init} was fitted as a function of pressure and temperature (2.11) for each station (A, B, C constants). This correction has the same functional form as the cell material deformation correction, which is therefore not applied separately.

$$C_{bot} - C_{init} = A + BP + CT \qquad (2.11)$$

The values of the constants are given in table 2.2, together with number of points used and standard deviation of fit for each station. We also calculated the mean conductivity offset (O) for each station as (2.12):

$$O = \overline{C_{bot} - C_{init}} = A + B\bar{P} + C\bar{T} \qquad (2.12)$$

where $\bar{P}$ and $\bar{T}$ are the mean pressure and temperature of the sample included in the fit for each station. Figure 2.5 shows O as a function of station number. In regions of very high salinity gradient (eg around stations 50-60), very fresh melt-influenced waters of salinity ~30 overlay waters of more ambient values (~34), over the upper 200 or 300 metres. In these conditions, Niskin bottles do not flush through sufficiently rapidly to contain water solely from the depth at which they are closed; rather, they contain an admixture of deeper waters. This results in the measured salinity being systematically too high, so that even though the worst misfit bottles are edited out before calculating the fit parameters, the 'final' calibration probably needs to be adjusted in these areas. Since the mean deep-water offset is relatively stable over the cruise, it may be appropriate to adjust the calibrated salinities in these cases to accord more closely with the deep-water value. Excluding one outlier, the mean offset for 151 stations is –0.0044 (sd 0.0061) mmho/cm.

Although the above reservation remains at the time of writing, the quality of the calibration process itself is attested by figure 2.6, which shows a plot of sample minus calibrated CTD conductivity versus upcast pressure. Taking all data below 500 dbar and excluding 50 outliers, the mean conductivity difference of 1460 points in the range ±0.011 mmho/cm is 0.0000 (sd 0.0012) mmho/cm.

The final step in the process is to apply derived values of A, B, C as corrections to upcast CTD conductivity profiles, to sort in ascending (deepening) order of pressure, to average into 2 dbar steps, then to calculate salinity (PPS-78; UNESCO, 1978).

CTD Dissolved Oxygen

Due to the difficulties mentioned in section 2.1.1, the calculation of CTD dissolved oxygen values remains to be completed.

Altimeter, Transmittometer, Fluorimeter

Fluorescence (f_{raw}) was converted to voltages (fvolts; 2.24); this is a calibration of the voltage digitiser in the CTD. Transmittance (tr_{raw}) was similarly calibrated to voltages (trvolt; 2.25), then converted to 1 m equivalent path length (tr1; 2.26). The altimeter (alt_{raw}) was calibrated to alt by 2.27.

$$fvolt = -5.0326 + 1.5359E-4 \times f_{raw} + 3.383E-14 \times f_{raw}^2 \qquad (2.24)$$

$$\text{trvolt} = -5.0326 + 1.5359\text{E-}4 \times \text{tr}_{\text{raw}} + 3.383\text{E-}14 \times \text{tr}_{\text{raw}}^2 \quad (2.25)$$

$$\text{trl} = 4.251 + 20.894 \times \text{trvolt} \quad (2.26)$$

$$\text{alt} = \pm 249.7 + 7.62\text{E-}3 \times \text{alt}_{\text{raw}} + 1.04\text{E-}10 \times \text{alt}_{\text{raw}}^2 \quad (2.27)$$

Digital Reversing Temperature and Pressure Meters

Two digital reversing temperature meters were used, T1545 and T995, and two reversing pressure meters, P6534 and P6394. T1545 and P6534 were at position one on the CTD rosette, T995 and P6394 were at position four. Table 2.3 summarises data from the reversing instruments.

Winch

Mikis Tsimplis

Winch data were recorded on a PC connected with the winch console and copied to the JRC level A data logging. The data is logged every 5 sec while the winch is working. The usual processing of the winch data involves merging with the CTD files of values corresponding to the same time. Unfortunately the PC clock was unstable and its difference to the master clock on board was not monitored. The cableout value was manually reset to zero during each CTD deployment at the time the CTD was at surface. The winch data file was divided into smaller files. The start and the end of each file corresponded to the cableout parameter being zero. Editing of the created files identified those that correspond to deployments of the CTD. All relevant parameters are available, but will not be merged onto CTD files on account of the timing problem.

2.2 LOWERED ADCP MEASUREMENTS

Katie Rubython

2.2.1 Description

The LADCP package at SOC consists of a RDI 150kHz BroadBand ADCP (Phase III) with a pressure case rated to 6000 meters and 4 downward facing transducers with 20-degree beam angles. Fitted centrally in the CTD rosette frame, the LADCP is powered during casts by a 48 volt (lead-acid) rechargeable battery pack housed in a second pressure case horizontally mounted near the bottom of the frame. As well as permanent connection to the ADCP, the battery pack pressure case is fitted with a recharge plug and a screw at the end cap which can be used to release any gas build-up as a result of charging. The communications connector of the ADCP is brought to the outside edge of the frame with a short extension cable, enabling easier access for the unit to be connected pre- and post-deployment.

The communications lead and power lead (both 15 metres in length) were connected to a dedicated PC and to a Wynall respectively. The Wynall is a purpose made 48v lead-acid charging unit. Unlike the CTD sensors which are sending a continuous flow of data to the computer onboard, the LADCP unit is set for recording internally prior to deployment then the communication and power sockets are sealed off with two blanking plugs. Prior to each cast the instrument was subjected to a number of tests and then sent a configuration command-file, which determines the mode of operation. One of the tests concerned the setting of the internal clock of the instrument to the ship's clock. The test results (jr44sss_cc.txt) and deployment files (jr44sss_cc.log) were recorded for each cast. The instrument was set to Water and Bottom Tracking Mode with 10-bin ensembles of 16-meter bins for the whole cruise. The rechargeable battery pack was connected for recharge at the end of each cast, and remained on charge until the next deployment. Keeping the batteries well charged both minimises the charging period and minimises any gassing of the batteries. Experience gained from this cruise and previous cruises has shown that there is no significant gassing of the batteries when used in this way. The pressure release screw on the end-cap was loosened at weekly intervals, with no audible evidence of gas being released.

On the second test station, the current profile produced from the LADCP was what has become known in LADCP-speak as an 'X-profile'; c.f.: http://www.ldeo.columbia.edu/~visbeck/ladcp/example/example.html). Although certain stations during the remainder of the cruise did exhibit some evidence of 'X-profiling', the effect was much less than the second test station and in general the data showed well matched up and down current shear profiles.

2.2.2 Data processing

The LADCP measures instantaneous scatterer relative velocities of the water column and these can be converted into profiles of absolute currents by an elaborate processing path. The scatterer velocities are measured by utilising the Doppler frequency shift, phase changes and correlation between coded pulses transmitted and received by four transducers. The speed of sound is taken to be 1500 m/s. Given the geometry of the transducer set, and the orientation/motion of the package, the along beam velocities are transformed into earth co-ordinates to give north, east and vertical current motion relative to the CTD package for each of the ensemble bins. The four beam configuration of the LADCP allows two estimates of the vertical velocity to be calculated, the difference between the two estimates of vertical velocity is recorded as an error velocity.

Initial processing includes the resolution of the velocity components output from the LADCP deck unit to true north and east components using values of magnetic variation. In order to remove relative velocities introduced by the motion of the package during the cast, shear profiles are computed by differentiating the velocities within each of the ensemble 16-bins. Then, the data is integrated up over the cast to produce a shear profile with a zero net velocity. This process also removes the barotropic component of the velocities, which must be reinstated either from the ship displacement (recorded from differential GPS data) or from the relative motion of the package over the sea floor (Bottom Tracking). The final velocity profile is therefore the sum of the baroclinic and barotropic components.

CTD data is used in the latter stages of the processing, firstly to correct the depths of the ensemble bins through the matching of the CTD data to the vertical velocity of the package as measured by the LADCP and secondly to provide in-situ sound speed values for these depths. The velocity data is then scaled to account for the difference between for the default value (1500m/s) and the in-situ value.

The processing of LADCP data is achieved using software developed by Eric Firing at the University of Hawaii. The software uses a combination of 'perl' scripts and MATLAB 'm' files to process the data. The perl scripts provide control files for a variety of C programs.

The main processing steps are as follows:

1) Extract binary ADCP files from instrument to the dedicated pc. The data files are named jsss_cc.000.

2) Binary data files are transferred to the unix system and then loaded into the CODAS database. The perl script scanbb.prl performs an initial interrogation of the data and produces a file jsss_cc.scn which is read by the script loadbb.prl and indicates which ensembles are loaded into the database. The magnetic variation is calculated from the geoeval.m matlab routine (values in mag_var.tab) and this data together with the station position and depth are also loaded into the database by loadbb.prl. The resulting database files are named as jsss***.blk.

3) The perl script domerge.prl calculates mean shear profiles (the baroclinic component of the current) and applied corrections and editing options which were kept constant throughout the cruise. The matlab routine do_abs.m then calculates absolute velocities and produced a standard set of profiles. In the step the uncorrected data (down, up and mean profiles) were viewed and plotted as unreferenced shear profiles with the depth-averaged set to zero.

4) The calibrated CTD data was interactively matched to the ADCP package vertical velocities using the matlab fd.m routine. This matching process produces real depths with in-situ speed of sound values. The depth and sound speed information is then added to the database using the add_ctd perl script. (domerge.prl has then to be rerun)

5) In order to restore the depth-averaged (barotropic) velocity component (equivalent to the ship's displacement) which was removed when first calculating the shear, the cast GPS data was used. For all stations south of 70N the gpsnmea (differential gps) navigation data was used. For stations north of 70N the gpsglos navigational data was used. In both cases the data was appended to larger files from day files and extracted from pstar fromat into ascii format. A matlab routine creates a monotonic time series with 1sec sampling and linearly interpolates for missing data. The data is filtered using a running mean over 5 seconds and then subsampled every 5 seconds and saved in a matlab sm.mat file.

6) Do_absN.m can then be run. This calculates absolute velocity profiles, with the barotropic component of the velocity calculated using the navigational data from the sm.mat

Bottom tracking raw files have been created from the LADCP binary data files (jsss_cc.000) using the BBBATCH.EXE pc routine. No further processing has been completed for this data. The aim is to calculate the barotropic component of the flow from this data to compare with the results gained using the navigational data.

In addition there is a tide model TPXO.3 which is based upon Topex/Poseidon altimetry crossover data. This can be run for each station position to obtain the contribution of tidal velocities to the current shears measured by the LADCP.

2.2.3 Data collection

A total of two test stations and 152 CTD stations were occupied, in depths ranging from 110m to 3756m. Data from station 128 proved to be unreliable, in that there was no downcast data in the binary files extracted from the LADCP unit. It was noted that the CTD package was covered in marine detritus (squid ?) from this cast and it was suspected that the LADCP may have been confused by returns from such a scatterer. No LADCP data was processed from this station.

Data from station 148 was recorded in the same deployment file as station 147, due to the LADCP having been left pinging on the deck between the stations. This was rectified by manually editing the C program scanbb.c to read in the specific number of records (nrec -which corresponds to the number of ensembles) for each station. Data file j147_01.000 is a copy of j148_01.000, both containing the raw data for both stations.

2.2.4 Problems

The RDI self contained LADCP proved reliable throughout the cruise with no attention required apart from routine inspection of the transducer faces. The charging system was generally robust, however the connection and disconnection of the power lead to the battery pack at each station eventually degraded the watertight integrity and the pin to socket contact. The lead was replaced at station 37 when charging began to be intermittent. Two battery packs were used. A loss of upcast data occurred at stations 121 and 122. The suspicion that this was due to battery pack failure at low temperatures was thought credible from the results of the Auto tests and Rub beams test performed through the BBTEST program which indicated that the LADCP unit was performing as expected. The pack was replaced for station 123. However this replacement pack failed to charge on recovery after station 134 but was retained for casts 135/136 on residual charge until the original battery pack was refurbished with four new batteries and changed prior to station 137. Due to a damaged O ring this pack leaked on it's first deployment and the unit was removed and replaced with the second unit, again the LADCP powered by residual charge only. The flooded unit was inspected and only the electronics board and ADCP power plug were damaged beyond re-use. The unit was rewired to operate without the electronics unit and refitted prior to station 141. No further battery problems occurred.

Previous experience has shown that severe corrosion of the battery lead pins/sockets can occur if the power lead is mated to the battery pack socket when not completely dry. This can also lead to problems when trying to communicate with the unit from the pc since the communication circuit requires an earth connection from the battery lead. Care was taken to ensure that the communication and battery lead sockets and blanking plugs were completely dry before being connected/disconnected to the battery pack sockets. Additionally the plugs were regularly greased with silicone grease to improve water dispersion. Care was also taken to pull the leads out of their sockets using the plug rather than the lead to try and ensure the continuity of the wiring in the lead/plug.

As a matter of routine the data was downloaded from the deck unit using a hyper-terminal routine BB-ADCP.ht. Occasionally this gave errors in downloading which seemed related to the quality of battery connection and also once when the LADCP recorder was nearly full. In these situations the data was downloaded using the BBSC program.

2.3 SF6

Mar ie-Jose Messias, Gareth Lee, Kevin I. C. Oliver, and Andrew J. Watson

2.3.1 Introduction and procedure

The distribution of the tracer Sulphur Hexafluoride (SF6) was surveyed along the track of the RRS Cruise JCR44 to the Nordics Seas, as part of the ARCICE programme. The cruise took place approximately 3 years after 320 kg of SF6 were released in the pycnocline near the centre of the Greenland Sea Gyre during the European Sub-Polar Ocean Programme phase II (ESOP2). The purpose of the experiment is to study convection, vertical dispersion and lateral dispersion in the Greenland Sea and exchange rates and pathways of water between the Greenland and surroundings seas. One particular interest of the SF6 survey was also in the observation of development of the elevated SF6 concentrations in the Greenland central gyre bottom water.

The water samples for SF6 were the first samples taken from freshly opened Niskin bottles as soon as the rosette was on deck. Occasionally, the SF6 sample was the second taken after oxygen during leg 4 (stations: 149, 147, 145, 143, 141, 139, 137) and a correction based a previous test of air exchange in the Niskin bottles was applied (Ledwell *et al.*, 1998). In sampling from the rosette, after one rinse of the bottle, the sampling tube was cleared of bubbles and pinched to slow the flow. Then the tube was quickly lowered to the bottom of the bottle, with the tube still pinched. The bottle was slowly filled with water. When the bottle was a quarter full, the pinch was released and the water was allowed to flow freely for the time required for 3 flushes of the bottle. The bottles were cold to start with and were stored underwater at close to 4°C until analysed.

2.3.2 SF6 Analysis

Analysis System

Samples were analysed using a purge and trap system coupled to a gas chromatograph (GC8A) with electron capture detection as described by Law *et al.* (1994). The system is essentially the same as used during the previous cruises during ESOP2. SF6 was extracted from sea water by purging a known volume of sea water with oxygen-free nitrogen (NOF) and then cryogenically concentrated onto a trap filled in with Porapak Q. The gases were injected to the chromatographic column after heating the trap at +70°C. The SF6 peak appeared 2 minutes after injection onto the column.

Analysis System Parameters:

Water sample volume	403 ml
Low trap temperature	< –55 °C using CC-100 Neslab cryocoolers

High trap temperature	80 °C
Sparge time	2 minutes
Sparge flow rate	200 ml/min
Sparge efficiency	95%
Gas standard loops volumes	0.297 ml, 0.750 ml
Standards	51 ppt, 97 ppt provided by Plymouth Marine Laboratory
Column	2 m, 1/8", molecular sieve, 5A, 80-100 um, at room temperature
Detector	Shimadzu ECD at 310°C, 2.0 nA
Analysis time	9.0 minutes

Calibration

A set of 4 secondary gas standards (20 ppt, 51 ppt, 97 ppt, 290 +/- 0.5%) prepared at PML (P. Nightingale and M. Liddicoat) was available. Lab pressure and temperature were recorded and incorporated to the calibration. The sensitivity of the GC has been checked by triplicate injection of the 51-ppt standard run routinely along the cruise. For the calibration of all the samples, an extensive multi-point calibration was performed twice during the cruise using 2 different injected standard volumes and the 4 standards above. The response of the GC was nearly linear for the range of concentration encountered below an area of 80 000 as Law et al, 1993) and a linear fit was used for the calibration of the preliminary data.

System blank

Sparged sea water from low SF6 concentration sample analyses was collected in sampling bottle at the drain of the system. This water is assumed to be absolutely free of SF6, and its analysis allows the monitoring of the system blank (blank including all the effects encountered by the samples during the analysis, but not a blank due to air contamination during sampling) used NOF gas bottle was observed up to station 75. In this case, the system blank was subtracted from the sample concentration. After station 75, the NOF gas bottle was changed and the system blank was imperceptible.

Sparge efficiency

The efficiency was monitored by resparging a sample. The sample concentration was corrected accordingly by dividing by the efficiency of the sparge. The slope of the curve on figure 2.8 gives an estimation of (1-E)/E, where E is the fraction of tracer extracted on each sparge.

Reproducibility and Precision

Duplicate samples from the same Niskin bottle were run to determine an average reproducibility. A preliminary result for the mean absolute difference was 0.036 fmol/l (table 2.4). The repeat

injection of standards revealed a standard deviation between 0.14% and 1.4% (table 2.5). An absolute limit on the precision of the peak area measurements of approximately 200 microvolt-seconds corresponds to 0.018 fM. This is due to the noise level of the instrument. It determines the minimum detectable level, which is nominally 0.035 fM, i.e., twice the rms. noise. This base uncertainty dominates for lower lever concentrations while uncertainty of 1 to 2% dominates for concentrations above 1fmol/l.

Air measurements

Ten atmospheric samples were collected in 100ml glass syringes at 79°52.22N and 00°53.63E. The SF6 atmospheric concentration measured was 4.84 ppt -/+ 0.05ppt.

Acknowledgements

RRS *James Clark Ross* is operated by the British Antarctic Survey. Many thanks are due to BAS, the PSOs and the captain, the first officer, the deck engineer and crew of the JCR for a productive and enjoyable cruise. Thanks are also due to Mark Stewart for computing assistance and the science party for their help especially in sampling, and their co-operation and kindness.

2.4 OXYGEN-18 AND BARIUM

1550 Oxygen-18 samples (150ml glass bottles) and 160 Barium (60 ml high-density plastic bottles) samples were collected for post-cruise analysis at UEA. The sampling did not require any particular procedure, apart from 3 rinses of the bottles.

2.5 OXYGEN

Adrian Wright and Simone Medonos

Dissolved oxygen samples were taken from every second station and from all stations in certain areas of interest. Dissolved oxygen samples were drawn from each Niskin bottle following the collection of samples for SF6 analysis and prior to sampling for salinity and chemical tracers. Between two and four duplicate samples were taken on each cast, from the deepest bottles at the same time that the samples themselves were taken. The samples were drawn through short pieces of silicon tubing into clear, pre-calibrated, wide necked glass bottles and were fixed immediately on deck with manganese chloride and alkaline iodide dispensed using precise repeat Anachem bottle top dispensers. Samples were shaken on deck for approximately half a minute, and if any bubbles were detected in the samples at this point, a new sample was drawn. The samples were transferred to the chemistry laboratory, and then shaken again thirty minutes after sampling and stored under water until analysis.

The temperature of the samples drawn from all depths were measured using a hand held electronic thermometer probe. The temperature was used to calculate any temperature dependent changes in the sample bottle volumes.

Samples were analysed in the chemistry laboratory approximately two hours after collection. The samples were acidified immediately prior to titration and stirred using a magnetic stir bar set at a constant spin. The Winkler whole bottle titration method with amperometric endpoint detection (Culberson, 1987) was used with equipment supplied by Metrohm. The spin on the stir bar was occasionally disturbed by the movement of the ship and also by the uneven bases on some of the glass bottles, leading to less effective stirring of the sample and thus longer titration times, although this probably did not effect the accuracy of the endpoint detection. The Anachem dispensers were washed out with deionised water, each time the reagents were topped up, to avoid any problems caused by the corrosive nature of the reagents.

The normality of the thiosulphate titrant was checked against an in-house potassium iodate standard of 0.01 N at the beginning of each analytical run and it was incorporated into the calculations. A total of five standards were used throughout the duration of the cruise. Thiosulphate normality decreased with time except for thiosulphate batch 2 (iodate batch 3) (see problems). Blank measurements were also determined at the start of each run to account for the introduction of oxygen within the reagents and impurities in the manganese chloride, as described in the WOCE Manual of Operations and Methods (Culberson, 1991). Thiosulphate standardisation was carried out by adding the iodate after the other reagents and following on directly from the blank measurements in the same flask. Changes in the thiosulphate normality are shown in figure 2.9 and table 2.6.

Calculating the mean oxygen concentration difference between 273 duplicate pairs within the range ±10 µmol/l excluded 33 pairs, leaving a mean difference of –0.27 (sd 2.04) µmol/l.

Problems

- The temperature range of the chemistry laboratory often varied throughout the cruise. The non-constant nature of the lab resulted in the frequent introduction of air bubbles in the Titrino which then had to be mopped up. The temperature of the laboratory was noted for each analytical run.

- At station 045 the Anachem dispenser for Alkaline Iodide solution was wrongly set to 2.5 ml. Due to the time lapse no resampling could be conducted and analysis could not be sufficiently completed. Due to the corrosive nature of Manganese Chloride the Anachem dispenser was changed at the start of the second leg. As a result, fewer bubbles were encountered whilst sampling.

- Occasionally problems were experienced with the temperature probe which was exchanged for a more reliable model at station 013. The new probe failed twice later on in the cruise and thus an alternative probe had to be used.

2.6 SALINITY

Hazel Thornton

Water samples were drawn from each Niskin bottle into 200ml glass sample bottles closed with disposable plastic inserts and screw-on caps. A procedure of rinsing the bottles and caps twice with sample water before filling to the base of the neck and sealing was employed for each sample. To reduce the risk of salt crystal formation and sample contamination the caps were wiped dry before being screwed on. The samples were stored in crates and allowed to equilibrate to ambient temperature in a temperature monitored laboratory for at least 12 hours before being analysed. Two duplicate samples were taken at each station during legs 2 and 3 of the cruise and one duplicate over the last leg.

Samples were analysed on the (ex-IOS) Guildline 8400B Autosal Laboratory salinometer. A high stability temperature control bath and heat exchanger maintain the sample at a precisely defined temperature during analysis avoiding the need for temperature compensation giving a precision of better than 0.0002 in salinity. Two other salinometers were carried to cover any possible problems, an old IOS 8400 and a BAS 8400B, but were not required. There were numerous analysts, HT, AC, MB, IJ, KG, LC, JH, NH, AK. The biology laboratory was run at a nominal

temperature of 19 °C however the temperature did vary considerably and had always to be checked before analysis began.

Standardisation was achieved by use of IAPSO standard sea water ampoules. Three different SSW batches were used, P132, P134 and P136. The salinometer was standardised before the analysis of each crate. Figure 2.10 shows the salinity standard history and highlights that the drift of the salinometer was acceptable under the imposed conditions. The period of increased drift can possibly be explained by the variations in ambient temperature of the laboratory during the time in the ice.

Calculating the mean salinity difference between 178 duplicate pairs within the range ±0.005 excluded 10 pairs, leaving a mean difference of 0.0002 (sd 0.0010).

3. HYDROGRAPHIC UNDERWAY MEASUREMENTS

3.1 NAVIGATION

Sheldon Bacon, Margaret Yelland and Luca Centurioni

In this section, we provide a brief description of the main navigation data streams. All data were edited in a similar manner: checking for time jumps in the basic 1 second data, followed by despiking and averaging into 30 second data. Additional editing parameters are decribed below. All data were also checked visually. It is suggested in Yelland and Pascal (2000) that some time jumps are caused by the Level C processing occasionally producing rounding errors when converting between decimal jday and seconds. Interpolation of gaps was left to post-processing.

The principal positional navigation stream (GPS_NMEA) was provided by a Trimble 4000DS differential GPS receiver, located on the Bridge, with antennae on the Monkey Island. Data with poor positional accuracy (indicated by HDOP > 4) were edited out. The base station for the reference signal was Aberdeen.

The secondary navigational stream (GPS_GLOS) was provided by an Ashtech GG24 system which combines the dithered signal from the U. S. GPS satellites with the undithered signal from the Russian Glonass satellites to produce a pseudo-differentially-corrected GPS signal. Data with poor positional accuracy (indicated by HDOP, PDOP, TDOP, VDOP > 10) were edited out. The GG24 is located on the Bridge; antennae are on the Monkey Island.

The Ashtech 3DF GPS (data stream GPS_ASH), located on the Bridge, uses four antennae on the Monkey Island to provide high-accuracy measurements of ship attitude (heading, pitch, roll) which are accompanied by measures of maximum measurement rms error (mrms) and maximum baseline rms error (brms). Data with poor positional accuracy (indicated by mrms > 0.008, brms > 0.09) were edited out.

The gyrocompass is a Sperry Mk. 37 Model D, located in the nav. aid power supply room on the Bridge level.

The RVS *Bestnav* stream was also recorded. This provides 30-second positional data using a hierarchical gap-filling method to create a continuous navigational record. Data are taken from the three satellite streams above; if there is a gap longer than a set threshold in the principal stream, positional information is derived from the secondary stream, etc. In the complete absence of satellite data, dead reckoning is used (not needed here).

3.2 VM–ADCP MEASUREMENTS

Jenny Hutchings, Nick Hughes, Pat Cooper and Mikis Tsimplis

The ADCP onboard the James Clark Ross is substandard because it is unable to sample adequately underway for most of the time irrespectively of the weather conditions. The state of the instrument is unacceptable for any routine oceanographic work and it reduces the research capability of JCR significantly.

The erratic behaviour of the instrument became obvious both to the scientific team and the BAS technical support immediately after the departure from Hull. In spite of repeated efforts to change the settings of the instrument the output was corrupted (at best) and persuaded all involved that the instrument is malfunctioning. The ship was slowed down for 30 min to test whether this malfunctioning was related to the ship movement but no improvement was achieved. Therefore the instrument was switched off and advice was sought from the BAS headquarters. The instrument was subsequently restarted according to the instructions received but again no improvement was observed.

While on station the instrument seemed to produce numbers and these were compared with the Lowered Acoustic Doppler Profiler which was deployed with the CTD package at each station. The various steps are described below but the general estimate indicates an average deviation of 6±5 cm/sec between the two instruments in an environment where the velocity is of the order of 10 cm/sec.

The discrepancy between the two instruments in addition to the failure of the ADCP underway indicates that the instrument is faulty and that it would be advisable for BAS to consider replacement of the instrument.

The ADCP data collected were nevertheless processed and stored. The various tests are described below.

3.2.1 General Description of the ADCP

The RD Instruments vessel-mounted acoustic Doppler current profiler (VM–ADCP) employs the Doppler principle to remotely measure speed and direction of water currents from a moving vessel. By transmitting a succession of acoustic pulses, and segmenting the resulting backscatter echoes into many depth cells (bins) over a depth range of 30 to 700 meters, computer analysis of the bins provides a detailed profile of current speed and direction throughout the water column. In waters where the bottom depth is within range, the ADCP bottom track feature measures earth referenced vessel speed. Combination of these measurements yields absolute (earth referenced) vertical current profiles from a moving vessel without inputs from other navigation systems.

The IBM XT/AT compatible computer based Data Acquisition System (DAS) processes the ADCP data in real time together with vessel attitude and heading data to produce vector averaged profiles in earth referenced coordinates. Processed and/or raw data is logged on floppy or hard disk and backed up on tape cartridge. Data may also be displayed in real time on the CRT or graphics plotter. The DAS software includes a menu driven user interface to allow operators to easily control the system via the keyboard.

3.2.2 ADCP Data measurement

The profiler transmits short acoustic pulses along four vertically inclined beams defined by highly directional transducers. Backscattered sound from plankton, small particles and small scale inhomogenities in the water is received by the transducer with a Doppler frequency shift proportional to the relative velocity between the scatterers and the transducer. Received echoes are amplified, digitized, and processed in real time by the ADCP's microprocessor which repeatedly executes a first moment (Doppler frequency) and second moment (spectral width) estimation algorithm. The resulting time series of measurements of the Doppler shift produces a range segmented profile of water velocity along the four beams. The Doppler shift and time delay of the backscattered bottom echo is also measured for each beam providing an earth referenced measurement of vessel velocity and water depth (bottom tracking). In addition to current profiling and bottom tracking, the ADCP also measures profiles of acoustic backscattering strength by measuring the amplitude of the backscattered echo. Backscattering strength profiling range and spatial resolution are the same as for current profiling. The ADCP also contains Built-In-Test (BIT) functions providing complete operational status verification and fault identification without the use of external test equipment. A status evaluation is automatically performed at the end of each data collection cycle and GO/NO GO status is recorded with measured data. Commanded BIT routines are used to isolate faults (see Section 5.5).

3.2.3 Real Time Processing

The data acquisition system receives profiler data via the IEEE-488 parallel or RS-422 serial interface and processes the data in real time. By knowing the precise beam geometry, three orthogonal current velocity components for each bin are computed from any three of the four beams. For each ping, the profiler checks the Doppler estimates for validity, and each bin in the profile is compensated for vessel pitch and roll using attitude gyro data, resolved into N/S and E/W (earth) coordinates using heading gyro data, and accumulated into a vector averaging array. These processing steps are repeatedly executed for each ping. At the completion of a selectable averaging interval (1-600 seconds), the means of the vector current profiles and bottom track velocities are calculated and made available for disk storage and graphic display. Each velocity data point on a plot represents the average current velocity through a horizontal "slice" of the

water column in the region bounded by the four beams. This velocity data is spatially averaged over the distance travelled by the vessel during the measurement interval.

3.2.4 Data Processing and Calibration

The ADCP 2 minute ensembles are fed through a printer stream directly into the ship's level C system. From here they were read into daily pstar formatted files for various corrections to be applied, and the absolute water and bottom velocities then determined, once the ship's velocity is known from navigation. The shipboard processing of the ADCP data is described here.

adpexec0 (data extraction): Extracts raw data from the RVS acquisition, writes to daily (conventionally midnight to midnight GMT) pstar formatted files.

adpexec1 (clock correction): A correction was applied to account for the clock drift of the PC logging the ADCP data. Several times a day the PC clock was compared to the ship's master clock, and the time drift calculated.

adpdepthedit (removal of multiple bottom echoes): In shallow waters, the ADCP data was merged with the SIMRAD depth measurements; all measurements apparently originating from below the sea floor (due to multiple echoes) were removed.

adpexec0.1 (sea chest oil temperature correction): The ADCP on the JCR is placed in a sea chest filled with silicone oil. As before (B. A. King, pers. comm.), a correction was applied to the derived water speed to account for the variation of the speed of sound in the oil. It should be noted that the correction is based on the assumption that the oil in the sea chest is known and not mixed with air or water. The correction applied is

$$U_{corr} = U_{old}(1 - 0.0048113 \times T + 0.000035695 \times T^2)$$

where T is the temperature of the oil. Applied to the raw water and bottom track velocities, this correction is of the order of 10%.

adpexec2 (gyro heading correction): As the gyro inherently has errors, it is important to correct gyro headings with data from a more accurate source, in this case the Ashtech GPS3DF. The Ashtech data was processed in the standard way, averaged into 2 minute bins, and used to correct the gyro heading ensemble by ensemble. There may still be large gaps or spikes in the heading data, these should be removed manually.

adpexec3 (calibration of the ADCP data): There is a misalignment between 'true' forwards direction and the direction of the ADCP transducers. This heading misalignment to be determined, phi, is defined by the gyro error and the Ashtech antenna array misalignment. There

is also a scaling factor, A, that should be applied to the ADCP water velocities. The determination of these two parameters will be described in a later section.

adpexec4 (determination of absolute velocity): Finally the absolute water velocity can be determined by merging with navigational data. The ship's velocity over the ground is derived over each two minute ensemble and then subtracted from the water velocity relative to the ship to give the absolute water velocity. The navigation data is described elsewhere. Two navigation products were used with the ADCP data. The GPSNMEA data was used up to 70°N, and this was used to determine absolute velocities through out the cruise. During the time when the ship was above 70°N, the GPSGLOS data was used. [For post-processing, we shall revert to GPS_NMEA throughout. SB.]

To find Calibration Coefficients A and phi

As the JCR returned to England via the North Sea, the ADCP was put into bottom tracking mode and the ship steamed in several straight sections maintaining a speed of around 5 knots. In regions where the sea floor is less than 300m depth, the bottom velocity data can be used to determine the calibration coefficients.

The bottom tracking data was processed in the standard fashion, and absolute bottom velocity determined without calibration (set A=1 and phi=0 in adpexec3). Time periods when the ship's heading was constant, the ADCP bottom data return above 50% and there was not significant data drop out over time were identified. It was estimated that sections of 30 minutes long would be acceptable to reduce the errors in the GPS positioning. The ADCP aboard the JCR performed very badly throughout the cruise, and there were few sections of decent bottom tracking data to use. A section of 1.5 hours on the last day of the cruise was used to determine A and phi.

The ship's speed and heading over the sea floor was determined from the ADCP absolute bottom velocity. The GPS ship's speed and heading was also determined, and the calibration coefficients found as

$$A = Ugps / Uadcp$$

$$PHI = PHIgps - PHIadcp$$

The speeds and directions derived are shown in table 3.1

Problems Encountered

There is an obvious problem with the ADCP on board the JCR. The depth penetration is less than 200m, and at times falls to unacceptably low levels. While the ship is steaming the data drop out is unacceptable, and the percentage of good returns typically below 25%. It is looks like we will

only be able to use data collected while the ship was on station. During bottom tracking mode, the data drop out was high and it was almost impossible to determine periods useful for the calibration of the data. This situation is unacceptable and the ADCP must be serviced.

3.2.5 Comparison between shipboard and lowered ADCP measurements

To investigate the performance of the VM–ADCP, a comparative study between this and the Lowered Acoustic Doppler Current Profiler (LADCP) was made. It was noted that the VM–ADCP did not produce meaningful data while the ship was steaming. On station the data looked more reasonable, though it was not known whether the good returns gave usable current measurements or the measurements were swamped by noise.

First visual comparisons were made between the VM–ADCP and LADCP profiles. The VM–ADCP measurements were acquired averaged over two minutes. This data was processed and calibrated as described in the previous section. Although bottom tracking had not been used to refine the calibration, it was still believed there was some value in comparing the uncalibrated absolute velocities as errors due to calibration should appear as constant bias. The average absolute current profiles in the north-south and east-west directions were found for the time period while the LADCP was deployed. Individual VM–ADCP returns exhibited similar structure, with a variability of 10 cm/s due to noise in the ship's position. This noise was assumed to be Gaussian, and the average velocity profile during the station used in comparison with the LADCP profile. The LADCP north-south and east-west absolute velocities were determined as described in Section 2.2. An average was found between upcast and downcast velocities, which was used in quantitative comparison with the station averaged ADCP velocities. It was noted at each station there was a bias between the ADCP and LADCP, which did not appear to be constant between stations. There was little similarity between the shape of the velocity profiles, indicating that the ADCP data might be unacceptably noisy.

A statistical analysis of the difference between LADCP and ADCP mean current measurements was performed. For 20 stations the vertically averaged difference, and standard deviation of this were calculated. The mean difference between ADCP and LADCP varies substantially between stations, and does not indicate a constant bias. Generally the standard deviation of the vertically averaged velocity was large, around 30 percent of the mean, which suggests there was little agreement between the ADCP and LADCP.

The ADCP returns good data for the top 200m meters of the ocean. During the LADCP deployment it takes about 10 minutes to travel 200m. To refine the comparative study, the ADCP data for the coincident time of the downcast and upcast was investigated. For five stations the ADCP data was averaged during the first 10 minutes of the LADCP downcast and last 10 minutes of the upcast. These mean profiles were compared to the LADCP downcast and upcast

quantitatively exactly as before. The mean differences and standard deviation were not substantially different from the station averaged values.

Possible sources of error in the ADCP absolute velocities are the calibration and oil temperature correction. Typical calibration coefficients are a scaling factor of 1.03 and vector offset of 2 to 3 degrees. These are too small to describe all the variation between the LADCP and ADCP velocities. An oil temperature correction was not applied to the data presented here, although a brief investigation found that taking the correction method from JCR cruise 26, the raw velocity data was reduced by seven percent. This is not as much variation as observed between the LADCP and ADCP. It is possible that the oil temperature correction is inaccurate. The problems with determining this correction have been documented elsewhere (B. A. King, pers. comm.), and it should be noted the lack of knowledge regarding the sea chest could introduce large unknown errors into the processed data.

In conclusion, the ADCP data was unacceptably noisy. It is unclear why this is so, though it would be worthwhile investigating the sea chest containing the ADCP for wear and tear. A study of the propagation of sound waves through the sea chest oil is suggested, and at the very least it should be determined what oil is used and whether the chest is full.

3.3 DOPPLER LOG

Phil Heath

Dual Axis Doppler Speed Logger
Manufacturer: Sperry Marine
Model: SRD421S
s/n: unknown

The Dual Axis Doppler Speed Log utilises the Doppler shifted returns form high frequency acoustic energy transmitted into the water to provide precise fore/aft and port/stbd speed data, distance travelled, and water depth below the transducer. The system processes bottom reflections to provide over the bottom speed in the presence of ocean currents, and/or it processes acoustic energy reflected from the water mass to provide through the water speed when desired or when the water depth is too deep to obtain bottom returns.

The system utilises a microprocessor controlled transmitter to generate a series of short duration ultrasonic pulses. These pulses are transmitted into the water by a three-channel transducer, which is mounted through the ship's hull. Each of the three return echo signals from either the water or the bottom is Doppler shifted in frequency from the transmitted signal by an amount which is proportional to the ship's speed, direction of motion, and signal transmission angle with respect to the ship's motion vector. The return signals are amplified and applied through scaling and signal detector circuits to generate Doppler shift data which is processed to calculate fore/aft and port/stbd speed vectors.

The system is generally used in bottom mode. The instrument then produces speeds relative to the bottom when the water depth is less than 200m, it then automatically switches to water mode. The water depth does not seem to be logged in the raw RVS file. So to determine whether the logged speed is relative to the bottom or to the water, depth information would need to be merged from another source.

The SRD421S has not been calibrated since the replacement of hardware, software and transducer while the ship was in dry dock prior to the JR44 cruise. Calibration requires extended periods (several days) of steaming at known constant speeds, and this has not been possible since the refit.

From casual observation by the ship's radio officer the speed indicated by the instrument is known be reading low, possibly by as much as 10% under some conditions.

3.4 ELECTROMAGNETIC LOG

Phil Heath

Aquaprobe Electromagnetic Log Mk.V
Manufacturer: Chernikeef Instruments Limited
Model: EM2020 MK5
s/n: A1167

The Aquaprobe Electromagnetic (EM) Log measures speed through the water by creating an alternating magnetic field in the sea water. This is achieved by energising a coil encapsulated inside the transducer. When sea water flows through the alternating magnetic field a voltage is generated perpendicular to the line of flow. Two small pick up beads in the face of the transducer detect this voltage. The master speed and distance indicator contains all analogue and digital circuits for amplifying and processing the signal to produce a speed and distance log.

The EM2020 has not been calibrated since the fitting of a new transducer while the ship was in dry dock prior to the JR44 cruise. Calibration requires the ship to be stationary with no ocean current. This is only practical while the ship is in floating dock. From casual observation by the ship's radio officer the speed indicated by the instrument is thought to be reading high.

Toward the end of the JR44 cruise the distance travelled indication of the EM and Doppler logs differed by about 500 nautical miles. It should be remembered that while the ship is on station it holds position with bow and stern thrusters, the currents produced by these will be detected by the EM logger, and by the Doppler logger when operating in water mode. Also the EM2020 adds all measurements to the total distance travelled, regardless of whether the water flow is forward or reversed through the sensor, where as the SRD421S subtracts any aft velocities.

Spot reading of distance travelled as indicated by the two systems, and the GPS distance travelled at 0120Z 27th August 1999 were:

SRD421S:	3391.2 nautical miles
EM2020:	3917.5 nautical miles
GPS:	3979.7 nautical miles

3.5 THERMOSALINOGRAPH

Sheldon Bacon, Margaret Yelland, Kevin Oliver

The JCR carries a Simrad EA500 echosounder, located on the Bridge. The transducer is 6 m below the waterline, depending on the ship's trim. The draught of the ship, measured midships, decreased steadily throughout the cruise from 6.23 m at the start to 5.75 m at the end.

Thermosalinograph (TSG) sea surface temperature measurements at 5 second intervals were de-spiked, rejecting records if temperature differed by more than 0.2 °C from a five point running median, using the PSTAR program "pmdian". Salinity was calculated using the "peos83" from conductivity and TSG temperature measurements, assuming a pressure of 0 bar, and were de-spiked by a similar method; records were rejected if salinity differed by more than 0.05 from a five point running median. TSG temperature and conductivity records were rejected at these points.

Data editing for all oceanographic variables was also necessary for times when the uncontaminated seawater supply was interrupted or impaired by the presence of sea ice. This editing was carried out manually. Fluorescence data were not edited or calibrated, except as aforementioned. It was observed that there was little correlation between TSG fluorescence and CTD 7 db fluorescence. Air temperature and air pressure were processed with the oceanographic variables; see section 4.1 for evaluation.

TSG temperature and conductivity were calibrated by comparison with calibrated CTD values; this exercise was repeated post-cruise with final calibrated CTD data. Figure 3.1 shows the comparison of temperature measurements using CTD data from 7 m depth (for all stations) to coincide with the depth of the JCR's uncontaminated seawater intake. The range of surface temperatures was from about –1 to +13 °C. A straight line fit of CTD to TSG temperatures (independent and dependent variables respectively) produced a slope of 1.00059 (standard error [se] 0.00343) with intercept 0.01526 (se 0.00965). The slope is not significantly different from 1 at ±1 se, the intercept is not significantly different from zero at ±2 se; thus TSG sea surface temperatures are good and useable.

Unfortunately the same is not true for all the TSG conductivity data. Figure 3.2 shows the difference between CTD conductivity at 7 m and TSG conductivity as a function of station number. The conductivity difference is well-behaved up to about station 45 with a mean difference of –0.47 mmho/cm (CTD minus TSG), after which it goes haywire. This coincides with the first switching off of the uncontaminated seawater pump on the approach to the East Greenland ice edge. The cause of the subsequent poor performance is not known, but is it either sensor failure or continued bubble import. These data are not useable. For stations 1-45, a fit of CTD minus TSG conductivity to CTD conductivity (dependent and independent variables; see

figure 3.3) produced a slope of 0.0387 (se 0.0066) and an intercept of –1.8836 (se 0.0190). This is equivalent to a correction function of Ctrue = 1.040 × Ctsg – 1.9594. The slope fit suggests that TSG conductivities are accurate to about 0.01 mmho/cm (for the early part of the cruise).

3.6 SIMRAD ECHO SOUNDER

Nick Hughes

The bathymetry equipment installed on *RRS James Clark Ross* consists of a Simrad EA500 Hydrographic Echosounder. The Simrad Echosounder was used during the cruise for bottom detection. While in bottom detection mode, the depth values were passed via an RVS level A interface to the level C system for processing.

Data was transferred to PSTAR format in daily chunks. Latitude and longitude from NMEA GPS data were merged into the data file to provide positional information. The file was then checked for negative time jumps.

The data was automatically despiked using the PMDIAN routine in PSTAR. In some files there was significant noise which this method failed to remove so the despiking was done manually using PSPIKE. Small gaps in the data were filled using straight line interpolation (PINTRP).

Despiked data was processed using the Carter Tables corrections to sound speed to yield corrected depth. In the final stage of the processing a one minute average was applied to the data.

3.7 BIOLOGICAL SAMPLING

Paul Andrews

Introduction

This section of the report describes tangential flow filtration of sea surface particulate material for algal alkenone analysis. A number of species of marine algae, particularly the ubiquitous coccolithophore *Emiliania huxleyi*, produce long-chain, di- and tri- unsaturated C_{37} methylketones (alkenones). *Emiliania huxleyi* has been found to increase the degree of unsaturation of its alkenones as sea temperature decreases, resulting in a lowering of the melting points of these lipids and so enabling these micro-organisms to maintain their cellular fluidity and function in colder climates. Since, therefore, the relative abundance of the alkenones within the algae changes according to the sea temperature, these compounds provide the basis for a recently-proposed organic geochemical palaeotemperature parameter, the UK_{37} index (Brassell *et al*, 1986). Additionally, these algae also produce a tetra- unsaturated C_{37} methyl ketone which has been proposed as an indicator of polar seas of lower temperature and salinity. Since the polar oceans play a crucial role in the global climate, a greater understanding of the distributions of alkenones in modern polar settings is very important for their subsequent use in geochemical palaeoclimate studies.

Sampling method

Using the ship's underway uncontaminated seawater supply system a seawater sample (volume > 100 litres) was collected into carboys. A concentrated particulate suspension (particle size > 0.1 μm) of approximately 1 litre in volume was obtained from the seawater sample using a Millipore Pellicon tangential flow filtration system fitted with two Millipore low protein binding "Durapore" microporous (pore size = 0.1 μm) filter membrane cassettes in parallel.

The particulate material, within which the algae of interest are included, was then isolated from suspension by filtration through a Whatman 70 mm GF/F glass fibre filter within a standard evacuated Buchner funnel/flask apparatus. The vacuum required was provided by a Brook Crompton Betts Model 8524 PVH-A12 corrosion resistant pump. The dry particulate–laden glass fibre filter was then placed into a clean 50 ml Teflon–capped Pyrex sample bottle using clean forceps. The filter was subsequently immersed within the sample bottle in 40 ml of a mixture of dichloromethane and methanol (3:1 volume ratio respectively) to extract the alkenones and pigments. The sample was then stored in the ship's –20 °C refrigerator to prevent any chemical degradation prior to analysis by gas chromatography at Newcastle University.

For each sample collected the ship's position, the sea surface temperature, the sea surface salinity and the sea surface fluorescence reading were recorded from the ship's data logging system.

Additionally, two procedural blanks were conducted for the sampling and filtration method using 50 litres of Millipore Super-Q purified water instead of seawater.

During the last ten days of the cruise a marked decrease in the water flow through the tangential flow filtration system at the recommended operating conditions was observed. This caused the overall filtration time to increase significantly with the result that the number of samples that could be realistically collected per day decreased from two to one. The probable cause for this problem was the reduction in the performance of the microporous membrane cassettes brought about by the intensive use they were subjected to. Two Millipore low protein binding "Durapore" microporous filter cassettes were used in parallel in the filtration system on this cruise. As an improvement on the system, the use of three or four cassettes in parallel would increase the speed of the filtration stage in the sampling procedure and the effect of membrane degradation would be reduced, thus allowing more samples to be collected.

4. CONTINUOUS METEOROLOGICAL MEASUREMENTS

JCR cruise 44 was made up of two parts, the hydrographic phase and the meteorology phase. The hydrographic work occupied the first and last thirds of the cruise, with the meteorology phase occupying the middle third, from 2000 GMT on day 216 to 2000 GMT on day 226. However, the distinction was more blurred in practice since much of the meteorological work was continuous throughout the cruise, and some hydrographic work continued during the Met Phase. For this reason, the meteorological work will be described in two parts. This Section describes the work which was continuous throughout the cruise whereas Section 5 describes the work which took place while the ship was in the Marginal Ice Zone (MIZ).

4.1 AIR-SEA/ICE FLUXES AND MEAN METEOROLOGY

Robin Pascal, Margaret Yelland and Phil Heath

4.1.1 Aims

The James Clark Ross was instrumented with an array of meteorological sensors in order to provide continuous surface measurements of the air-sea/ice fluxes of momentum and sensible and latent heat, the radiative fluxes and mean meteorological parameters such as air pressure, sea surface temperature etc. The prototype AUTOFLUX system (AutoFlux Group, 1996; Pascal, Yelland and Clayson, 2000) was used for data acquisition and initial processing. These data will be used in support of the hydrographic program and the LES modelling of air-sea/ice fluxes.
Information on the AUTOFLUX system can be found at;
http://www.soc.soton.ac.uk/JRD/MET/AUTOFLUX/

4.1.2 Instrumentation

The Southampton Oceanography Centre's Meteorology Team instrumented the JCR with a variety of meteorological sensors. These were supplemented by two additional instruments provided by BAS (a chilled mirror dewpoint sensor and a fast response IR hygrometer), and data from the ship's Ocean Logger.

The mean met sensors (Table 4.1) measured air temperature and humidity, air pressure, sea surface temperature, incoming and reflected shortwave (300-3000 nm) radiation and incoming longwave (4-50 micron) radiation. Additional parameters obtained via the Ocean Logger (not shown in the Tables) were air pressure (from a Vaisala digital barometer in the UIC lab), air temperature and sea surface temperature from the thermosalinograph (TSG) intake at a depth of 7 m (Section 3.5). The surface fluxes of momentum and heat were obtained using the fast-

response instruments in Table 4.2. The sonic anemometers provided mean wind speed and direction data in addition to the momentum flux estimates.

The positions of the instruments are indicated in Figure 4.1. Where possible, the instruments were mounted on the ship's foremast in order to obtain the best exposure. The main exception was that of the fast-response hygrometer which needed regular attention. Since access to the foremast was dependent on weather/sea conditions, this instrument was located on the port bridge wing where it could be tended as required. Although this position gave unrestricted access to the hygrometer, it was relatively badly exposed and an additional sonic anemometer was placed alongside it in order to estimate the degree of flow distortion at that location. The effects of flow distortion on the measurements will be quantified after the cruise using a computational fluid dynamics model of the ship (Yelland *et al.*, 1998)

4.1.3 The AutoFlux logging system.

All the SOC and BAS instruments were logged using the SOC AutoFlux system which was undergoing its initial trial during the cruise. The system was based around two Unix workstations; the first workstation, "southerly" (SO), was used for data acquisition, and the second, "sowesterly" (SW), for data processing. Both workstations were networked but were set up in stand-alone mode and not integrated into the ship's system. Each workstation was cross mounted with the other, allowing easy data transfer between workstations and the sharing of devices installed on either station. The AutoFlux data acquisition system on SO ran multiple real time data acquisition and system programs, and the workstation was equipped with 8 extra serial ports for the multiple serial communications required. SO also had the greatest level of extra features, such as an auto-boot function and other system software designed to make the data acquisition as robust and reliable as possible. These applications were:

Powerchute: Both systems were attached to the UPS but only SO has the UPS manager powerchute installed. This monitors UPS loads, utility supply etc and includes a background process which provides orderly shutdown of the host computer in the event of an extended AC power failure. The software allowed the systems to survive a 20 second mains blackout (at 16:10 GMT, day 214), which was severe enough to blow fuses in some systems, without interruption of the data acquisition.

Program Monitor: Runs the data acquisition programs and continues to monitor that they are currently active. If an acquisition program crashes it is automatically re-started and an indicator is set.

Time Sync: This program reads in time either from a GPS receiver or, as in this case, from the ship's clock and adjusts the workstation time if the error is greater than 1 second. Jumps greater than 10 seconds are flagged and control is passed to the user before any adjustments are made.

Data were backed up to both CD (on SO) and Exabyte tapes (on SW). Complete backups (of both systems to both media) and subsequent removal of data from the hard disks were required approximately every 7 days. Such backups took about a few hours and data acquisition was halted during this time.

4.1.4 Data acquisition

Data were acquired continuously throughout the cruise using various logging programs on SO. These were:

"Gmet" – This acquires the mean meteorological variables and was set up to sample the 22 channels of data listed in Table 4.1. Each sensor is attached to a Rhopoint module which converts the sensor output into digital data, and communicates it to the logging system via an RS485 network. The sensors are usually interrogated once every 10 seconds but due to the number of sensors and long cables runs it was found that the program was unable to poll every sensor within that time, and so the sampling interval was increased to 12 seconds.

"Gillhs", "Gillr2", "Gillr2b" and **"Fhumid"** – These programs logged and processed data from the three sonic anemometers and the fast-response hygrometer. The programs are very similar. To take the HS sonic as an example, 16 sections of data were obtained every 15 minutes, each section consisting of 1024 data samples which are output from the anemometer at a rate of 20Hz. At the end of the 16 sections the data are processed to produce spectra and quality control parameters. The different data rates of the four instruments and number of sections obtained in a 15 minute period are listed in Table 4.2.

4.1.5 Instrument problems and system downtime.

The SOC sea surface temperature **"soap"** (a thermistor trailed over the side of the ship) did not function properly at any time during the cruise. Different sensors and electronics were tried to no avail. The problem was assumed to be a wiring fault but this was not traced successfully. Sea surface temperature data were obtained instead from the TSG when in open water, and from the Tascos when in ice.

Data from SOC's **pressure sensor,** located on the bridge, was very noisy. Data from the ship's sensor in the UIC lab was used instead.

The **long wave sensors** on the "bird table" (the small platform on top of the foremast extension) were popular perches for sea birds.

The BAS chilled mirror **dewpoint** sensor functioned intermittently and needed frequent attention. The heating cycle was not always successful at clearing the mirror, especially when in freezing conditions.

The two half-hemisphere **shortwave sensors** on the port side of the foredeck suffered occasionally from moisture ingress at the rhopoint connections. The downwards-looking sensor of this pair was suspected of a calibration offset and the two were exchanged (up for down) on day 215 at 14:18 GMT. Post-cruise calibrations will be performed.

The mountings of the **HS sonic** anemometer became loose and the instrument swung round to starboard sometime before 06:00 day 216. This was corrected when access was permitted to the foremast at 13:00. Advantage was taken of access to the foremast to examine the rhopoint junction box in order to trace the problem with the soap. As a result, **all data logging** was stopped from 13:00 to 15:00 day 216.

The **sonic anemometers** and the **fast-response hygrometer** suffered from icing intermittently while the ship was in the MIZ. The HS seemed more sensitive to icing and the clearing of ice from this instrument was dependent on access to the foremast. The R2 sonic on the foremast extension was less accessible but fortunately also less sensitive.

Tasco1 (sky) seemed dubious from day 221.0 to 230.0, during which time the value gradually increased from about 2.5 degrees to 3 degrees. However, the Tasco2 (sea) temp performed well throughout, suggesting that the mirror for Tasco1 may have been misaligned. The correction for sky temperature will be approximated using data from the long wave sensors during this period.

All data logging was stopped for system backups. These took place during the periods; day 212 06:30-10:00, day 220 09:40-14:00, day 225 14:30-16:50, day 227 19:15-22:20, day 234 12:15-14:40.

4.1.6 Initial results.

The various **air temperature** sensors were compared. The SOC psychrometers are accurate to about 0.05°, which was borne out by a comparison of the port and starboard instruments; the difference between the two psychrometers was 0.05° (s.d. 0.10°) over the whole cruise, for both the wet bulb and the dry bulb temperatures. The difference between the two psychrometers was largest (0.1°) for relative wind speeds below 4 m/s and decreased to less than 0.04° for winds above about 10 m/s. This may suggest that the fan on the port psychrometer (which read relatively high) was not working quite as well as it should.

The air temperature was also obtained from the ship's sensor on the foremast and from a PRT mounted alongside the dewpoint mirror on the bridge wing. Compared to the dry bulb temperature from the SOC starboard psychrometer, the ship's sensor underestimated the air temperature by 0.8° (s.d. 0.2°) on average. In the mean, the PRT was in good agreement with the psychrometer (a mean overestimate of 0.02°) but was rather noisy (s.d. 0.5°).

A comparison of the wet bulb depressions from the psychrometers and the dew point depression from the chilled mirror showed that data from the wet bulbs looked reasonable when the air temperatures were below zero (minimum dry bulb reading was -3°), suggesting that the water in the plastic reservoirs did not freeze. An exception to this occurred during the period from day 219.1 to day 220.6, when the port psychrometer wet bulb gave the same values as the dry bulb, suggesting that the port reservoir froze solid. The starboard wet bulb seemed OK during this period.

As mentioned in Section 4.1.5, the SOC **sea surface temperature** "soaps" did not function. SST was obtained instead from the ship's thermosalinograph (TSG). Compared to the near-surface CTD data from 80 casts, the SST from the TSG was high by only 0.01° (s.d. 0.03°). When the ship was in the MIZ the TSG intake was switched off to prevent it becoming clogged with ice. During this time the SST/ice temperature was obtained from the two IR Tasco radiometers, one of which was pointed upwards to obtain the sky temperature (required to correct the data from the downwards-looking sensor for the sky effect). A comparison of 46 near-surface CTD temperatures showed that on average the SST from the Tascos was high by 0.01° and was rather scattered (s.d. 0.6°). This large scatter is to be expected since the Tascos measure the temperature of the "skin" of the sea surface which can differ from the bulk temperature by up to 1°.

The AutoFlux system logged **air pressure** data from a SOC sensor placed in the bridge (at a height of about 15 m above sea level). This was compared to the Ocean Logger data which was obtained from a sensor in the UIC lab (7 m above sea level). The SOC sensor produced very noisy data which was on average 1.2 mb greater than that from the Ocean Logger. The difference between the data from the SOC sensor on the bridge (not corrected for height) and that from the sensor in the UIC (corrected to sea level) would be around 1.5 mb, suggesting that the Ocean Logger data are indeed corrected to sea level.

Figure 4.2 shows the time series of 1 hour averaged air temperature, sea/ice temperature and air pressure from the starboard SOC psychrometer, the TSG/Tascos and the Ocean Logger sensor respectively. Sea surface temperatures were obtained from the TSG except for the periods from day 215.8 to 220.5 and from 221.35 to 228.0, during which times the temperatures were obtained from the Tascos.

There were a total of five **shortwave** sensors deployed during the cruise. The first measured the total incoming shortwave radiation and was located on the "bird table" on top of the foremast extension. The other four all had half of their hemispherical domes blacked out using 1/2 hemisphere covers made (supposedly) of brass coated with chrome. These were deployed in pairs, boomed out to either side of the ship, but were turned off and brought inboard when the ship was in rough seas. The purpose of these instruments was to measure the reflected shortwave radiation. In each pair, one sensor was oriented to look upwards and the other downwards. The orientation of each pair was checked by comparing the total radiation measured by the two upwards looking 1/2 hemispheres with that measured by the sensor on the foremast extension. If the orientation of the 1/2 hemispheres was correct, the two estimates of total incoming shortwave should agree. The comparison was good, with the two 1/2-hemispheres producing a total incoming flux about 1 W/m2 (s.d. 8 W/m2) larger than that obtained from the sensor on the mast.

Figure 4.3 shows the two estimates of the total incoming shortwave. Two periods can be seen where the two upwards looking 1/2 hemispheres disagree with the mast sensor; these occurred during days 206.5 to 208.4 and from 219.0 to 222.64. The first period of bad data was due to the sensors losing their 1/2 hemisphere covers during a storm, and the second was due partly to the connectors to the port 1/2 hemisphere sensors getting damp and partly to both pairs of 1/2-hemispheres being twisted round by heavy seas while on passage between days 219.9 and 221.35. The 1/2-hemisphere covers were meant to be made of chrome covered brass, but when they were brought inboard at the end of the cruise some rust stains were visible at the edge of the covers. This did not seem to affect the data since the comparison with the sensor on the mast still looked good even during the last days of deployment (to day 239.5)

The data from the two downwards-looking sensors were examined by looking at the ratios of up/down flux data. This indicated a problem with the port downwards 1/2-hemi from day 213.25 to 215.5 which read low by about 20 W/m2 or more, possibly due to moisture in the connectors.

Examination of the night time data obtained at the beginning and end of the cruise (when the sun went below the horizon) suggested that the downwards looking sensor on the starboard side over-estimated by 2 or 3 W/m^2. All the shortwave sensors will be calibrated again after the cruise.

A comparison of the two upwards-looking **longwave** sensors on the foremast "bird table" showed that the data from the "LW2" instrument was rather noisy, and data from "LW1" is to be preferred. Data from this latter instrument is also shown on Figure 4.3.

Three fast-response anemometers (all made by Gill Instruments Ltd.) were used to measure the **wind speed and direction** as well the momentum flux. These were: an R2 on the foremast "bird table", an HS on the foremast platform, and another R2 on the port bridge wing. The last

instrument was used to estimate the severity of the flow distortion in the region of the fast response hygrometer. The HS seemed the most sensitive to icing, but could be cleared of ice when access to the foremast was permitted. The R2 on the bird table was not accessible but luckily seemed least sensitive to ice. True and relative wind speeds and direction are shown in Figure 4.4. The true wind speed (U10n) has been corrected for ship speed over the ground, for atmospheric stability and to a height of 10 m. A wind blowing onto the bow of the ship is indicated by a relative wind direction of 180°.

The one minute U10n values from the R2 on the mast and the HS were compared for winds blowing within 30 degrees of the ship's bow. On average the HS wind speeds were larger by 0.13 m/s (s.d. 0.28 m/s) or 2%. The wind directions agreed to within 1° in the mean.

Wind speed and direction were also obtained from the ship's anemometer, mounted alongside the R2 on the "bird table". A direct comparison of the relative wind speeds was possible for these two anemometers since they were both mounted at the same height. The ship's anemometer overestimated the relative wind speed by 0.3 m/s (s.d. 0.4 m/s) on average, and the wind directions agreed to within 0.3 degrees on average.

Heat and momentum fluxes will be calculated after the cruise.

4.2 RADIOSONDE ATMOSPHERIC PROFILES

Robin Pascal

Vaisala RS80-15G radiosondes, provided by the UK MET Office, were launched twice a day (at 1130 and 2330 GMT) to measure the temperature and water vapour structure of the troposphere and provide wind speed and direction profiles. At the end of each profile a TEMP message (WMO message FM35) was generated and sent to Bracknell via INMARSAT C for weather forecasting purposes. Additional flights (at 0530 and 1730 GMT) were launched during the Met Phase but were operated in Research mode during which the production of TEMP messages are not available. Data were acquired via an RS232 connection from a PC to a DigiCORA MW15 GPS receiver, and logging software was operated during each flight producing a real-time display and logged files of PTU (pressure, temperature and humidity), raw wind data and an averaged profile file. In addition, output from the DigiCORA was also logged in a flight file detailing system test information, sonde serial number, GPS position, ground check calibration corrections and time of flight.

During the early part of the cruise problems were encountered when operating the DigiCORA in TEMP mode. On a number of occasions, flights which had been successfully launched were prematurely terminated by the DigiCORA and a second balloon had to be launched. The reason

for this is not fully understood, although it appears that the maximum interpolation time for pressure, temperature or humidity had been exceeded. After the first 15 flights the frequency of this problem decreased. Nearly all of the successfully launched sondes reached the 100 mbar level, with the majority going on to nearer 50 mbar. Only 2 flights (numbers 3 and 49) failed to produce any wind data (a great improvement on previous experience where approximately 10% failed). The PC data from flight 24 was lost due to incorrect connect to the logging PC, although the TEMP message was successfully produced. A total of 90 sondes (Table 4.3) were launched from the bridge navigation deck aft of the wheelhouse (Figure 4.1). Balloons were inflated in a special restrainer designed to hold the balloon in a safe position even in strong winds. Sondes were launched successfully from this position throughout the cruise demonstrating that with its high position relative to the A-frame and lack of obstructions that this is an excellent point for radiosonde deployments. Launches were possible for a wide range of relative wind directions, so that it was not normally necessary for the ship to alter course.

Substantial data processing was carried out onboard, with the data initially displayed and logged in real-time on a PC. On a daily basis files were transferred to the SUN computers and converted into PSTAR format. Plots of temperature, relative humidity, wind speed and direction against pressure were generated. The data were further despiked then interpolated at 5 mbar intervals so that distance run verses height sections of temperature, humidity, wind speed and direction could be produced.

4.3 MONITORING OF NON-METHANE HYDROCARBONS IN THE ARCTIC TROPOSPHERE

Jim Hopkins

4.3.1 Why monitor hydrocarbons?

Hydrocarbons are emitted into the atmosphere from a variety of sources, their emission can be anthropogenic (man-made) or biogenic (naturally occurring). Build-up of hydrocarbons in the atmosphere can have direct harmful effects on health as carcinogens or causing respiratory illness, they are also involved in many reaction schemes the by-products of which can be considerably more harmful then their parent compounds. Tropospheric Ozone, a potent greenhouse gas and thought to be a cause of asthma, is one such example and is produced during the oxidation of hydrocarbons in the presence of NO_X.

The major removal pathway for hydrocarbons is via reaction with the hydroxyl radical (OH). The hydroxyl radical is the most important oxidising species in the atmosphere and is generated by a reaction involving ozone and water vapour in the presence of sunlight (310 nm).

4.3.2 Why monitor hydrocarbons here?

The ocean environment is generally very 'clean' with respect to hydrocarbons. This is due to the high concentration of water vapour which aids the production of OH and therefore destruction of hydrocarbons. In the Arctic marine environment, however, the presence of water vapour will be limited due to colder temperatures resulting in a decrease in OH concentration. If this is the case then we would expect that any hydrocarbons transported to or produced by the Arctic ocean would slowly build-up resulting in higher concentrations than would otherwise be expected. In such environments where OH is limited, alternative reaction pathways for the hydrocarbons may dominate such as reaction with the nitrate radical and also halogen atoms.

4.3.3 How do we monitor hydrocarbons?

A unique fully automated programmed temperature vaporisation – gas chromatography – flame ionisation detection system (PTV-GC-FID) is used to acquire and analyse one sample (1.5 litres) every hour and fifteen minutes (*approx.*). The sample is acquired at the front end of the ship and pumped through a 100 m length of Teflon tubing, coated with a stainless steel braid for extra robustness, to the main laboratory where the PTV-GC-FID is situated. The sample is firstly dried by being passed through a Dreschel flask held at –8 °C and a magnesium perchlorate trap. The hydrocarbons are then preconcentrated by passing over an activated charcoal trap held at low temperature (-25 °C) at a known flow rate (75 ml min^{-1}). All of the hydrocarbons are adsorbed onto the surfaces of the charcoal while the bulk of the sample (nitrogen and oxygen) passes straight through. Once the required volume of sample has passed through the trap, it is heated (350 °C) to desorb all of the trapped compounds which are then passed onto an aluminium oxide PLOT column (50 m, 0.53 mm i.d., $Na_2SO_4Al_2O_3$) in the GC system for analysis.

4.3.4 Results so far

Currently the results exist as a time-series of their concentration during the ships passage to and from the Arctic. Reconciliation of this data with back trajectories will give further indication of the source and age of the air mass. The time-series for ethene and propene shown in Figure 4.5 are seen to give good correlation during certain time periods, implying a common source for these two compounds. Later filtering of the data with respect to wind direction will remove any data points recorded when the sample was contaminated by the ships emissions.

4.3.5 Problems encountered

The system ran successfully throughout the cruise, with the exception of one day when we entered the ice and the end of the sample line froze over, the ice blocking the tube was removed and the system returned to normal working order.

The only other problem encountered was the regular saturation of the magnesium perchlorate traps used to remove water from the sample. These traps contained 6 cm^3 (*approx.*) magnesium perchlorate and needed to be replaced roughly twice a week, larger drying traps should have been used.

4.4 CLOUD OBSERVATIONS AND WEATHER NARRATIVE

Phil Heath

Hourly visual observations of cloud cover and type were made by the scientific staff. The ship staff also made hourly cloud observations in addition to their usual 6-hourly weather observations whenever possible. Figure 4.6 shows the difference between the two sets of observations for the total cloud cover in oktas. It can be seen that, in general, the two agreed well.

The 6-hourly weather obs made by the ship's staff are summarised below.

Day 205, 24 July 1999: Started off bright, becoming cloudy (7+) by mid morning. No significant wx all day. Winds light to moderate SW becoming NW later. Visibility good.

Day 206, 25 July 1999: Started off bright, becoming cloudy (7+) by mid morning. Overcast until 1700, some breaks in the cloud by evening, overcast again by nightfall. Slight showers of rain in the morning. Winds W to NW force 6 becoming 7 by 1800. Visibility moderate to good all day.

Day 207, 26 July 1999: Overcast with only occasional breaks all day. Dry in the morning with some rain in afternoon an evening. Winds W force 5 to 7. Visibility moderate to good.

Day 208, 27 July 1999: Overcast with only occasional breaks all day. Intermittent drizzle with occasional rain throughout the day. Winds W force 7 becoming 6. Visibility moderate.

Day 209, 28 July 1999: Overcast all day. Some rain and intermittent drizzle in afternoon and evening. Winds W force 4 to 5. Visibility good.

Day 210, 29 July 1999: Cloudy at first, clearing by 0400, broken cloud throughout the day. No significant wx. Winds force 4-5 WNW. Visibility Moderate to good.

Day 211, 30 July 1999: Broken cloud until evening, then becoming overcast. Slight drizzle and slight intermittent rain before midnight. Winds force 4-5 WNW. Visibility good.

Day 212, 31 July 1999: Starting overcast, then fog by 0400 continuing until 0700, then overcast, fog 1000 - 1400, clearing in afternoon then overcast with intermittent fog until

midnight. Intermittent slight drizzle in early morning, fog as stated, no other significant wx. Winds force 4 becoming lighter during fog, S becoming W later. Visibility variable.

Day 213, 1 August 1999: Overcast until 1500 then clearing to half cover, becoming cloudy again by nightfall. Patchy fog in early morning and again before midnight. Winds force 3-4 SW. Visibility variable.

Day 214, 2 August 1999: Overcast or Sky obscured all day. Fog all afternoon, then again from 2000 until midnight. Winds 2-4 W to NW. Visibility variable.

Day 215, 3 August 1999: Overcast all day, sky occasionally obscured by fog. Fog until 0400, then again at 0700 and 1600 to 2000. Winds light N and NW. Visibility variable.

Day 216, 4 August 1999: Start of the "Met Phase". Overcast with low Stratus 1000. Clearing at midday with a small amount of thin Cirrus. Then sky obscured by fog or overcast with Stratocumulus for the rest of the day. Intermittent drizzle in the early morning. Fog from 1500 to 2200, a short break at 1700 revealing a cloud free sky above. Winds Very light and variable. Visibility variable.

Day 217, 5 August 1999: Cloud observations varied throughout the day. During the periods when the fog cleared thin altostratus was reported. This may well have been thin stratus at a deceptive height. The fog became shallow at 1800 revealing a cloud free sky above. The only significant wx was the fog. This varied in thickness throughout the day, only clearing significantly at 0400. Winds were light southerly. Only poor visibility was reported throughout the day.

Day 218, 6 August 1999: Sky overcast or obscured by fog all day except for the fog being shallow at 00 and 01Z when a virtually cloud free sky was revealed, and a clearing at 1600 - 1700 also revealing a blue sky with a trace of cirrus. The only reported wind observation showed calm at 0600.

Day 219, 7 August 1999: The sky remained overcast when not obscured by fog. Patchy fog throughout the day was accompanied by slight intermittent snow from 1400 onward. Winds northerly force 4. Visibility varied with the fog but was never better than moderate.

Day 220, 8 August 1999: On day 219 at 2200 observations ceased until 1200 on day 220. This was an open water passage. I think we must have had a party! From 1200 until midnight the sky remained completely overcast. There was no significant wx reported. Winds were NNW force 5 at 1800. Visibility was moderate.

Day 221, 9 August 1999: The overcast remained until 0800. The cloud then gradually cleared to a blue sky by 1100. From 1800 to midnight the cloud gradually returned to seven oktas of

Stratocumulus. Slight drizzle and sleet was reported in the morning. Winds were force 7 from the north at midnight moderating to easterly 4 by midday. Visibility was reduced by sea spray in the morning, becoming good later.

Day 222, 10 August 1999: The sky remained overcast all day. There was continuous slight rain in the afternoon and evening. Winds were light easterlies becoming northerly later. Visibility poor to moderate.

Day 223, 11 August 1999: The overcast sky became obscured by fog before 0300. This continued until 1800 when the fog lifted slightly to form low stratus. Winds were light and variable.

Day 224, 12 August 1999: The sky remained overcast until being obscured by fog by 1700. The fog remained until 2300. Intermittent slight rain at 0300 and slight drizzle at 2200 was the only other significant wx. Winds were force 3 to 4 from the north.

Day 225, 13 August 1999: Complete overcast with low stratus remained until 0900. Intermittent fog in the afternoon and evening obscured only the 8 oktas of stratocumulus that lay above. Intermittent slight drizzle at 0300 and 0400. Winds force 3 from the north throughout. Visibility never better than moderate due to patchy fog and mist.

Day 226, 14 August 1999: Again complete overcast all day. Fog from 1700 to 1900, followed by slight snow sleet and mist until midnight, ending the met phase of the cruise. Winds were light NW throughout. Visibility never better than moderate due to patchy fog and mist. **End of "Met Phase".**

Day 227, 15 August 1999: Fog and overcast during the watch of the dark side 0000Z - 0400 gave way to a bright sunny day, but by 1900 the stratocumulus returned to cover the sky. No significant wx was recorded, winds were force 3 - 4 from the SW. Visibility was moderate to good later in the day.

Day 228, 16 August 1999: Broken stratocumulus (7+ oktas) remained all day. A solar halo was noted suggesting cirrostratus above. No significant wx was recorded until 2300 when it started to rain slightly, winds light SE becoming calm by 1800. Visibility was good throughout.

Day 229, 17 August 1999: 8 oktas of stratocumulus producing continuous rain and drizzle persisted solidly throughout the day. Winds were light and variable throughout. Visibility moderate.

Day 230, 18 August 1999: Overcast all day with intermittent slight rain and drizzle. Winds light and variable. Visibility moderate.

Day 231, 19 August 1999: Cloudy skies until 1700 when the lower stratocumulus broke up to give a blue sky. Cloudy again by midnight. Slight snow around midday. Winds force 4 from NE becoming light and variable later. Visibility moderate becoming good later.

Day 232, 20 August 1999: Cloud clearing by 0200 with a green flash observed at sunrise around 0240Z. Cloud cover remained less than half until 0800, then increased and became variable throughout the day. There was intermittent slight rain around midday. Winds light and variable with good visibility throughout.

Day 233, 21 August 1999: Total cover of stratus and stratocumulus throughout the day. Intermittent rain until midday. Winds force 3 to 5 from the south becoming SW. Visibility moderate.

Day 234, 22 August 1999: Total cover of stratus and stratocumulus throughout the day. Occasional slight drizzle throughout with fog at 1800. Winds force 4 from the west. Visibility moderate.

Day 235, 23 August 1999: Mainly cloudy with breaks around midday. Slight intermittent drizzle in early afternoon. Winds force 4 SW, becoming light at midday, then increasing to SW force 7 by 1800. Visibility good.

Day 236, 24 August 1999: Clear skies around midnight allowed the Northern Lights to be observed by some. Cloud increased during the day to 8 oktas by 2300. No significant wx was reported. Visibility good until after 2300 when fog descended.

Day 237, 25 August 1999: Thick fog persisted from midnight until 1200, this then lifted to low stratus. 1500 - 1900 Stratocumulus increasing in height. 2000 - 2100 Altocumulus covered the sky with some cirrus visible. At 2200 fog descended becoming dense by midnight. No observations were made in the bridge observational met.

Day 238, 26 August 1999: Thick fog persisted until 0700. The sky remained cloudy until 1800, after which there was intermittent fog. Wind easterly force 4 at 1800, force 4 - 5 from the NE at 1800. Visibility variable.

Day 239, 27 August 1999: The last day of met observations started with fog at midnight, lifting slightly at 01Z and 02Z observations before returning until 0600. The sky remained cloudy until 1900 when observations ceased. The wind at 1200 was force 6 from 110 degrees. At 1200 the visibility was between 4 and 10 km. No other observations were entered in the bridge met log.

5. METEOROLOGICAL MEASUREMENTS IN THE MARGINAL ICE ZONE

5.1 INTRODUCTION AND NARRATIVE

Margaret Yelland

This section summarises activities undertaken while the ship was in, or on the edge of, the MIZ. The first 24 hours were technically part of the hydrographic part of the cruise. The ship first encountered the ice edge on day 215.833 (03/08/99 20:00). Each Met Phase station contained two parts: 1) two or more hours of continuous measurement with the ship held head to wind during which a CTD dip was also performed if ice conditions permitted, and 2) a period of two or more hours with the wind on the port beam during which surface profiles of the atmosphere were obtained using the tethered balloon (Section 5.2). The duration of the stations varied, with the longest stations usually taking place between 20:00 of one day to 04:00 of the next, since the captain did not want the ship to manoeuvre in the ice unless he or the first mate were present on the bridge. Table 5.1 lists the ship activities while in the MIZ as recorded by the navigation officers. Additional activities such as deployments of the PIMMS and sonar buoys and radiosonde launches are also listed in Table 5.1 and are discussed separately in Sections 5.4, 5.6 and 4.2 respectively.

The original aims of the MIZ measurement program were a) to find an "ideal" lead with a minimum open water fetch of 200 m surrounded by 10/10 ice cover and then sample as the LES model results suggested., and b) to sample in a range of sea-ice concentrations from 1/10 to 10/10 cover. Since ideal leads are hard to find it was initially planned to travel north from the first Met Phase station (number 54 on day 216 20:00 to 217 06:00) in 7/10 ice cover into the low concentration or open water of the Northeast Water. However, ice conditions deteriorated quickly once the Met Phase began and it was impossible to make sufficient headway northwards after Station 54. Station 55 (77 20.0 °N, 12 18.7 °W) took place in 9/10 ice cover amongst vast floes which had seriously impeded progress such that the ship's passage speed had been reduced to less than 2 knots and the ship had been unable to make any progress northwards in the preceding 6 hours. As well as being more concentrated than suggested by the SSMI satellite images (Section 5.3), the ice was also relatively old and thick. It was therefore decided that the original plan be discarded and that the ship should head eastwards into open water and then proceed to 80 °N in the open water and re-enter the ice further north. This allowed us a) to rendezvous with the AWI aircraft *Polar2*, and b) to study a region where the sea ice was younger and thinner, i.e. more easily penetrated by the ship. It was also thought that the remote sensing information available was more reliable further north due to the lack of melt-pools which had been common at 77 °N and were thought to cause the SSMI images to under-estimate the sea-ice concentrations in that area. Stations 56 and 57 were performed in 3/10 and 2/10 ice cover respectively as the ship headed eastwards to open water. Figure 5.1a shows the ship's track for stations 51 to 57.

After steaming north east in open water for about 32 hours the ship re-entered the ice edge at 80 23 °N, 8 14 °E. Figure 5.1b shows the ship's track for stations 58 to 74. Station 58 took place in 3/10 ice cover, after which the ship steamed into the ice for station 59 in 9/10 cover. Stations 60 to 65 were performed as a section across the ice edge in order to investigate the development of the surface layer upwind and downwind of the edge. Station 60 took place on the ice edge, which ran roughly east-west, while the wind blew from the north. The wind stayed roughly off-ice for station 61 at a distance of 200 m downwind from the edge but became lighter and more variable during station 62 at 400m downwind of the edge. Station 63 took place 800 m "downwind" of the edge but the wind direction became very variable with fog present, making it difficult to keep the ship at the correct downwind distance. Station 64 took place in foggy conditions on the ice edge itself which was becoming very broken up and ill-defined due to the variable wind direction. Station 65 took place 500 m into the ice in fog. The HRPT images suggested that the fog cleared towards the west so the ship steamed south west in open water following the ice edge until midnight on day 223/224 whereat station 66 took place on the ice edge which was again confused. Stations 67 to 73 were again performed as a section through the more well-defined ice edge slightly further south, while the wind was blowing off-ice. Station 67 was initially on the ice edge but a tongue of ice moved across the stern of the ship after the first few hours, making the ship 100 m upwind of the ice edge. Station 68 was intended to be downwind of the ice edge but this plan was revised when the scientists on the *Polar2* informed us of their intention to perform a laser altimeter section across the ship's position towards the end of the day. Since we wanted the ship to be on-station in the ice during the aircraft section, station 68 took place about 500 m upwind of the ice edge. The aircraft flew overhead at 23:30 on day 224. The ship then resumed the ice-edge section by taking a position 200 downwind of the ice edge for station 69, then 400m downwind for station 70. Station 71 took place 800 m down wind of the edge before the ship returned to the ice-edge for station 72 (since the earlier ice edge station was actually 100 m upwind of the edge). Finally, as the ship headed southwards towards the start of the next hydrographic line, the final stations 73 and 74 took place in 7/10 and 9/10 ice cover respectively.

Figures 5.2 shows the true wind direction (from) and the true wind speed corrected to 10 m and neutral conditions, plus ice concentration in tenths averaged from the various visual observations obtained (Section 5.4). It can be seen that during the first fetch section (stations 60 to 65) the wind speed was initially about 4 m/s and blowing almost perpendicular off the ice-edge, but then decreased to around 2 m/s and became very variable in direction with the final 3 stations taking place in fog. Because of this it is thought that this section is unlikely to provide much useful information. However, the second fetch section is much more promising; the wind stayed constant at around 5 m/s and blew off-ice continuously. It is hoped that this second "fetch" section through the ice edge can be used for the LES modelling program in lieu of the "ideal lead"

experiments originally envisaged. It is also thought that a reasonable range of different ice concentrations and conditions were obtained during the limited 10 day measurement period.

5.2 TETHERED BALLOON PROFILING

Ian Jones and Alison Coals

5.2.1 Aims

The varying ice concentration of the Marginal Ice Zone induces changes in the lower parts of the atmospheric boundary layer. In particular, alterations to the surface roughness and surface fluxes where open water is found amidst sea-ice effects alterations to the temperature, humidity and wind velocity profiles near the ice/ocean-atmosphere interface. Traditional ways of studying these profiles include use of radio-sondes as well as fixed instrumentation at given heights on the ship. However, the resolution of radio-sondes in the lower atmosphere is not great and fixed instrumentation, by its nature, only gives information at one or two heights. For this reason tethered balloon flights were employed to fill out the details of the changing profiles in the bottom few hundred metres of the atmosphere, enabling much greater resolution data to be obtained in this region of interest.

5.2.2 Equipment

For this purpose a medium sized helium filled balloon was used. This was approximately 6 metres long and 2 metres in diameter at its largest circumference. The balloon was tethered to a manual winch bolted to the ship's deck matrix. Two different gearing ratios were engineered into the winch, one to pull a normal load, the second giving sufficient mechanical advantage to pull a far heavier load. This latter gearing was included as a safety measure lest the pull from the balloon should prove too large, but in fact was never needed. The tethering line was a reel of 400 lb breaking strain, polyester line. The purpose of the balloon was to lift an internally recording sonde.

The sonde incorporated temperature and relative humidity sensors, mounted beneath a radiation shield, a pressure sensor and a wind speed sensor utilising a pitot tube. A compass including pitch and roll sensors was also contained within the sonde. The wind direction measured was that in which the pitot tube was pointing, requiring this to be angled towards the wind. This was achieved by hanging the sonde in line with the balloon, which itself was sufficiently aerodynamic to always point into the wind.

5.2.3 Flights

Flights were carried out on all stations during the Meteorological Phase, up to heights of no more than 300 metres, as follows:

Station 54, 4 flights; Stn 55, 2; Stn 56, 2; Stn 57, 1; Stn 58, 2;
Stn 59, 5; Stn 60, 4; Stn 61, 5, Stn 62, 4; Stn 63, 7; Stn 64, 7;
Stn 65, 4; Stn 66, 5; Stn 67, 6; Stn 68, 10: Stn 69, 6; Stn 70, 6;
Stn 71, 7; Stn 72, 11; Stn 73, 6; Stn 74, 5.

5.2.4 Problems

Problems came in two categories; those with flying the sonde and those with the sondes themselves. The problems in flying the instrument, though potentially great, proved to be surmountable. Despite a number of large structures on the ship, the balloon and balloon line never came into contact with any alien body and the sonde was always released and retrieved with minimal difficulty. Similarly, after initial experimentation, the sonde could be hung without difficulty in line with the balloon, so that the pitot was angled towards the wind. In still conditions the error in this was small, although increased significantly in regions of turbulence, when the instrument shifted position considerably. There was also a small tilt in the instrument, but this is detected by the pitch sensor and can therefore be taken into account in the data analysis. A more rigid fastening would be needed if such work was carried out in areas where large quantities of turbulence might be expected.

On the whole the equipment used proved to be very successful. In the conditions encountered the balloon was a useful tool for raising and lowering the sonde, keeping steady at most times and giving ample lift. It should be noted though, that no high wind speeds were encountered where extra difficulties with the balloon might be expected.

The manual winch operated well, gave control over the speed of the ascent and descent of the balloon as well as sufficient pull to bring back the balloon without difficulty in any of the winds encountered. There were no problems with the line during the experiment either, although some very slight fraying was evident towards the end. For work with a balloon of this size which has large static lift, so that line drag is not an important factor, a thicker diameter line would offer less fraying potential without adversely affecting the measurements.

The sondes worked reasonably well in the conditions, although some features could be improved. Firstly, the use of a pitot for measuring wind speed has the disadvantage that moisture within the pitot can cause the instrument to malfunction. As the relative humidity was high during most of the flights much care had to be taken of the sonde both during and between flights. This problem would need to be addressed for further work, although even in the moist conditions encountered

here many successful flights were undertaken. Secondly, there was evidently some time lag in the response of the temperature sensor. It is expected that this problem can be overcome during post-processing. Both the relative humidity sensor and the temperature sensor also had some trouble in very moist conditions, if moisture settled on to the sensors, although this problem occurred only rarely.

5.2.5 Calibrations

Accurate calibration of the sondes was planned for after the cruise, thus during the cruise, the manufacturers' nominal calibrations were used. Tests were performed on board the ship to check that these calibrations were sufficiently accurate to allow the data to be interpreted meaningfully. The pressure sensors were calibrated against the barometers in the UIC room and on the bridge, whilst the relative humidity was tested against a hygrometer. Temperature sensors were tested against a hand-held thermometer and the ship's psychrometers. The wind-speed measurements were tested against the sonic anemometer on the bridge wing and against a hand-held anemometer. All these tests suggested a reasonable degree of accuracy for the existing calibrations. A further calibration of the sondes' wind speed and temperature data was carried out by strapping the sondes next to the sonic anemometer and psychrometers on the fore-mast for several hours. This experiment confirmed that readings from the sonde were reasonable. The temperature sensor was estimated to be accurate to a couple of tenths of a degree of the psychrometers, however, the aforementioned time lag in the temperature response was also evident. Wind speeds were within a few tens of centimetres per second of the sonic anemometer wind speeds as long as the pitot tube was pointing towards the wind. At angles greater than 45 degrees from the true wind the sonde gave much less accurate readings.

5.2.6 Profiles

Two example profiles are shown in figure 5.3, as well as those obtained from radio-sondes released at a similar time. The plots show the wind speed and temperature against height on the evening of 9/8/99 between 21.10 and 21.30 (Station 59) in an area of approximately 10/10ths ice concentration. Sampling took place at 1 Hz, with the data shown being averaged over 10 second periods. Apart from this averaging no processing has been done to the balloon-sonde data in the plot. Also shown are the radio-sonde profiles in the lower boundary from the radio-sonde ascent started at about 23.30.

The two temperature profiles are qualitatively similar, but are offset by between 1 and 2 degrees throughout the profile. This is in part caused by a temperature drop of nearly a degree in the time between the balloon and radio-sonde flights (see fig 4.2). The radio- and balloon-sondes should be accurate to within a few tenths of a degree though, implying that the time lag in the

balloon-sonde response is responsible for an error of around 0.5 – 1 degree. Post-processing of the raw data will be needed to investigate this.

The wind speed profiles are very different. Radio-sonde wind speed profiles are not always accurate near the surface though, and wind speeds during the relevant time period from the ship's instruments of 6-9 m/s (see figure 4.4) are much closer to those being measured by the balloon-sonde, suggesting that the balloon-sonde measurements are those which are likely to be correct. It's also interesting to note the spike in the balloon-sonde profile at around 100 m, where much turbulence had been evident during the flight. This illustrates the difficulty of this method of measuring in regions of turbulence.

5.3 REMOTELY-SENSED ICE OBSERVATIONS

Jenny Hutchings

The meteorological phase aimed to take measurements in regions with various sea ice conditions. As the ice is in fast retreat in August and conditions change on a weekly basis it was important to keep track of the ice conditions the weeks preceding the phase. Daily monitoring of the sea ice state using several sources of information aided cruise planning.

The most comprehensive data set were "egg" charts provided by the National Ice Centre, U.S.A, and relayed to the ship once a week (by Ben Moat, SOC). These are compiled from direct observations and satellite monitoring, in particular making use of passive microwave data and Radarsat. They report the sea ice concentration, ice type and floe size. There were two sections in the meteorological phase, one on the north-east Greenland shelf at 78 °N travelling Northwest from 76°N, 9 °W towards 77 °N and 12 °W, the other at 80 °N and 0 to 10 °E. The ice conditions in the two regions were quite different. On the first section the ice was close and consisted of a variety of first year, second year and multiyear ice. Floes varied in size from meters to tens of meters, though there were a few floes over 100 m. For the week preceding this section, the egg charts reported similar conditions, describing the ice as thick (2 m) multiyear and first year ice. On the second section the ice was predominantly medium thickness (70–120 cm) first year ice. When the ship remained in the marginal ice zone, within 500 m of the ice edge, the ice consisted of brash and small (< 20 m) ice cakes. On the two occasions that the ship ventured further into the pack, the pack closed in and small floes (20–50 m) were prevalent. The egg charts reported thicker ice and did not indicate floe size. Therefore, it appears that the egg charts reported regional conditions satisfactorily, though failed to resolve the marginal ice zone.

Daily estimates of sea ice concentration, extracted with the NASA Team algorithm (Cavalieri *et al.*, 1984) from SSMI passive microwave radiometers on board DMSP/NOAA satellites, were used in preliminary planning. These did not show much variation during the week before and during

the meteorological phase. Along the East Greenland shelf the ice was reported to be between 40–60 % concentration. The ice to the north and east, above Spitsbergen, was recorded with higher concentrations of 80–100 %. The egg charts were in agreement with the concentration above 80 °N, but were in disagreement further south and closer to Greenland, reporting concentrations greater than 80 %. The ship observed concentration in this region was above 80 %; see figure 5.4 which shows ice cover data from routine ship observations. It is well known that the NASA Team algorithm performs badly during the summer, probably due to the presence of melt ponds (eg El Naggar, Garrity and Ramseier, 1998). In the region where the SSMI sea ice concentrations were most inaccurate it was estimated that there was 30–50 % coverage of melt ponds, which could explain some of the difference. Above 80 °N there were fewer melt ponds, and the SSMI concentrations were in better agreement with observations.

As the SSMI data was deemed to be unreliable, egg charts and AVHRR images were relied upon. AVHRR images were sent to the ship by High Resolution Picture Transmission (HRPT) every time a satellite passed over the ship's position. Each image had five channels, three visible and two infrared. False colour images were created from these, and the colour table modified to aid distinction between ice and cloud. Four out of ten days were cloud free in the regions of interest. During 8, 9 and 11 August the ice edge where the ship spent the second part of the meteorological phase was visible; see figure 5.5. We also occasionally received via email processed AVHRR images sent by the Satellite Group at Plymouth Marine Laboratory. An example is shown in figure 5.6, which is constructed from $4.8 \times (\text{band1} \pm 0.59 \times \text{band2})$, which nicely highlights the ice on the north-east Greenland shelf.

There was agreement between the ship observed ice edge and the other estimates of ice edge position. The ice edge for the SSMI data was taken to be where the ice concentration falls below 15 %. Ice edge position was also provided by NAVTEX Ice Reports, prepared by The Meteorological Institute of Tromsø, Norway, for 3 and 10 August. The edge position given by all these sources is shown in figure 5.7, superimposed upon the SSMI ice concentration for 5 August. Note that the ship-observed ice edge is in agreement with the NAVTEX edge, and falls in the region of 15–30 % SSMI sea ice concentration. Given that the NAVTEX, ship-observed and SSMI ice edges are not coincident in time, and the ice edge was moving north, it can not be said how accurately 15 % concentration gives the ice edge in the SSMI data.

The most reliable source of information on sea ice conditions was the NOAA egg charts, which agreed best with observed ice conditions during the meteorological phase. The SSMI data alone was unreliable, underestimating ice concentration by 20 % or more. The AVHRR images were of limited help in determining the ice edge, though could not provide more detailed information. The most reliable ice monitoring can only be performed by amalgamating all available information, compensating for the weakness of the remotely sensed data. Although the egg

charts reported large scale ice conditions better than the other sea ice monitoring products, they could be improved by assimilating still more information.

It is instructive to compare the ship observations (fig. 5.4) with SSMI data (fig. 5.8, showing the wider area of the north-east Greenland shelf and Fram Strait). We see that where the SSMI predicts low ice concentrations, we ran in fact into heavy ice cover. In particular, the SSMI data show a south-east to north-west trending zone of low ice cover on the Greenland shelf, ending near the Greenland coast in about 80–81 °N. On the part of the track heading east on about 77 °N, from about 13 °W to 9 °W, we encountered 7/10–10/10 cover. The SSMI data presumably shows something like surface liquid water fraction, which is very different from open water fraction.

5.4 IN-SITU OBSERVATIONS OF SEA-ICE

Margaret Yelland, Robin Pascal and Phil Heath

Visual observations of the ice conditions were made every hour. Two independent sets of observations were obtained from a) the science team and b) the officers on the bridge. The observations were coded using the WMO "Egg Code". The two sets are tabulated in Tables 5.2 and 5.3. Also shown in Table 5.3 are the 6-hourly observations made by the navigating officers as part of their synoptic meteorological observations.

The visual observations were supplemented by the SOC Colour Quickcam camera (made by Connectix) which took periodic digital pictures of both sea state and ice coverage during the cruise. The camera is designed for producing digital pictures on a PC and simply plugs into the PC's parallel and keyboard ports. It is capable of producing 24-bit colour photos at 640 X 480 pixels. The software provided with the camera, QuickPICT and QuickMovie, allowed easy setup and was used in auto capture mode and was set to take a picture every 15-60 minutes. The image files produced were saved in JPEG format, and were transferred daily to Zip disk to avoid the hard disk becoming full. The camera was installed in a corner of the bridge, facing towrds the bows of the ship, with a 486 laptop PC and placed hard against the window to avoid any unwanted reflections. The system worked well throughout the cruise.

SPRI operated a second camera system during the cruise. This is discussed in Section 5.8.

5.5 TRIALS OF PIMMS BUOYS

Robin Pascal

PIMMs is an acronym for Polar Ice Motion Monitoring Buoys. On this cruise, we had the following aims: Verification of hull design including drift performance relative to ice and survivability in more extreme ice conditions. Initial testing of the interface circuitry for air and sea temperature measurements and the performance of the application program in the EL-2000G data communicator. Operational characteristic for instrumentation and batteries at low temperatures and the success rate of message transmission.

The main controller of a PIMMs buoy is the STELLAR EL-2000G data communicator which is a microprocessor based VHF transceiver that allows communication with the ORBCOMM Satellite communication system. This system is designed for the sending and receiving of short email messages from and to the unit via uplinks and downlinks with the satellites and earth station gateways. The EL-2000G utilises a built-in GPS card to establish the unit's position, and also

contains communication management, position determination algorithm, housekeeping and application software modules.

The internal application software has been set up to control the frequency of position measurements, sample the unit's analogue and digital inputs, log the data and format a message every specified logging session. For the PIMMs buoy the two analogue inputs are used to measure air and sea temperatures from the measurement of platinum resistance thermometers (PRTs) via interface circuits. One digital input is used to indicate the sign of the air temperature sensor to increase the sensors resolution. In the interface electronics the air temperature range is set for 0 - 20˚C for a 0 - 5 Volt output and with the sign bit gives a complete range of ± 20 ˚C. For greater accuracy the sea temperature has a more limited range of -2 - 10 ˚C for 0 - 5 Volt output.

The application settings were such that each logging session takes the form of:

Time, position , speed, heading, digital ch.1, analogue ch.1, analogue ch.2, unit internal temperature, internal battery voltage, external power on/off.

dd/mm/yyyy hh:mm:ss, xx.xxx, xx.xxx, xx.x, xx.x, x, x.xxx, x.xxx, xx.x, xx.x, NNN

On departure the PIMMs buoy was stowed on the after deck with as clear a sky view as possible. The buoy was first powered up on Day 207 after assembly of the internal components, a Stellar EL-2000G Orbcomm Communicator and interface circuits for the sea and air temperature sensors, which were powered by two STR Pb sealed Gel 12 Volt, 45 Ah batteries. The buoy was left transmitting messages until the MET phase of the cruise where on an opportunistic basis the buoy was deployed in the marginal ice zone in various ice concentrations. Also during this phase the buoy's position on the ship was changed to make deploying the buoy more convenient, but gave the buoy a poorer sky view, reducing the number of good satellite passes. Initially the message format was set for positions every 15 minutes with two positions per message, generating one message every 30 minutes; this was changed to one position per message every 15 minutes at the start of the MET phase to increase the no. of messages produced. Before each deployment the communicator was reset causing all old messages to be lost in an effort to make it clearer as to when the messages generated during the deployment were transmitted.

Generally the buoy performed well and seemed to behave very well in the ice. Although the buoy tended to drift off relative to the ice flows when in open water, this relative drifting stopped the moment the buoy was in any form of ice or brash. When caught in ice or squeezed by larger flows the buoy either popped out or was lifted up rather than being pushed under.

By day 209 the buoy was only in range of the near polar orbiting satellites and messages were sent in Globalgram mode where the messages are limited to 219 chars and are stored on the satellite and later down loaded to a gateway. It was disappointing to find that only one of the 4 near polar

orbiting satellites (id 2) could be seen by the communicator. Unfortunately this greatly limited the number of satellite passes seen, typically 3 - 4 good passes each day.

For this experiment the buoy was powered by two gel cell batteries, to give 45 Ah at 24Volts, and with an approximate current of 110 mA at 24 V this should give a maximum duration of 17 days but there would some reduction due to low temperatures. The battery voltage was periodically measured and after 14 days was reduced to 8.9 volts but with the communicator still functioning.

5.6 ON-ICE ACTIVITIES

Arthur Kaletzky and Nick Hughes

We planned to measure sound speeds in sea ice in-situ using methods and equipment described in Resummon, M.H. (1998). As holes had to be drilled in the ice to embed the ultrasound source and receiver, we also planned to do some amount of sea ice coring and sampling. These activities were not performed for the following reasons:

1. The apparent failure of a key component of the Reisemmann experiment (the "composition box" or modulator), possibly due to damage during shipment or during a practice setup on the aft deck.

2. The inability to find an ice floe which complied with BAS ice docking criteria (large stable floe of 300m diameter or greater, strong enough not to crack when directly impacted by the JCR's bow, which is BAS standard ice mooring practice) and biological safety criteria (isolated floe in the Marginal Ice Zone widely separated from other floes or in an area believed to be clear of polar bears and in excellent visibility).

5.7 SONAR BUOYS

Arthur Kaletzky

Acoustic thermometry and ice thickness measurement using a very low frequency source and sonobuoys.

The aim of this experiment was to test the feasibility of receiving clear signals from a distant, powerful 19.6Hz source using military-surplus sonobuoys and of using the received waveforms and arrival times to estimate average temperature and ice thickness along the source-buoy transect.

The principles of this approach for temperature are well established in underwater acoustics literature but generally for shorter ranges (e.g. Jensen et al, 1994). The determination of ice thickness from arrival time was originally suggested by Jin and Wadhams (1989). Recently, Mikhalevsky and co-workers have put into service a powerful 19.6 Hz source moored off the north tip of Franz Josef Land (Mikhalevsky, et al., 1999). The source is battery-powered, and thus is restricted to transmitting only once in 96 hours, at midnight UTC, controlled by a local rubidium clock. We obtained some standard wideband military-surplus sonobuoys, mostly from Mikhalevsky's group, in order to receive the signal during the CATS-MIAOW cruise. The sonobuoys have wideband (10-6000Hz) hydrophones, and simply modulate all acoustic signals received onto VHF-FM and rebroadcast this. The sonobuoys are powered by salt-water batteries which are activated immediately on immersion, and are thus single use expendable devices. As the buoys are designed for deployment from fixed-wing aircraft, some preparation, including parachute and protective packaging removal, is required before deploying over the side of a ship.

A more important difficulty is the need to determine buoy position at the time of acoustic signal reception very accurately. Jin and Wadhams cite a requirement to measure arrival time to an accuracy of 0.005 sec., which translates to a position accuracy of 70-75m. Ideally, an expendable GPS receiver with buoy-ship telemetry, such as is present in Vaisala radiosondes would be used but this technology was not available for this cruise. The next best approach would be to determine ship position very accurately (DGPS) and double-range the buoy using, e.g., precisely timed acoustic sources (at a much higher frequency than 19.6Hz, to avoid confusion with the primary signal) at the bow and stern, in conjunction with accurate measurement of local water temperature and thus sound speed. Unfortunately, such shipboard sonar sources were not available for this cruise. Thus, the only method left was sighting the buoys (whose visibility was enhanced by attaching party balloons) from the gyro-stabilized sights on the bridge wings. On one occasion, it was possible to move the ship around and get bearings from 3 separate ship positions just after the reception period, thus getting an increased position accuracy (+-50m?).

Precise timing of the reception was also a problem initially, but fortunately P. Cooper of BAS was able to provide a 1Hz pulse (modulated onto a higher frequency) driven by the ship's master

clock. This was fed into the R. channel of a stereo recording system, whereas the sonobuoy hydrophone (mono) signal was fed into the L. channel after being received and demodulated by a ICOM IC-R100 receiver. Initially, a Sony DAT digital recorder was used, but after encountering problems with labelling and recording the sessions we switched to using a SoundblasterLive audio board recording directly onto a 13Gb hard disc in a Windows-95 PC. The wall clock time of session start was noted, and the first recorded R. channel clock pulse rising edge was assumed to be the start of the following second. It should be noted that the wall clock (Radiocode) time does not correspond exactly to the correct GPS time and is about 1.5 seconds out. While we hope to be able to compensate for this using listings of the RVS gps_ash stream sec variable which show what the difference was (sampling rate 2Hz) it would be very desirable for future acoustic work for the ship's Radiocode system to be exactly synchronized to GPS.

A separate VHF antenna had to be set up (sbd. aft rail of Nav. Deck) as we were not permitted to use the ships operational VHF antenna system and a scientific VHF antenna had recently been removed. A long length of low-loss coax had to routed from there to the main lab where our receiving and recording equipment was set up. It may be advisable to have some scientific radio space in a quiet part of the Nav. Deck or near it in the future.

For much of the cruise, the ship was in the acoustic shadow of Svalbard relative to the source. The first attempt was made shortly before 00:00 03AUG, at 75deg48.00'N 008deg29.39'W. An older buoy from SPRI stock was used. It never began transmitting and appeared to sink. From then on, we used only buoys donated by Mikhalevsky's group.

On 07AUG, a listening session was held at 77deg 00.7549N 009deg 00.4150W using a Magnavox AN/SSQ-41B sonobuoy. Subjectively, a low rumble was heard at a plausible time on the monitoring headset, but this cannot be definitive due to the very high level of ambient noise in the main lab and the use of low-grade consumer headphones (it proved not feasible to match the aircraft noise reduction headphones we also brought with us as land based supplies were needed to do the impedance matching). We should avoid sharing lab space with atmospheric chemistry or other noisy activities in the future. The presence of a usable signal will have to be determined by digital signal processing on land, to be performed independently by us and by Mikhalevsky's group.

On this first occasion 2 buoys were used - the first one began transmitting normally but then became silent. As there was time remaining before reception start, we launched a second buoy shortly before midnight. This transmitted normally, was sighted and fixed, and provided a recording of the sounds received. Afterwards, an attempt to listen to the first-launched buoy was successful, and for a long time we received clicks (later determined to be the ship's scientific SIMRAD), biological-sounding noises (irregularly-spaced clicks) and sloshing sounds. The second buoy, which was still in sight, was then recovered by the ship's crew but the hydrophone was

apparently severed before or during the recovery. It was decided not to attempt to recover any more sonobuoys.

An apparently successful session was also held on 11AUG, at 80deg 24.31'N, 005deg 38.55'E, and another on 15AUG at 79deg 18.1431'N 000deg 30.9086'E. This session was the occasion of the accurate position fix by moving the ship and sighting from 3 different DGPS-determined points and also the first use of direct recording to disc via the Soundblaster board.

In all cases, shipboard digital signal processing (MATLAB on both jruf and tr-03, our Win-95 PC) , is apparently not adequate to the task of determining whether a signal did arrive, when , and what the waveform was. Thus we will not know whether these experiments were successful until some time after we return.

A final listening session was held on 27AUG at 66deg 53.488'N, 20deg 49.336'W. A somewhat different sonobuoy, Sparton Electronics AN/SSQ-41B(400) was used. In this case, the cruise schedule did not allow for loitering in the buoy area, so the ship sailed on at ~8kts after the buoy was launched over the side. In any case, sighting the buoy would have been difficult because of darkness and fog. However, a good signal was received from the buoy for the next ~30mins (~5nm range) and some apparently promising waveforms were seen on the computer display.

It should be noted that in all other cases while the ship was not far from the buoy, it was generally using bow thrusters to keep station or heading for higher-priority experiments. Although the Ross seems to be a very quiet ship underway, that is not true when bow thrusters are in use. The ship noise level appeared to be much lower in the last deployment, with the ship steaming away, then it was in the earlier ones with the use of bow thrusters. The ideal situation is, of course, to have the merely drifting about 0.5-1nm away, but that requires dedicated ship time.

We gratefully acknowledge the help of D. Trewitt (Deck Eng.), P. Cooper (BAS electronics), R. Kilroy and J. McCarthy (Bridge), and K. von der Heydt (WHOI) during the course of this work, and to S. Sawhill of SPRI, who suggested attaching balloons to sonobuoys.

5.8 ICECAM

Nick Hughes

The IceCam is a data gathering system designed and built at the Scott Polar Research Institute (University of Cambridge) to provide visual ground truth information for interpreting satellite images. The units are designed for easy deployment on available ships-of-opportunity and consist of a single box which is positioned overlooking the bow of the vessel. The system is built around a Pentium 133 PC motherboard running the Linux operating system. On being powered-up the

unit starts to gather information from its sensors which are linked to the computer through Advantech Adam RS-485 industrial data collection modules. Digital camera images are recorded every 5 minutes and environmental data is logged every minute. The modular design of the system allows additional sensors to be plugged in through an expansion port. In the prototypes the following instrumentation available:

i) Digital camera. This is a small golf-ball shaped unit (3Com/US Robotics BigPicture which looks out of a glass window on the leading face of the IceCam box. This provides a low resolution (320x240), full-colour (24-bit) image. Work is being carried out to develop driver software for more advanced digital cameras with the aim of obtaining full PAL resolution (768x576).

ii) Global Positioning System (GPS). Positional information and cruise track is provided by a Motorola Encore GT GPS board. This communicates with the IceCam's onboard computer through an RS-232 serial port.

iii) Clinometers (_2). The unit contains two Schaevitz Accustar clinometers. These are mounted at right angles to each other to provide pitch and roll measurements of the unit up to ±60 degrees. The aim is to use these for geometric reconstruction of the camera images into ice maps which can be compared directly with satellite images.

iv) Thermistors (_2). These are used to provide external and internal temperature information.

The first prototype unit was the most complete of two systems available and was prepared for deployment during the first week. It was during this stage that minor internal damage was discovered and repaired delaying deployment. The cause of the damage is believed to have been transit to and from an abortive deployment on board *USCGC Polar Star* (WAGB-10) during June/July. This unit was deployed on entering sea ice towards the end of CATS Leg 1 on the "monkey island" (flying bridge) rail overlooking the bow using a metal mounting frame clamped to the superstructure.

On initial power up the unit functioned for 14 hours before the Un-interruptable Power Supply (UPS) monitoring the electricity supply shut down the unit safely but unexpectedly. Attempts to restart the unit failed so it was returned to the laboratory where it started up. An inspection of the files created by the computer revealed that the GPS unit was not functioning and that bugs existed in the code for logging the environmental sensors. Several days were then spent in re-deploying and checking the instrument. On each occasion the unit worked in the laboratory and on deck but not when mounted on the railing. The cause was eventually found to be in the UPS unit which appears to have an undocumented feature in that it shuts down when the battery life is reduced beneath a certain level. In this case the unit had cooled so that battery life was reduced

thereby preventing the unit from restarting. The solution was to remove the UPS and rely on the stability of the ship board power supply.

The unit was returned to its position minus the UPS and worked without downtime throughout the rest of the cruise. On return a number of issues need to be addressed before the next deployment.

i) UPS. The unit needs to have some form of internal temperature control to protect the UPS. Work with the units in the laboratory resulted in excessive heat generation. This was thought to be sufficient to act as protection during a field deployment. The unit now needs to be re-engineered so that cooling and heating can be carried out by the unit in response to temperatures registered by the internal thermistor.

ii) GPS. The GPS board, aerial and cable combination was not tested together before deployment due to lack of time. The logging software has been run using GPS boards of the same type and is bug free. The GPS board is responding correctly to the software so the fault is likely to be that the unit is not seeing satellites due to a cable or aerial problem.

iii) Sensor logging software. Sensor data is being recorded but the status information file contains wrong values. The software requires debugging.

The environmental data will be superimposed as captioning on the image on return to SPRI. Software to do this post-processing during data collection will be written for future deployments.

Data and images from this cruise will be made available at:

http://www.spri.cam.ac.uk/people/neh25/IceCam.html

6. COMPUTING

Mark Stewart

In addition to the equipment described below a wide variety of computing equipment was supplied by the various scientific parties. This included Sun workstations, Macs, PCs running Linux, PCs running NT and PCs running OS/2. Network connections and services such as Email, printing and file store were provided for these systems as required.

NetWare File Server

Compaq Proliant 1200 running NetWare 4.11 with 164 MB RAM, 3 x 9GB disks configured as a RAID 5 disk array and a DLT 4000 tape drive. The main services provided included a GroupWise message store, access to printers, an application/data file store for PCs and a POP server.

PCs

3 Viglen PCs running NT 4 were available for general data processing. User file store, print services and applications were provided by the NetWare file server. Applications installed included Corel Suite, Office 97, Netscape, Minitab 12, Lotus 97, Lan WorkPlace Pro, GroupWise, Exceed (X Terminal emulator) and Dr. Solomon (Virus checker). A PC running Windows 95 was dedicated to running the Dartcom SIAMIV software so that satellite images could be viewed and printed.

Unix File Server

Sun Ultra 60 running Solaris 2.7 with 512 MB RAM, 4 x 9GB disks, 1 x 4GB disk, DLT 4000 tape drive and a DAT DDS2 tape drive. The Ultra 60 provided print services, access to file store and applications. Two 9GB disks were available for scientific data. These disks were backed up to the DLT 4000 drive twice a day. Applications used included TeX, Matlab and Pstar as well as C and FORTRAN compilers.

Printing

Available printers included a HP LaserJet 4M Plus (providing HP PCL and PostScript monochrome printing on A4 media), a HP DeskJet 1600CM/PS (providing HP PCL and PostScript colour printing on A4 media) and a HP DesignJet 650c (providing PostScript colour printing on A0 media).

Electronic Mail

The GroupWise 5.2 message store on the NetWare server was accessed by either POP (Eudora and Netscape) or GroupWise clients. Daily Email transfers between the ship and the Internet were carried out using an Inmarsat B connection to BAS HQ in Cambridge.

Data Logging

Data from a variety of devices were logged using the RVS ABC system. The Level C component was a Sun SPARCstation 10 running SunOS 4.1.4 with 32MB RAM, 2 x 4GB disks, 1 x 2.1 GB disk and a DAT tape drive. Backups were made twice a day using the DAT drive.

Network

The network on the JCR is currently a mixture of UTP, thin Ethernet and thick Ethernet. Connections from cabins and from some of the Labs used thick Ethernet. The majority of clients accessed central computing services via a UTP network based on three 3Com SuperStack II switches.

REFERENCES

AutoFlux group, 1996: AutoFlux - an autonomous system for monitoring air-sea fluxes using the inertial dissipation method and ship mounted instrumentation. Proposal to MAST research area C - Marine Technology, 38 pp. + appendices

Brassell, S. C., G. Eglinton, I. T. Marlowe, U. Pflauman and M. Sarnthein, 1986: Molecular stratigraphy: a new tool for climatic assessment. *Nature* **320**, 129-133.

Carter, D. J. T, 1980: Echo-sounding correction tables (formerly Matthews' tables); 3rd edition. Ministry of Defence Hydrographic Dept., Taunton, U. K., 150 pp.

Cavalieri, D. J., P. Gloersen and W. J. Campbell, 1984: Determination of sea ice parameters with the NIMBUS-7 SMMR. *J. Geophys. Res.* **84** 5355-5369.

Culberson, C. H. and S. Huang, 1987: Automated amperoteric oxygen titration. *Deep-Sea Res.* **34** 875-880.

Culberson, C. H., 1991: WOCE Operations Manual (WHP Operations and Methods). WHPO Report 91/1, Woods Hole, 15 pp.

El Naggar, S., C. Garrity and R. O. Ramseier, 1998: The modelling of sea ice melt-water ponds for the High Arctic using an airborne line scan camera, and applied to the Satellite Special Microwave / Imager (SSM/I). *Int. J. Remote Sensing* **19** 2373-2394.

Holliday, N. P., 1999: CTD data quality on RRS *Discovery* Cruise 242, September–October 1999. Southampton Oceanography Centre Internal Document No. 62, 28 pp.

Jin, G. and P. Wadhams, 1989: Travel time changes in a tomography array caused by a sea ice cover. *Prog. Oceanogr.* **22** 249-275.

Law, C. S., A. J. Watson and M. I. Liddicoat, 1994: Automated vacuum analysis of sulfur hexafluoride in seawater: derivation of the atmospheric trend (1970-1993) and potential as a transient tracer. *Marine Chemistry*, **48** 57-69.

Ledwell, J. R., D. C. E. Bakker, K. I. C. Oliver and A. J. Watson, 1998: Sulfur Hexafluoride Sampling and Analysis. Cruise report FS Polarstern, Cruise ARKTIS XIV/2.

Meteorological Office, 1996: Ships' code and decode book. The UK Met Office publication Met.O.509. The Stationary Office, London.

Mikhalevsky, P. N., A. N. Gavrilov and A. B. Baggeroer, 1999: The Transarctic Acoustic Propagation Experiment and Climate Monitoring in the Arctic. Preprint to IEEE Journal of Oceanic Engineering.

Pascal, R. W., M. J. Yelland and C. H. Clayson, 2000: The AutoFlux logging system – draft handbook. Southampton Oceanography Centre, Southampton, U. K., 68pp. (available at http://www.soc.soton.ac.uk/JRD/MET/AUTOFLUX/DOCS/handbook.pdf)

Resummon, M.H., 1998: Ultrasonic transmission properties of sea ice, PhD thesis, Univ. of Cambridge

Saunders, P. M., 1990: The International Temperature Scale of 1990, ITS-90. *International WOCE Newsletter*, No. 10, p. 10.

UNESCO, 1981: Background papers and supporting data on the Practical Salinity Scale 1978. UNESCO Tech. Papers in Marine Science No. 37, UNESCO, Paris, 144 pp.

Yelland, M. J., B. I. Moat, P. K. Taylor, R. W. Pascal, J. Hutchings and V. C. Cornell, 1998: Wind stress measurements from the open ocean corrected for air flow distortion by the ship. J. Phys. Oceanogr., 28(7), 1511-1526.

Yelland, M. J. and R. W. Pascal, 2000: RRS James Clark Ross, U. K. to Falklands Passage, AutoFlux Trials Cruise, 11 September – 17 October 2000. Southampton Oceanography Centre, Cruise Report, No. 32, 36 pp.

Table 2.1: Station summary. Columns show: station number (stn nbr); date as year-month-day (YYMMDD) and time as hour-minute-second (HHMMSS); latitude and longitude derived from differential GPS (for the bottom of the CTD cast, where appropriate); corrected water depth from Simrad echo sounder (depth); height off bottom at bottom of CTD cast as measured by altimeter (alt); maximum pressure measured by CTD during cast (pmax); number of Niskin bottles fired (N btl); and whether various tracers were sampled on the cast. Note that during the Meteorological phase, not all stations had CTD casts. The "=" sign in the comments field indicates a repeat station, followed by the number of the station repeated.

stn nbr	Date YYMMDD	Time HHMMSS	lat	lon	depth m	alt m	pmax dbar	N btl	O2	SF6	O18	Ba	I 129	Comments
1	990726	003838	63 59.690 N	004 0.600 E	1616	8	1633	24						Test 1
2	990726	034350	63 59.988 N	003 59.946 E	1620	8	1637	24		*				Test 2
3	990726	195742	64 44.802 N	010 6.942 E	346	10	341	10	*					Leg 1 start
4	990726	232438	65 2.160 N	009 50.496 E	358	7	355	10		*	*			
5	990727	023344	65 19.980 N	009 32.502 E	294	8	289	10	*					
6	990727	054815	65 39.054 N	009 13.878 E	446	9	443	13		*	*			
7	990727	092549	65 58.026 N	008 54.582 E	298	9	295	10	*	*				
8	990727	130820	66 16.998 N	008 34.578 E	330	9	325	11						
9	990727	164351	66 34.968 N	008 15.282 E	317	9	313	10	*	*	*			
10	990727	192328	66 48.030 N	008 1.170 E	449	9	447	13		*				
11	990727	220142	67 3.198 N	007 44.472 E	1015	6	1025	12	*	*	*			
12	990728	004143	67 15.000 N	007 30.738 E	1457	7	1471	14		*				
13	990728	034142	67 30.996 N	007 12.156 E	1374	9	1387	14	*		*			
14	990728	065326	67 47.028 N	006 53.376 E	1275	9	1283	18		*				
15	990728	101051	68 4.080 N	006 32.682 E	1506	9	1517	16	*	*	*			
16	990728	130030	68 12.000 N	006 22.656 E	1947	7	1975	18						
17	990728	171650	68 32.004 N	005 57.690 E	2482	9	2517	20	*	*	*			
18	990728	210637	68 40.140 N	005 47.832 E	3007	3	3059	22		*				
19	990729	014331	68 58.506 N	005 22.692 E	3196	6	3251	20	*	*	*			
20	990729	063345	69 16.302 N	004 58.620 E	3220	9	3273	22		*				
21	990729	112106	69 34.602 N	004 33.102 E	3226	9	3277	24	*	*	*			
22	990729	171939	69 52.176 N	004 7.758 E	3223	9	3277	24		*				
23	990729	215104	70 9.930 N	003 41.412 E	3221	8	3275	23	*	*	*	*	*	
24	990730	022840	70 28.308 N	003 13.362 E	3220	8	3275	23		*				
25	990730	070514	70 46.506 N	002 44.658 E	3168	8	3221	23	*	*	*			
26	990730	113343	71 2.364 N	002 18.654 E	3140	8	3189	24		*				

CONTENTS

27	990730 155545	71 21.294 N	001 47.016 E	2263	19	2307	20	*	*	*			
28	990730 200444	71 38.928 N	001 16.926 E	2348	10	2403	24		*				
29	990731 000811	71 56.490 N	000 44.832 E	2421	9	2443	24	*	*	*			
30	990731 041309	72 14.232 N	000 11.850 E	2272	42	2277	24		*				
31	990731 081642	72 31.734 N	000 21.402 W	2308	22	2493	24	*	*	*			
32	990731 124137	72 48.996 N	000 55.938 W	3150	10	3199	24		*				
33	990731 170339	73 5.430 N	001 30.264 W	3122	9	3173	24	*	*	*			
34	990731 212243	73 22.836 N	002 6.876 W	2839	11	3073	23		*				
35	990801 013251	73 39.990 N	002 46.128 W	2911	9	2959	21	*	*	*			
36	990801 051052	73 47.796 N	003 2.982 W	2967	9	3025	22		*				
37	990801 103325	74 6.522 N	003 47.244 W	3536	9	3599	24	*	*	*	*	*	
38	990801 151759	74 22.314 N	004 26.544 W	3532	9	3593	24		*				
39	990801 200132	74 38.952 N	005 10.278 W	3513	9	3573	24	*	*	*			
40	990802 004351	74 55.362 N	005 53.838 W	3485	8	3547	24		*				
41	990802 052016	75 11.316 N	006 38.658 W	3447	8	3509	24	*	*				
42	990802 112302	75 36.954 N	007 54.498 W	2981	9	3031	24	*	*	*			
43	990802 151327	75 26.628 N	007 23.484 W	3316	10	3367	24	*	*	*			
44	990802 195959	75 40.692 N	008 8.166 W	2473	9	2519	24	*	*	*	*	*	
45	990802 232918	75 45.648 N	008 22.980 W	2009	9	2033	24		*	*	*		
46	990803 055430	75 54.330 N	008 49.512 W	1478	10	1493	18	*	*	*	*	*	
47	990803 091153	76 1.380 N	009 12.120 W	932	9	941	19	*	*	*			
48	990803 112913	76 5.754 N	009 27.174 W	462	9	463	12	*	*	*			
49	990803 135748	76 15.474 N	009 59.850 W	278	10	273	9		*	*			
50	990803 182641	76 32.682 N	011 0.054 W	311	9	305	9	*	*	*			
51	990803 235248	76 41.574 N	011 52.620 W	314	9	309	9	*	*	*			
52	990804 075227	76 48.660 N	012 0.036 W	325	9	319	10	*	*	*			
53	990804 122644	77 3.906 N	013 0.048 W	251	9	247	8	*	*	*			
54	990804 205912	77 17.922 N	013 58.452 W	260	9	253	8	*	*	*			Leg 1 end
55	990805 192500	77 20.0 N	012 18.7 W										Met phase start
56	990807 004609	76 58.590 N	008 58.374 W	357	8	349	12	*	*	*			
57	990807 163553	77 4.050 N	006 12.432 W	291	8	295	11	*	*	*			
58	990809 131334	80 27.408 N	008 18.186 E	908	10	907	24	*	*	*			
59	990809 190000	80 24.9 N	007 01.0 E										
60	990810 093829	80 22.986 N	005 59.094 E	566	9	567	16	*	*	*			
61	990810 154500	80 24.2 N	005 46.9 E										
62	990811 012938	80 25.152 N	005 42.834 E	572	8	573	16	*	*				
63	990811 041800	80 24.7 N	005 43.6 E										

64	990811 102500	80 24.65 N	005 38.18 E											
65	990811 180000	80 28.2 N	005 27.1 E											
66	990812 005617	80 9.900 N	003 23.544 E	1634	10	1657	24	*	*	*				
67	990812 115800	80 05.39 N	002 22.2 E											
68	990812 182800	80 05.1 N	001 56.2 E											
69	990813 042300	80 03.8 N	001 15.3 E											
70	990813 111400	79 59.87 N	001 02.62 E											
71	990813 191838	79 56.838 N	001 1.200 E	2759	10	2809	24	*	*	*				
72	990814 010000	79 55.3 N	000 59.3 E											
73	990814 071800	79 05.1 N	001 01.0 E											
74	990814 144000	79 52.5 N	000 54.2 E											Met phase end
75	990815 053607	78 59.868 N	001 26.010 W	2583	9	2621	24		*					Leg 2 start
76	990815 104420	78 57.060 N	000 51.774 E	2511	9	2547	23	*	*	*	*	*		
77	990815 144102	78 51.216 N	002 9.984 E	2493	9	2527	24		*	*				
78	990815 181725	78 50.082 N	003 25.566 E	2315	10	2345	24	*	*	*	*	*		
79	990815 213413	78 49.914 N	004 30.228 E	2392	9	2427	24		*	*				
80	990816 005941	78 50.010 N	005 41.802 E	2513	8	2551	24	*	*	*	*	*		
81	990816 042605	78 50.052 N	006 41.922 E	1710	9	1731	24		*	*				
82	990816 070614	78 50.040 N	007 29.586 E	1144	10	1153	21	*	*	*	*	*		
83	990816 093301	78 50.196 N	008 9.438 E	922	10	927	18		*	*				
84	990816 114355	78 50.088 N	009 0.888 E	214	7	207	8	*	*	*				Leg 2 end
85	990816 201538	78 12.096 N	010 33.186 E	264	8	257	8	*	*	*				Leg 3 start
86	990816 214215	78 6.594 N	010 5.040 E	210	8	203	7		*	*				
87	990817 003853	77 55.980 N	009 11.400 E	1072	9	1079	19	*	*	*				
88	990817 032711	77 47.358 N	008 29.700 E	1879	8	1905	24		*	*				
89	990817 064436	77 38.394 N	007 48.954 E	2893	10	2991	24	*	*	*		*		
90	990817 102443	77 32.490 N	007 22.668 E	3324	9	3387	24		*	*		*		
91	990817 134442	77 28.188 N	007 3.786 E	2696	24	2739	24	*	*	*				
92	990817 164700	77 23.556 N	006 41.394 E	2356	8	2393	24		*	*				
93	990817 205731	77 8.094 N	005 38.490 E	2530	8	2565	24	*	*	*				
94	990818 011608	76 51.498 N	004 32.556 E	2925	8	2973	24		*	*				
95	990818 053626	76 34.602 N	003 29.322 E	2732	10	2779	22	*	*	*				
96	990818 101759	76 17.010 N	002 27.774 E	3123	9	3171	24		*	*	*	*		
97	990818 170604	75 59.304 N	001 27.486 E	3240	9	3293	24	*	*	*				
98	990818 213247	75 40.104 N	000 26.418 E	1838	5	1863	24		*	*				
99	990819 014616	75 23.106 N	000 24.930 W	3700	8	3765	24	*	*	*				
100	990819 064315	75 5.100 N	001 16.740 W	3676	9	3739	24		*	*	*	*		

101	990819 115422	74 45.708 N	002 9.864 W	3626	9	3687	24	*	*	*	*	*	
102	990819 170306	74 25.902 N	003 1.398 W	3576	10	3635	24		*	*			
103	990819 220138	74 6.750 N	003 48.930 W	3562	8	3633	24	*	*				=37
104	990820 031004	73 46.308 N	004 37.290 W	3194	9	3431	24		*	*			
105	990820 081031	73 25.092 N	005 25.278 W	2924	9	2971	24	*	*	*			
106	990820 125541	73 3.990 N	006 10.752 W	2599	9	2639	24		*	*		*	
107	990820 172720	72 42.798 N	006 54.318 W	2543	10	2581	24	*	*	*			
108	990820 215052	72 21.492 N	007 36.150 W	2568	7	2611	24		*	*			
109	990821 021153	72 0.390 N	008 15.834 W	2487	7	2527	24	*	*	*			
110	990821 062205	71 36.792 N	008 58.368 W	1012	10	1073	18		*	*			
111	990821 091745	71 25.692 N	009 17.724 W	2296	9	2327	24	*	*	*	*	*	
112	990821 132743	71 14.598 N	009 36.690 W	459	8	469	13		*				
113	990821 171320	70 51.198 N	010 15.372 W	1253	10	1263	24	*	*	*			
114	990821 211016	70 28.800 N	010 50.850 W	1578	11	1593	24		*				
115	990822 010509	70 6.798 N	011 24.390 W	1839	8	1861	24	*	*	*			
116	990822 051048	69 43.698 N	011 58.260 W	1727	9	1745	24		*				
117	990822 092615	69 20.100 N	012 31.548 W	1762	9	1781	24	*	*	*			
118	990822 133428	68 57.000 N	013 2.898 W	1842	10	1861	24		*				
119	990822 173614	68 35.106 N	013 31.656 W	1804	9	1823	24	*	*	*	*	*	
120	990822 213021	68 12.606 N	014 0.156 W	1488	8	1509	24		*				
121	990823 011644	67 49.602 N	014 28.194 W	1141	6	1159	23	*	*	*			LADCP down only
122	990823 044758	67 25.896 N	014 56.346 W	856	15	869	19		*				LADCP down only
123	990823 072445	67 8.808 N	015 15.936 W	196	10	185	7	*	*	*			
124	990823 104929	66 46.296 N	015 41.118 W	238	10	235	9	*	*	*			Leg 3 end
125	990823 223712	66 20.010 N	020 13.074 W	119	8	109	4	*					Leg 4 start
126	990824 001010	66 27.420 N	020 21.024 W	179	9	169	5		*	*		*	
127	990824 013346	66 34.800 N	020 29.130 W	291	9	293	7	*					
128	990824 025249	66 42.216 N	020 37.272 W	350	36	353	7		*	*	*	*	No LADCP
129	990824 041329	66 49.608 N	020 45.432 W	287	9	287	7	*					
130	990824 053658	66 57.090 N	020 53.490 W	181	9	173	5		*	*		*	
131	990824 070719	67 4.530 N	021 1.572 W	208	8	207	5	*					
132	990824 083256	67 11.976 N	021 10.086 W	277	10	277	7		*	*	*	*	
133	990824 095907	67 19.236 N	021 18.450 W	309	12	309	7	*					
134	990824 113554	67 26.718 N	021 27.408 W	529	9	533	8		*	*		*	
135	990824 131050	67 34.116 N	021 35.976 W	645	10	649	8	*					
136	990824 144052	67 41.406 N	021 44.850 W	675	9	679	8		*	*	*	*	
137	990824 161424	67 48.600 N	021 53.208 W	736	10	741	9	*	*				No LADCP

138	990824 182128	67 55.896 N	022 2.094 W	791	9	795	9		*	*	*	*	
139	990824 200754	68 3.096 N	022 10.824 W	870	9	875	9	*	*				
140	990824 220038	68 10.398 N	022 19.878 W	1167	9	1175	10		*	*	*	*	
141	990825 001820	68 17.592 N	022 28.848 W	1276	8	1287	11	*	*				
142	990825 023155	68 24.780 N	022 37.908 W	1385	8	1399	12		*	*	*	*	
143	990825 045403	68 31.992 N	022 47.130 W	1463	9	1477	12	*	*				
144	990825 071821	68 39.192 N	022 56.400 W	1498	9	1513	13		*	*		*	
145	990825 094809	68 46.296 N	023 5.670 W	1390	9	1401	12	*	*				
146	990825 120415	68 53.394 N	023 15.048 W	836	10	843	9		*	*	*	*	
147	990825 133853	69 0.552 N	023 24.492 W	390	9	391	7	*	*				
148	990825 145852	69 7.650 N	023 34.068 W	266	10	263	6		*	*		*	
149	990825 170758	69 14.814 N	023 43.878 W	201	11	187	5	*	*				
150	990825 183029	69 21.906 N	023 53.634 W	157	10	147	4		*				Leg 4 end
151	990825 202318	69 21.894 N	023 53.640 W	156	10	145	4		*				Tail start =150
152	990825 225050	69 7.692 N	023 34.194 W	270	9	269	6	*					=148
153	990826 014646	68 53.196 N	023 15.054 W	838	10	845	13		*	*			=146
154	990826 043954	68 39.102 N	022 56.640 W	1498	9	1513	19	*	*	*	*	*	=144
155	990826 080808	68 24.828 N	022 37.878 W	1386	9	1399	18		*	*	*	*	=142
156	990826 110602	68 10.386 N	022 19.854 W	1168	9	1177	16	*	*	*	*	*	=140
157	990826 134112	67 55.890 N	022 2.040 W	791	10	795	13		*	*		*	=138
158	990826 152509	67 48.600 N	021 53.292 W	736	8	743	11	*	*	*			=137
159	990826 170301	67 41.400 N	021 44.568 W	675	10	679	11		*	*			=136
160	990826 192541	67 26.688 N	021 27.354 W	529	10	531	10	*	*	*			=134
161	990826 220200	67 11.874 N	021 10.158 W	276	10	275	7		*	*			=132
162	990827 010331	66 49.656 N	020 45.258 W	288	9	289	7	*	*	*			=129
163	990827 021805	66 42.186 N	020 37.074 W	352	25	351	8		*	*			=128
164	990827 034501	66 34.782 N	020 29.100 W	292	19	291	7	*	*	*			=127
165	990827 062323	66 20.016 N	020 13.212 W	117	10	107	4		*	*			Tail end =125

Table 2.2: Conductivity calibration statistics for each station (stn). A, B, C are constant, pressure coefficient and temperature coefficient respectively; O is mean offset (see text for description), N is number of samples included in each station fit and sd is standard deviation of fit (note units – values are normal units × 1000); Pbar and Tbar are mean pressure and temperature of fitted samples for each station.

stn	A mmho/ cm	B mmho/ cm dbar	C mmho/ cm °C	O mmho/ cm	N	sd µmho/ cm	Pbar dbar	Tbar °C
2	-1.6578	-3.39E-05	-5.37E-02	-1.7953	24	1.53	746.4	2.09
3	-1.8301	-2.10E-04	-2.44E-02	-2.0842	8	6.12	160.8	9.01
4	-1.7626	-2.41E-05	-3.97E-02	-2.1233	7	2.50	179.2	8.97
5	-1.6965	-9.04E-05	-4.66E-02	-2.1126	9	2.61	125.7	8.68
6	-1.7624	-2.52E-05	-3.87E-02	-2.0546	10	8.61	233.0	7.40
7	-1.6778	-1.12E-04	-4.76E-02	-2.1017	9	8.59	124.3	8.61
8	-1.6790	-1.01E-04	-4.77E-02	-2.0981	10	8.06	146.6	8.48
9	-1.6882	-7.83E-05	-4.78E-02	-2.1208	7	6.75	143.2	8.82
10	-1.6571	-3.83E-05	-5.25E-02	-2.0894	11	2.42	175.8	8.11
11	-1.6876	6.13E-06	-4.92E-02	-1.9635	9	0.96	366.8	5.65
12	-1.6574	-2.88E-05	-5.29E-02	-1.8373	10	10.71	623.9	3.06
13	-1.6527	-3.40E-05	-5.41E-02	-1.9640	12	1.63	385.2	5.51
14	-1.6486	-4.09E-05	-5.44E-02	-1.8502	17	1.21	550.5	3.29
15	-1.6499	-3.77E-05	-5.41E-02	-1.8670	15	1.30	535.9	3.64
16	-1.6544	-3.10E-05	-5.34E-02	-1.8375	18	0.88	787.0	2.97
17	-1.6587	-2.66E-05	-5.24E-02	-1.8268	19	2.31	1026.4	2.69
18	-1.6587	-2.64E-05	-5.27E-02	-1.8259	22	1.07	1163.4	2.59
19	-1.6596	-2.54E-05	-5.22E-02	-1.7848	19	2.64	1394.3	1.72
20	-1.6604	-2.55E-05	-5.21E-02	-1.7804	21	1.90	1404.6	1.62
21	-1.6600	-2.57E-05	-5.25E-02	-1.7623	23	1.09	1446.4	1.24
22	-1.6585	-2.59E-05	-5.25E-02	-1.7705	23	0.60	1352.3	1.47
23	-1.6588	-2.55E-05	-5.25E-02	-1.7379	21	0.64	1479.8	0.79
24	-1.6590	-2.54E-05	-5.25E-02	-1.7793	21	1.73	1377.6	1.63
25	-1.6588	-2.59E-05	-5.26E-02	-1.7681	22	0.73	1264.5	1.45
26	-1.6596	-2.54E-05	-5.23E-02	-1.7650	23	1.39	1450.2	1.31
27	-1.6565	-2.78E-05	-5.29E-02	-1.7701	19	0.97	1063.2	1.59
28	-1.6571	-2.77E-05	-5.26E-02	-1.7380	24	1.07	1093.1	0.96
29	-1.6592	-2.53E-05	-4.94E-02	-1.6891	24	5.08	1046.5	0.07
30	-1.6583	-2.61E-05	-4.98E-02	-1.6869	24	2.88	931.8	0.09
31	-1.6588	-2.52E-05	-4.93E-02	-1.7034	22	3.61	1015.4	0.38
32	-1.6557	-2.54E-05	-4.77E-02	-1.6842	22	3.67	1456.5	-0.18
33	-1.6565	-2.51E-05	-4.75E-02	-1.6702	24	0.95	1310.9	-0.40
34	-1.6478	-2.44E-05	-3.42E-02	-1.6561	18	1.69	1219.7	-0.62
35	-1.6542	-2.53E-05	-4.42E-02	-1.6512	19	0.87	1215.2	-0.76
36	-1.6574	-2.44E-05	-4.56E-02	-1.6565	20	1.06	1234.8	-0.68
37	-1.6562	-2.47E-05	-4.61E-02	-1.6689	23	0.99	1553.1	-0.56
38	-1.6610	-2.45E-05	-5.09E-02	-1.6712	23	0.76	2193.5	-0.85
39	-1.6593	-2.43E-05	-4.87E-02	-1.6829	22	1.13	2004.1	-0.52
40	-1.6503	-2.59E-05	-4.29E-02	-1.6646	22	3.05	1908.1	-0.82
41	-1.6539	-2.43E-05	-5.00E-02	-1.6715	23	0.89	1975.5	-0.61
42	-1.6616	-2.52E-05	-5.31E-02	-1.6728	20	0.97	1396.9	-0.45
43	-1.6609	-2.44E-05	-4.99E-02	-1.6778	21	1.57	1891.4	-0.59

44	-1.6617	-2.40E-05	-4.83E-02	-1.6838	22	1.52	1207.9	-0.14
45	-1.6590	-2.73E-05	-5.08E-02	-1.6811	20	1.78	1107.6	-0.16
46	-1.6570	-2.98E-05	-5.27E-02	-1.6980	14	0.89	867.3	0.29
47	-1.6386	-5.04E-05	-5.97E-02	-1.6914	16	1.18	499.0	0.46
48	-1.6301	-8.35E-05	-5.71E-02	-1.6517	10	1.79	210.8	0.07
49	-1.5941	-3.37E-04	-3.96E-02	-1.6549	8	2.68	136.6	0.37
50	-1.6141	-1.80E-04	-5.02E-02	-1.6398	5	2.57	185.2	-0.15
51	-1.4643	-7.84E-04	-1.22E-02	-1.5978	6	9.24	177.1	-0.44
52	-1.4249	-9.06E-04	-3.94E-04	-1.5645	5	12.71	154.2	-0.39
53	-1.0188	-3.27E-03	1.25E-01	-1.5772	5	14.55	153.4	-0.46
54	-1.5637	-4.25E-04	-8.66E-02	-1.5311	6	17.96	134.0	-1.03
56	-1.5606	-3.91E-04	-3.94E-02	-1.6091	9	12.45	171.2	-0.47
57	-1.5509	-6.23E-04	-2.89E-02	-1.6360	10	6.13	119.0	0.38
58	-1.6454	-4.72E-05	-5.50E-02	-1.7472	20	3.57	444.9	1.47
60	-1.5650	-1.69E-04	-7.09E-02	-1.8298	13	12.44	284.6	3.05
62	-1.6645	-2.35E-05	-5.07E-02	-1.8269	12	1.45	286.8	3.07
66	-1.6596	-2.84E-05	-5.15E-02	-1.6969	19	1.21	908.5	0.22
71	-1.6627	-2.64E-05	-5.26E-02	-1.7010	21	1.45	1383.9	0.03
75	-1.6644	-2.45E-05	-4.91E-02	-1.6983	12	1.53	1115.4	0.13
76	-1.6639	-2.55E-05	-5.06E-02	-1.7222	21	2.06	1186.2	0.55
77	-1.6618	-2.66E-05	-5.14E-02	-1.6978	19	0.96	1212.2	0.07
78	-1.6619	-2.79E-05	-5.28E-02	-1.6991	19	0.68	1132.3	0.11
79	-1.6603	-2.84E-05	-5.15E-02	-1.7064	21	2.86	1128.5	0.27
80	-1.6628	-2.60E-05	-5.06E-02	-1.6948	20	1.89	1228.8	0.00
81	-1.6625	-2.65E-05	-5.14E-02	-1.7288	24	1.96	793.8	0.88
82	-1.6554	-3.42E-05	-5.33E-02	-1.7693	20	1.75	581.9	1.77
83	-1.6642	-2.38E-05	-5.17E-02	-1.8068	17	1.62	478.3	2.54
84	-1.6208	-1.54E-04	-5.68E-02	-1.9306	7	4.31	91.1	5.21
85	-1.6007	-1.83E-04	-6.03E-02	-1.8742	6	2.42	129.6	4.14
86	-1.4204	-6.23E-04	-8.91E-02	-1.9460	5	9.82	114.2	5.10
87	-1.6643	-2.59E-05	-5.13E-02	-1.7761	17	2.27	548.2	1.90
88	-1.6629	-2.71E-05	-5.19E-02	-1.7344	24	1.88	906.5	0.90
89	-1.6638	-2.51E-05	-5.05E-02	-1.6887	21	1.44	1542.4	-0.27
90	-1.6756	-2.22E-05	-5.10E-02	-1.7559	21	2.01	990.7	1.14
91	-1.6657	-2.48E-05	-5.12E-02	-1.7303	23	1.14	1246.8	0.66
91	-1.6664	-2.44E-05	-5.11E-02	-1.7240	23	1.99	1266.7	0.52
92	-1.6637	-2.67E-05	-5.18E-02	-1.7244	24	1.11	1039.9	0.64
93	-1.6621	-2.71E-05	-5.15E-02	-1.7098	20	1.27	1065.9	0.37
94	-1.6630	-2.44E-05	-4.89E-02	-1.6877	23	2.11	1313.6	-0.15
95	-1.6632	-2.51E-05	-4.93E-02	-1.6997	21	2.58	1123.5	0.17
96	-1.6636	-2.50E-05	-5.02E-02	-1.6952	24	1.09	1377.3	-0.06
97	-1.6617	-2.62E-05	-5.17E-02	-1.6798	24	1.76	1374.6	-0.35
98	-1.6611	-2.54E-05	-4.82E-02	-1.6693	24	3.58	806.2	-0.25
99	-1.6604	-2.47E-05	-4.74E-02	-1.6745	24	0.87	1641.0	-0.56
100	-1.6766	-2.55E-05	-6.69E-02	-1.6600	22	0.82	1696.4	-0.89
101	-1.6613	-2.45E-05	-4.74E-02	-1.6689	24	0.54	1726.2	-0.73
102	-1.6598	-2.46E-05	-4.71E-02	-1.6623	22	0.89	1528.9	-0.75
103	-1.6600	-2.49E-05	-4.68E-02	-1.6751	24	1.60	1662.4	-0.56
104	-1.6605	-2.54E-05	-4.93E-02	-1.6638	23	0.78	1670.8	-0.79
105	-1.6615	-2.53E-05	-4.95E-02	-1.6622	22	0.88	1355.4	-0.68
106	-1.6597	-2.57E-05	-4.72E-02	-1.6748	24	0.92	1103.9	-0.28
107	-1.6605	-2.54E-05	-4.83E-02	-1.6598	22	0.46	1211.5	-0.65
108	-1.6603	-2.50E-05	-4.65E-02	-1.6728	24	0.68	1182.9	-0.37

109	-1.6620	-2.35E-05	-4.61E-02	-1.6758	24	0.86	1001.3	-0.21
110	-1.6605	-2.54E-05	-4.66E-02	-1.6784	15	0.67	550.8	0.08
111	-1.6609	-2.49E-05	-4.66E-02	-1.6648	21	0.44	1117.8	-0.51
112	-1.6574	-3.37E-05	-4.95E-02	-1.7238	10	1.35	226.6	1.19
113	-1.6591	-2.83E-05	-4.89E-02	-1.6917	23	2.32	606.4	0.32
114	-1.6595	-2.79E-05	-4.98E-02	-1.6817	23	1.36	758.7	0.02
115	-1.6585	-2.93E-05	-5.04E-02	-1.6918	24	1.71	793.4	0.20
116	-1.6589	-2.90E-05	-5.01E-02	-1.6741	23	0.84	822.6	-0.17
117	-1.6589	-2.90E-05	-4.98E-02	-1.6734	23	2.62	830.2	-0.19
118	-1.6578	-3.06E-05	-4.97E-02	-1.6715	23	1.95	854.9	-0.25
119	-1.6588	-2.85E-05	-4.96E-02	-1.6757	23	1.12	848.0	-0.14
120	-1.6587	-2.95E-05	-4.96E-02	-1.6840	24	1.18	597.0	0.15
121	-1.6574	-3.17E-05	-4.93E-02	-1.6927	22	1.77	488.0	0.40
122	-1.6541	-3.69E-05	-5.06E-02	-1.7117	18	2.52	452.5	0.81
123	-1.8123	2.40E-04	-2.78E-02	-1.9409	5	1.21	105.1	5.54
124	-1.7391	2.16E-05	-3.75E-02	-1.9410	7	0.57	142.5	5.47
125	-0.6680	-1.47E-03	-1.72E-01	-1.9818	4	3.63	68.5	7.03
126	-1.6339	-6.85E-05	-5.49E-02	-2.0221	4	0.52	96.3	6.95
127	-1.4537	-5.32E-04	-7.48E-02	-1.8787	7	2.14	154.3	4.58
128	-1.5792	-2.29E-04	-6.20E-02	-1.8793	6	1.22	197.4	4.11
129	-1.5009	-5.31E-04	-6.83E-02	-1.8444	7	3.36	154.2	3.83
130	-1.5015	-4.17E-04	-6.94E-02	-1.9463	5	0.80	100.0	5.81
131	-1.3629	-5.68E-04	-8.89E-02	-1.9666	5	1.83	106.5	6.11
132	-1.4913	-5.97E-04	-7.07E-02	-1.8198	7	2.79	153.0	3.35
133	-1.4890	-6.15E-04	-7.13E-02	-1.8344	7	2.69	157.1	3.49
134	-1.6619	-2.32E-05	-4.81E-02	-1.7776	7	1.75	247.8	2.29
135	-1.6569	-3.43E-05	-5.12E-02	-1.7244	7	1.41	285.3	1.13
136	-1.6548	-3.27E-05	-4.59E-02	-1.7322	7	3.11	218.5	1.53
137	-1.6756	6.37E-06	-3.59E-02	-1.7129	9	10.19	312.7	1.09
138	-1.6506	-4.48E-05	-5.86E-02	-1.6617	8	0.75	357.4	-0.08
139	-1.6564	-3.24E-05	-4.71E-02	-1.6709	8	0.77	367.6	0.05
140	-1.6353	-4.90E-05	-3.63E-02	-1.6591	8	1.42	438.9	0.06
141	-1.6506	-4.49E-05	-6.84E-02	-1.6529	10	1.94	540.3	-0.32
142	-1.6483	-4.73E-05	-6.92E-02	-1.6584	9	1.69	624.5	-0.28
143	-1.6435	-4.67E-05	-6.19E-02	-1.6666	10	2.25	682.0	-0.14
144	-1.6528	-3.58E-05	-5.63E-02	-1.6609	11	0.70	757.1	-0.34
145	-1.6520	-4.23E-05	-6.44E-02	-1.6655	10	0.43	678.5	-0.24
146	-1.6061	-1.23E-04	-3.90E-02	-1.6597	9	2.99	324.9	0.35
147	-1.5283	-4.16E-04	-2.12E-02	-1.5940	7	4.15	177.1	-0.38
148	-1.5045	-6.15E-04	-3.04E-02	-1.5759	6	9.16	132.5	-0.33
149	-1.5633	-6.96E-04	-8.51E-02	-1.5593	4	0.86	125.9	-1.08
150	-1.4130	-1.81E-03	-7.00E-02	-1.5036	4	29.44	79.8	-0.77
151	-1.4848	-1.87E-03	-1.20E-01	-1.5460	4	2.26	80.8	-0.75
152	-1.5257	-5.23E-04	-6.05E-02	-1.5565	5	10.92	159.6	-0.87
153	-1.6493	-4.38E-05	-5.69E-02	-1.6943	11	2.28	427.5	0.46
154	-1.4299	-4.85E-05	-6.67E-02	-1.4420	18	1.09	716.2	-0.34
155	-1.6479	-5.13E-05	-7.28E-02	-1.6639	16	1.57	758.7	-0.32
156	-1.6393	-4.59E-05	-3.86E-02	-1.6617	16	1.63	599.7	-0.13
157	-1.6544	-2.95E-05	-3.33E-02	-1.6734	13	0.68	414.0	0.20
158	-1.6669	-1.29E-05	-4.26E-02	-1.7182	11	1.75	348.8	1.10
159	-1.6551	-3.60E-05	-4.96E-02	-1.7247	11	7.73	343.1	1.16
160	-1.6988	6.35E-05	-4.10E-02	-1.7529	10	6.34	260.8	1.72
161	-1.5429	-4.35E-04	-6.36E-02	-1.8287	7	2.27	151.8	3.46

162	-1.5170	-4.23E-04	-6.69E-02	-1.8778	7	2.96	153.5	4.42
163	-1.4017	-7.63E-04	-8.60E-02	-1.7906	7	3.69	200.2	2.75
164	-1.5465	-1.87E-04	-6.82E-02	-1.9088	5	1.09	202.4	4.76
165	-1.6683	-3.10E-04	-4.52E-02	-2.0113	4	5.68	61.4	7.17

Table 2.3: Upcast CTD value minus reversing instrument value for pressure and temperature, excluding outliers. n is the number of points in the mean, compared with ntot, the total number of data points.

Instrument (units)	mean	sd	n / ntot
T1545 (°C)	-0.0052	0.0055	125/146
T995 (°C)	-0.0050	0.0083	81/108
P6534 (dbar)	6.45	2.68	132/142
P6394 (dbar)	4.77	2.26	133/144

Table 2.4: SF6 duplicate sample comparison.

Station	1st value fM	2nd value fM	Absolute difference fM	Percentage difference %
20	0.1377	0.1185	0.0192	
20	0.7448	0.7480	0.0031	
22	0.8452	0.8786	0.0333	
23	0.8186	0.8672	0.0486	
24	1.2512	1.2214	0.0298	2.3824
38	0.6009	0.5083	0.0926	
38	0.5232	0.4511	0.0722	
38	0.4620	0.3867	0.0753	
38	0.3887	0.3887	0.0000	
38	0.3303	0.3777	0.0475	
56	1.4991	1.5415	0.0424	2.8257
57	1.8144	1.7964	0.0180	0.9944
58	1.4383	1.4650	0.0267	1.8544
60	1.9074	1.9196	0.0122	0.6375
60	1.9611	1.8866	0.0745	3.8000
60	1.9729	1.9976	0.0247	1.2525
62	1.6403	1.6372	0.0031	0.1913
62	1.5693	1.6207	0.0514	3.2742
66	0.2149	0.1796	0.0353	
66	0.2479	0.2506	0.0027	
66	3.5328	3.5889	0.0561	1.5877
66	4.8891	4.8671	0.0220	0.4493
66	1.6517	1.6619	0.0102	0.6174
66	1.3642	1.3763	0.0122	0.8913
66	1.7180	1.7285	0.0106	0.6164
71	0.1071	0.0628	0.0443	
71	0.4201	0.4279	0.0078	
71	0.9162	0.9374	0.0212	
76	1.5752	1.5662	0.0090	0.5727
77	3.7167	3.6944	0.0224	0.6015
78	7.1385	7.2272	0.0886	1.2418
95	0.1318	0.1334	0.0016	
95	0.1157	0.1345	0.0188	
100	0.4919	0.4871	0.0047	
101	0.5338	0.5330	0.0008	
101	7.6245	7.6261	0.0016	0.0206
102	0.3895	0.3832	0.0063	
102	4.7091	4.6734	0.0357	0.7580
103	0.3420	0.2926	0.0494	
103	18.7308	18.9277	0.1969	1.0512
104	0.4216	0.4107	0.0110	
104	13.5138	13.5283	0.0145	0.1074
105	0.1918	0.2087	0.0169	
105	14.7932	14.5665	0.2267	1.5325
113	0.5730	0.5876	0.0145	
114	0.1404	0.1789	0.0384	
118	0.0702	0.0902	0.0200	
128	2.0058	1.9745	0.0314	1.5643

128	1.6250	1.6266	0.0016	0.0965
130	1.4991	1.5391	0.0400	2.6688
130	1.6858	1.6717	0.0141	0.8376
134	2.4769	2.4793	0.0024	0.0950
136	1.3583	1.3657	0.0075	0.5487
136	1.5446	1.5877	0.0431	2.7933
137	2.4385	2.5609	0.1224	5.0185
137	2.2898	2.3730	0.0832	3.6314
142	0.5354	0.5299	0.0055	
142	1.8211	1.8176	0.0035	0.1938
144	3.5697	3.6077	0.0380	1.0658
145	3.4226	3.4465	0.0239	0.6991
148	1.4179	1.4403	0.0224	1.5768
150	1.6175	1.6085	0.0090	0.5577
153	1.3936	1.4183	0.0247	1.7731
153	1.6375	1.6576	0.0200	1.2216
154	3.2453	3.2335	0.0118	0.3626
155	0.5554	0.5707	0.0153	
155	3.9776	3.9207	0.0569	1.4298
155	3.6952	3.7034	0.0082	0.2229
155	2.7750	2.8213	0.0463	1.6678
156	1.0253	1.0272	0.0020	0.1913
156	2.1722	2.2039	0.0318	1.4626
156	3.0868	3.0378	0.0490	1.5883
156	3.6905	3.6222	0.0682	1.8493
157	2.5703	2.6024	0.0322	1.2513
157	2.6205	2.6185	0.0020	0.0748
157	2.3855	2.3188	0.0667	2.7951
158	2.5169	2.5361	0.0192	0.7636
158	1.8239	1.8054	0.0184	1.0108
158	1.5697	1.5936	0.0239	1.5242
159	2.4875	2.4530	0.0345	1.3876
159	2.3243	2.3549	0.0306	1.3162
160	2.2310	2.2035	0.0275	1.2307
160	1.6995	1.6874	0.0122	0.7154
161	2.0784	2.0823	0.0039	0.1887
161	2.0364	2.0270	0.0094	0.4622
161	1.8439	1.7937	0.0502	2.7228
162	1.9290	1.8917	0.0373	1.9317
162	1.7132	1.7360	0.0227	1.3278
164	1.6658	1.7289	0.0631	3.7909
164	1.6172	1.5838	0.0333	2.0616
		Mean:	0.0327	0.9437

Table 2.5: SF6 standard repeats.

Standard	Analysis number	Mean SF6 area	STDEV area	%STDEV
290 ppt*0.75 ml	11	34479	48	0.14
51 ppt*0.297 ml	10	3590	50	1.4
51 ppt*0.75 ml	10	8390	50	0.54

Table 2.6: Average thiosulphate (thio) normality, and variation seen, for each batch of thiosulphate. The iodate weight, batch number and station from which it was first used is also shown.

Station Numbers	Iodate batch	Thio batch	Iodate weight (g)	Thio normality	
JR44				Mean	± 1 SD
003-013	1 (from 003)	1	0.3590	0.10086919	0.00053743
015-043	2 (from 015)	1	0.3621	0.10086919	0.00053743
044-045	3 (from 044)	2	0.3581	0.10031977	0.00021657
046-071	4 (from 046)	3	0.3560	0.10090893	0.00037522
076-107	5 (from 076)	3	0.3581	0.10090893	0.00037522
109-139	6 (from 109)	4	0.3568	0.10140977	0.00036512
141-164	7 (from 141)	5	0.3575	0.10196306	0.00010351

Table 3.1: VM-ADCP calibration results. Speed in cm/s, direction (dirn) in degrees (earth coordinates).

Section	ADCP		GPS			
	speed	dirn	speed	dirn	A	phi
A	515.40	166.53	515.55	166.71	1.00029	0.18
B	521.67	166.07	521.45	166.20	0.99958	0.13
C	508.04	166.81	508.72	166.95	1.00134	0.14
mean					1.0004	0.15

Table 3.2: Biological filtration sample information, where GMT is Greenwich Mean Time, samp # is sample number and Blk is blank number, Lat is latitude, long is longitude, Vol is the volume of seawater (or Millipore purified water for the blanks) sampled (litres), sal is the sea surface salinity and Fluor is the fluorescence reading.

Date	GMT	Samp #	Lat	Long	Vol	Temp	Sal	Fluor
25/7/99	14.06	1	621156N	031175E	140	13.2	34.73	6.4
26/7/99	08.32	2	641014N	052103E	140	12.8	34.72	9.1
27/7/99	10.43	3	655788N	085445E	140	11.9	34.21	26.2
28/7/99	08.21	4	675301N	064606E	140	11.0	35.12	24.9
28/7/99	13.50	5	681202N	062265E	140	11.0	35.12	25.8
29/7/99	10.19	6	693460N	043310E	140	9.6	35.10	19.5
30/7/99	08.41	7	704659N	021093E	140	9.3	35.06	24.9
30/7/99	13.28	8	710707N	021093E	140	9.2	35.17	21.7
31/7/99	09.40	9	723217N	002041W	130	6.6	34.92	5.1
31/7/99	15.31	10	730327N	012589W	140	5.5	34.72	4.0
1/8/99	12.14	11	740699N	034660W	140	5.1	34.71	7.7
2/8/99	13.03	12	753518N	074895W	140	5.2	34.59	9.4
3/8/99	09.58	13	760164N	091308W	140	0.4	30.29	10.1
3/8/99	15.06	14	762120N	091308W	140	1.0	30.20	7.8
11/8/99	13.00	15	802497N	053309E	140	4.7	33.97	69.1
12/8/99		Blk 1			50			
14/8/99	13.08	16	795197N	010161E	140	1.8	33.30	10.9
15/8/99	12.56	17	785150N	015925E	140	2.2	33.38	6.1
16/8/99	10.54	18	784998N	083724E	140	7.1	35.01	9.3
16/8/99	16.16	19	784447N	085992E	140	7.1	34.24	9.5
17/8/99	12.03	20	773227N	072161E	140	6.7	35.22	9.5
17/8/99	16.57	21	772361N	064127E	140	6.7	35.00	9.7
18/8/99	08.26	22	762171N	024396E	140	5.9	35.02	9.5
18/8/99	13.33	23	760125N	013382E	140	5.7	34.86	9.5
19/8/99	10.29	24	744588N	026899W	110	5.3	35.16	10.4
21/8/99	12.54	25	711604N	093416W	140	6.4	34.81	9.5
22/8/99	11.02	26	691505N	123822W	140	6.8	34.73	11.7
23/8/99	15.07	27	665286N	172092W	140	8.5	34.42	13.9
24/8/99	12.08	28	672790N	212905W	140	6.2	34.00	14.5
25/8/99	08.28	29	684170N	225940W	140	4.3	31.07	14.1
25/8/99	16.33	30	691244N	234057W	140	2.4	30.57	13.3
26/8/99	11.57	31	680944N	221860W	140	4.5	32.85	14.2
27/8/99	11.01	32	660489N	182556W	140	6.3	33.45	16.7
28/8/99		Blk 2			50			

Table 4.1: The mean meteorological sensors. Left to right, the columns show; sensor type, channel number and variable name, rhopoint address, serial number of instrument, calibration applied, position on ship.

Sensor	Channel, var. name	Addr.	serial #	Calibration $Y = C0 + C1*X + C2*X^2 + C3*X^3$	Sensor position	Parameter (accuracy if known)
Psychro-meter	1 psydp	$ARD	IO2001 DRY	C0 -10.29715 C1 3.856204e-2 C2 1.493662e-6 C3 2.775097e-10	Foremast platform. To port of HS sonic.	wet- and dry-bulb air temperatures , and humidity (0.1º)
Psychro-meter	2 psywp	$ERD	IO2001 WET	C0 -10.37121 C1 3.860973e-2 C2 1.506655e-6 C3 2.92417e-10		
Psychro-meter	3 psyds	$VRD	IO2003 DRY	C0 -10.43654 C1 3.852675e-2 C2 1.659024e-6 C3 2.022177e-10	Foremast platform. To starboard of HS sonic.	wet- and dry-bulb air temperatures , and humidity (0.1º)
Psychro-meter	4 psyws	$WRD	IO2003 WET	C0 -10.23283 C1 3.873807e-2 C2 1.420081e-6 C3 2.796214e-10		
SST "soap"	5 soap	$DRD	PD0004/53	C0 55.25209 C1 -7.879586e-2 C2 8.265113e-5 C3 -7.791395e-8	Over starboard side of foredeck	sea surface temperature
Tasco sky	6 Tasco1	$JRD		C1 1	Bow	sea "skin" temperature
Tasco sea	7 Tasco2	$KRD		C1 1	Bow	
Dew Point	8 dewpnt	$SRD	107939-02	C1 1	Port bridgewing	humidity
Kipp & Zonen SW1	9 swus	$9RD	CM11903290	C1 0.2062	Stbd side of foredeck	half-hemisphere incoming SW
Kipp & Zonen SW1	10 swds	$8RD	CM11871958	C1 0.22124	Stbd side of foredeck	half-hemisphere reflected SW
Eppley LW Dome	11 LW1Td	$HRD	31170 Td1	C1 1	foremast top forwards position	incoming LW radiation
Body	12 LW1Ts	$QRD	31170 Ts1	C1 1		
Thermopile	13 LW1E	$2RD	31170 E1	C1 1		
Eppley LW Dome	14 LW2Td	$BRD	27960 Td2	C1 1	foremast top aft position	incoming LW radiation
Body	15 LW2Ts	$6RD	27960 Ts2	C1 1		
Thermopile	16 LW2E	$CRD	27960 E2	C1 1		
Kipp & Zonen SW	17 Swmast	$8RD	CM11840606	C1 1	foremast top	incoming SW radiation
Vaisala Pressure	18 press	$TRD	S113002	C0 600 C1 4.6	bridge	air pressure
Kipp & Zonen SW2	19 swup	$XRD	CM11902836	C1 0.2198	Port side of foredeck	half-hemisphere incoming SW radiation
Kipp & Zonen SW2	20 swdp	$YRD	CM11903289	C1 0.2041	Port side of foredeck	half-hemisphere reflected SW radiation
Dew point Volts (BAS)	21 100R	$RRD	100R	C1 1	Port bridgewing	air temperature at dew point sensor
Dew point PRT (BAS)	22 PRT	$URD	PRT	C1 1	Port bridgewing	

Table 4.2: The fast response sensors.

Sensor	Program	Location	Data Rate	Sect-ions	derived flux
Gill Horizontally Symmetrical Research Ultrasonic Anemometer	gillhs	Port side of foremast platform	20 Hz	16	momentum and heat
Gill R2 Research Ultrasonic Anemometer	gillr2	Foremast top	21 Hz	16	momentum
Gill R2 Research Ultrasonic Anemometer	gillr2b	Port bridgewing	21 Hz	16	momentum
M100 Infrared Hygrometer (BAS)	fhumid	Port bridgewing	10 Hz	8	latent heat

Table 4.3: List of radiosonde flights. SSD = Sounding stop detected, H = height, M = mode.

NO.	JDAY	TIME	FILE NAME	FLIGHT FILE	LAT deg N	LONG	CAP	H mbar	M	COMMENT
1	205	11:25	2051220	-	57.37	1.20E	OFF	47	R	
2	206	12:13	2061308	-	61.87	3.08E	OFF	71	R	
3	206	23:55	2062349	-	63.98	4.00E	OFF	82	R	No Winds
4	207	12:01	2071152	-	64.36	6.90E	OFF	902	T	SSD
5	207	14:10	2071409	-	64.46	7.78E	OFF	68	T	No Temp sent
6	207	23:15	2072312	-	64.95	9.92E	OFF	1000	T	SSD
7	207	23:45	2072344	-	65.04	9.84E	OFF	761	T	SSD
8	208	11:47	2081141	FLIGHT008	66.06	8.82E	ON	61	T	
9	208	23:23	2082320	FLIGHT009	67.10	7.70E	OFF	911	T	SSD
10	209	0:17	2090011	FLIGHT010	67.21	7.57E	OFF	60	T	
11	209	11:45	2091140	FLIGHT011	68.11	6.49E	ON	38	T	
12	209	23:22	2092319	FLIGHT012	68.70	5.76E	OFF	133	T	
13	210	11:38	2101133	FLIGHT013	69.58	4.55E	OFF	60	T	
14	210	23:40	2102338	FLIGHT014	70.16	3.69E	OFF	310	T	Poor Signal
15	211	11:40	2111128	FLIGHT015	71.04	2.32E	OFF	880	T	SSD
16	211	12:05	2111202	FLIGHT016	71.04	2.31E	OFF	43	T	
17	211	23:25	2112321	FLIGHT017	71.92	0.79E	OFF	92	T	
18	212	11:35	2121130	FLIGHT018	72.79	0.87E	OFF	151	T	
19	212	23:20	2122317	FLIGHT019	73.39	2.12W	OFF	47	T	
20	213	11:32	2131125	FLIGHT020	74.11	3.78W	ON	43	T	
21	213	23:18	2132313	FLIGHT021	74.83	5.64W	OFF	6760	T	
22	214	11:52	2141145	FLIGHT022	75.62	7.91W	OFF	53	T	
23	214	23:14	2142312	FLIGHT023	75.80	8.40W	OFF	/	T	No PC data
24	215	11:37	2151132	FLIGHT024	76.09	9.45W	OFF	731	T	
25	215	12:09	2151205	FLIGHT025	76.10	9.45W	OFF	62	T	

CONTENTS

NO.	JDAY	TIME	FILE NAME	FLIGHT FILE	LAT deg N	LONG	CAP	H mbar	M	COMMENT
26	215	23:29	2152336	FLIGHT026	76.69	11.75W	OFF	41	T	
27	216	11:40	2161136	FLIGHT027	77.01	12.83W	OFF	73	T	
28	216	2316	2162309	FLIGHT028	77.30	131.98W	OFF	61	T	
29	217	5:44	2170539	FLIGHT029	77.31	14.08W	OFF	56	T	
30	217	11:37	2171135	FLIGHT030	77.33	8.31W	OFF	904	T	SSD
31	217	12:02	2171158	FLIGHT031	77.33	13.53W	OFF	66	T	
32	217	17:36	2171732	FLIGHT032	77.34	12.53W	OFF	38	T	
33	217	23:21	2172316	FLIGHT033	77.32	12.31W	OFF	63	T	
34	218	5:37	2180531	FLIGHT034	77.32	12.22W	OFF	68	R	
35	218	11:43	2181135	FLIGHT035	77.17	10.90W	OFF	50	T	Poor Winds
36	218	17:30	2181725	FLIGHT036	77.11	9.56W	OFF	40	R	
37	218	23:10	2182308	FLIGHT037	77.00	8.31W	OFF	38	T	
38	219	6:00	2190557	FLIGHT038	76.87	8.99W	OFF	49	R	
39	219	11:27	2191125	FLIGHT039	76.84	8.31	OFF	61	T	
40	219	17:20	2191716	FLIGHT040	77.07	6.21W	OFF	42	R	
41	219	22:12	2192208	FLIGHT041	77.06	6.22W	OFF	53	T	
42	220	23:24	2202318	FLIGHT042	79.15	5.57E	OFF	59	T	
43	221	5:46	2210535	FLIGHT043	79.91	9.48E	OFF	81	R	Winds 775+ mb
44	221	11:42	2211137	FLIGHT044	80.43	8.19E	OFF	120	T	
45	221	17:26	2211722	FLIGHT045	80.44	7.98E	OFF	51	R	
46	221	23:31	2212329	FLIGHT046	80.46	6.95E	OFF	45	T	
47	222	6:03	2220558	FLIGHT047	80.45	7.19E	OFF	42	R	
48	222	11:48	2221146	FLIGHT048	80.39	5.87E	OFF	45	T	
49	222	18:10	2221808	FLIGHT049	80.40	5.79E	OFF	52	R	No Wind Data
50	222	23:31	2222329	FLIGHT050	80.40	5.64E	OFF	91	T	
51	223	5:47	2230545	FLIGHT051	80.41	5.76E	ON	62	R	
52	223	11:38	2231123	FLIGHT052	80.41	5.62E	ON	53	T	
53	223	17:42	2231737	FLIGHT053	80.48	5.52E	OFF	42	R	
54	223	23:15	2232311	FLIGHT054	80.24	4.14E	OFF	49	T	
55	224	5:42	2240538	FLT055	80.16	3.37E	OFF	55	R	
56	224	11:39	2241133	FLT056	80.08	2.70E	OFF	73	T	TEMP via Telex
57	224	17:37	2241733	FLT057	80.09	2.01E	OFF	46	R	
58	225	1:50	2250147	FLT058	80.05	1.45E	OFF	52	T	Late launch
59	225	5:52	2250548	FLT059	80.06	1.22E	OFF	70	R	
60	225	11:39	2251136	FLT060	80.00	1.04E	OFF	67	T	
61	225	17:08	2251703	FLT061	79.97	0.96E	OFF	43	R	
62	225	23:14	2252309	FLT062	79.93	1.07E	OFF	44	T	Poor signal
63	226	5:54	2260551	FLT063	79.92	1.01E	OFF	58	R	
64	226	11:46	2261144	FLT064	79.88	1.05E	OFF	53	T	
65	226	17:33	2261731	FLT065	79.86	0.91E	OFF	39	R	
66	226	22:48	2262246	FLT066	79.44	1.20E	OFF	58	T	
67	227	11:36	2271133	FLT067	78.95	0.86E	OFF	51	T	
68	227	23:09	2272304	FLT068	78.83	4.50E	OFF	48	T	
69	228	11:37	2281135	FLT069	78.83	8.95E	OFF	67	T	
70	228	23:22	2282318	FLT070	78.12	9.42E	ON	53	T	Rain

CONTENTS

NO.	JDAY	TIME	FILE NAME	FLIGHT FILE	LAT deg N	LONG	CAP	H mbar	M	COMMENT
71	229	11:45	2291142	FLT071	77.54	7.38E	ON	73	T	Rain
72	229	23:18	2292314	FLT072	77.05	5.31E	ON	50	T	Rain
73	230	11:46	2301144	FLT073	76.28	2.46E	OFF	50	T	
74	230	23:26	2302323	FLT074	75.61	0.27E	OFF	47	T	
75	231	11:42	2311140	FLT075	74.76	2.16W	OFF	46	T	
76	231	23:19	2312315	FLT076	74.11	3.82W	OFF	50	T	
77	232	11:45	2321142	FLT077	73.13	6.04W	OFF	66	T	
78	232	23:24	2322319	FLT078	72.40	7.60W	OFF	57	T	
79	233	12:02	2331200	FLT079	71.43	9.30W	ON	58	T	
80	233	23:32	2332329	FLT080	70.32	11.09W	OFF	46	T	
81	234	11:43	2341140	FLT081	69.20	12.71W	OFF	60	T	
82	234	23:15	2342312	FLT082	68.17	14.05W	OFF	46	T	
83	235	11:34	2351131	FLT083	66.77	15.69W	OFF	52	T	
84	235	23:51	2352328	FLT084	66.35	20.24W	OFF	909	T	SSD
85	236	0:31	2360028	FLT085	66.46	20.35W	OFF	54	T	
86	236	11:59	2361157	FLT086	67.45	21.46W	OFF	44	T	Unwinder jammed
87	236	23:39	2362327	FLT087	68.23	22.40W	OFF	52	T	
88	237	11:39	2371136	FLT088	68.86	23.21W	OFF	51	T	
89	237	23:33	2372329	FLT089	69.13	23.57W	OFF	48	T	
90	238	11:42	2381139	FLT090	68.17	22.33W	OFF	502	T	lost at 500 mbar
91	238	23:20	2382317	FLT091	67.12	21.08W	OFF	58	T	
92	239	11:46	2391143	FLT092	66.72	18.23W	OFF	53	T	
93	240	1:08	2400104	FLT093	66.01	12.85W	OFF	55	T	
94	240	11:36	2401130	FLT094	64.56	9.80W	OFF	44	T	

Table 5.1: The scientific log kept by the navigation officers while the ship was in the MIZ The abbreviations are: HTW, head-to-wind; TB, tethered balloon profile; v/l, vessel.

Day, time.	Ice conc.	Station notes	Position
03/08/99 jday215			
2000		Entered ice edge	76 35.1N 11 09.2 W
2100	5/10	Ice edge runs east-west.	
2200	6/10		
2300	8/10		
2339		**STATION. CTD 51.**	76 41.74N 11 52.93 W.
2343		Sonde. Stay head to wind (HTW)	
04/08/99 jday216			
0100	2/10	HTW	
0200	2/10	HTW	
0300	3/10	HTW	
0400	3/10	HTW	
0450		**v/l underway.**	
0500	3/10	open pack	
0730		**STATION CTD 52.**	76 48.6N 12 00.0W
0800	3/10	open pack	
0900 to 1200	3/10	open pack	
1212		**STATION CTD 53.**	77 03.95 N 13 00.06 W
1256		**underway**	
2000		**MET PHASE STARTS**	
2032		**STATION MET 54**	77 18.03 N 13 58.73W
2214		Tethered balloon (TB).	77 17.72N 13 58.52W
05/08/99 jday217			
0406		TB finished. HTW	77 18.4N, 14 04.6W
0610		**underway**	
0900	9-10/10		

Day, time.	Ice conc.	Station notes	Position
1000	9-10/10	Jerry "vessel testing qualities of ice floes, which prove very hard, up to 2.5m thick, looks rotten with lots of melt pools but has continuous hard ice beneath the pools!"	
1100	6/10		
1200		sonde Jerry "ship had difficulty working this patch. If caught in consolidated parts, would be most unlikely to be able to extricate herself"	77 20.6N 13 22.3 W
1300	2/10	Enters open pack lead until 13:30	
1400	7/10	close pack between big and occasionally vast ice floes	
1500	8/10	close pack between big and occasionally vast ice floes	
1600	9/10	Vast floes with limited very close pack leads between	
1700	9/10	fewer melt pools covering ~30 % of floe surface	
1741		radiosonde	
1800	9/10		
1900	9/10		
1925		**STATION MET 55**	77 20.0N, 12 18.7W
1940		PIMMS	
2000	9/10	TB prep	
2040	9/10	TB flown	
2333	9/20	TB down	77 19.4 N, 12 18.45W
0100	9/10		
06/08/99 jday218			
0230	9/10	PIMMS recovered	
0300	9/10	polynya remains full of close pack - NO CTD	
0410		**v/l underway**	
0500	10/10	big and medium floes, closed? ice between floes	
0537		sonde	
0600	8/10		
0700	8/10		
0800	7/10	small medium and big floes with pools between and new ice	
0900	5/10		
1000	5/10		
1100	3/10		
1143		sonde	77 09.56N, 10 53.81W

Day, time.	Ice conc.	Station notes	Position
1200	7/10		
1300	9/10	vl making good ESE track	
1400	8/10		
1500	5/10		
1530	2/10	open pack lead	
1600	3/10		
1700	4/10	in pools between big/vast floes	
1800	4/10	in pools between big/vast floes	
1900	4/10	in pools between big/vast floes	
1931		**STATION MET 56.** HTW	77 01.0N, 9 01.4W.
1938		SPRI sonar buoy deployed	
1940		PIMMS deployed	
2000	2/10	in pools between big/giant floes	
2017	2/10	TB	77 00.95N, 9 00.8W
2230		recover PIMMS??	
2308	2/10	sonde	76 59.6N, 8 53.21W
2331	2/10	deploy sonar buoy	76 59.36N 8 58.98 W
07/08/99 jday219			
0005		HTW	
0037		CTD 76 58.7N 8 58.4W	
0100	3/10		
0200	3/10		
0238		start PIMMS recovery	
0254		PIMMS recovered	76 56.8N 09 01.3W
0300	2/10		
0400	3/10		
0405		**underway**	
0428		opportunistically recovered SPRI sonar buoy (or bits of it)	
0500	3/10	in pools between big/giant floes	
0600	4/10	in pools between big/giant floes (sonde)	
0700	7/10	in pools between big/giant floes	
0800	8-9/10	small floes and bits	
0900	3/10		
1000	3/10		
1100	4/10		
1200	4/10		
1300	4/10	areas of 5/10 with 3/10 between. all small floes	76 55.8N 07 11.1W
1400	8/10		76 56.96N 06 51.6W
1500	4/10		76.59.5N 06 32.7W
1600	2/10	**STATION MET 57** open pack lead	77 04.2N 06 12.1W

CONTENTS

Day, time.	Ice conc.	Station notes	Position
1625		CTD no 56	
1700	1/10	HTW	
1922		uncontam. seawater on	
2006		TB	77 03.19N, 6 13.07W
2245		**v/l underway**	
08/08/99 jday220		on passage North	
09/08/99 jday221		on passage North	
0827	3/10	ice edge ENE	80 21.32N, 8 25.34E
0854 *Truewind direction 090*		**STATION MET 58** wind direction true from 090	80 22.97N, 8 14.17E
0925		TB	
1000	3/10		
1235		HTW CTD	
1248			80 27.2N, 08 27.2E
1612		**v/l underway**	
1800 *1st year .5 to 2m thick*	10/10	pack and brash	
1900 *small open pool*		**STATION MET 59**	80 24.9N, 07 01.0E
2000 *wind from 0900 6 m/s*		HTW	
2035		TB	80 25.42N, 6 57.4 E
10/08/99 jday222			
0030		HTW	
0100	8-9/10		80 28.3N, 07 02.9E
0200	9/10		
0300	9/10		80 28.1N, 07 11.6E
0500	9/10		80 27.3N, 07 12.4E
0602	9/10	**v/l underway**	80 26.9N, 07 10.21E
0800	v/l at ice edge	ice edge runs north of line 250 to 70 deg	80 22.4N, 6 59.4E
0900 *On ice edge. Start of fetch section Wind off ice.*		**MET STN 60** HTW	80 22.89N 6 00.89E
0912		PIMMS deployed	
0921		CTD	
1006		CTD in	
1315		off HTW - PIMMS recovery	
1356		TB	
1519		ice edge north of line 100 to 280 deg	
1528		**v/l underway**	
1545		**MET STN 61** HTW 200m off ice edge	
1600			80 24.2N, 05 46.9E
1640		wind backed, change heading to 025	
1700		ice edge 110,290 deg	80 24.12N, 05 46.46E
1900		ice edge 110,290 deg	80 23.67N, 05 46.15E
1909		TB	
2055		**v/l underway**	

Day, time.	Ice conc.	Station notes	Position
2107		**MET STN 62** 400m off ice edge	
2212		TB	80 23.89N, 5 41.0E
2333			80 24.34N, 5 37.95E
11/08/99 jday223			
0005		thrusters off (sonar)	
0020		thrusters on. v/l drifted in to ice edge - move off	
0055		400m off edge. HTW Polarstern visit	
0115		CTD wind backs to S	80 24.9N, 05 37.9E
0130		wind varying NNW to WSW	
0158		CTD in	80 25.1N, 05 39.3E
0200		wind from 340, HTW	
0205		ice edge 110,290 deg wind backs to 310	
0310		HTW 250	
0400		**v/l underway**	80 25.2N, 05 42.7E
0418		**MET STN 63** stem 800m upwind of edge	80 24.7N, 05 43.6E
0438		HTW 250 degT ice edge 110,290 deg	
0500			80 24.6N, 5 44.3E
0530		wind veered 335. HTW stem 800m downwind of edge	
0547		radiosonde	80 24.1N, 5 46.7E
0600		ice edge 110, 290deg	80 23.8N 5 48.1E
0630		wind variable 250/050	
0700			80 22.9N, 5 48.7E
0740		TB	
0937		**v/l underway**	
1025		**MET STN 64** at ice edge	80 24.65N, 5 38.18E
1040		TB	
1310		HTW 030 deg	
1400		wind direction variable	
1500 *FOG*		ice edge becoming scattered and broken	80 25.9N, 05 31.3E
1600		wind variable ice edge 110,290 deg	
1612		**v/l underway**	
1700	9/10		80 28.5N, 5 32.0E
1715		2 miles into ice still foggy and no wind. Head back out.	
1800	8/10	**MET STN 65** 500m into ice edge 115,295	80 28.2N, 5 27.1E
1807		TB	
1900	6/10	plus brash	80 28.1N, 5 26.3E

Day, time.	Ice conc.	Station notes	Position
2000	7/10	plus brash	80 28.3N, 5 27.3E
2006		**v/l underway**	
2018		leaves pack ice heads SW in open water	80 28.07N, 5 25.64E
12/08/99 jday224			
0010		**MET STN 66** HTW just in ice edge	
0024		CTD deployed	80 10.0N, 03 24.3E
0150		CTD in. v/l now 320m and 036 deg from station rel to ice edge	
0205		HTW on station	
0500	5/10 to 6/10 strip	open water to SE, 8/10 - 9/10 to NW, N	
0600	5/10 to 6/10 strip	open water to SE, 8/10 - 9/10 to NW, N	
0635		deploy PIMMS	
0700		TB	80 09.2N, 03 18.9E
0700	5/10 to 6/10 strip	open water to SE, 8/10 - 9/10 to NW, N	
0800	5/10 to 6/10 strip	open water to SE, 8/10 - 9/10 to NW, N	
1002		v/l moved to recover PIMMS	
1022		**v/l underway**	
1158 *start of fetch section. Winds 5-6 m/s off ice.*		**MET STN 67** at ice edge position	80 05.39N, 2 22.20E
1210		TB	
1504		HTW v/l 1/2 ships length into ice	80 05.57N, 2 06.68E
1530		ice tongue moves in astern, making v/l 100m from ice edge	
1700	9/10	small floe+brash	
1800	9/10	small floe+brash	
1808		**v/l underway** into ice and upwind	
1828 *wind 025 4 m/s*		**MET STN 68** HTW 580m North of last station	80 05.1N, 1 56.2E
1900	8/10	small floe	80 04.8N, 1 54.8E
2000	8/10	small floe	80 04.2N, 1 51.1E
2200		v/l underway towards Polar2 rendezvous	
2240		v/l stopped HTW	80 03.38N, 1 43.53E
2322		VHF contact with Polar2	
2331		Polar2 flies from port to stbd over v/l	
13/08/99 jday225			
0010		TB	

Day, time.	Ice conc.	Station notes	Position
0100	9/10	small floes, open water to south	80 03.2N, 1 29.6E
0150			80 03.4N, 1 25.2E
0200	9/10	small floes, open water to south	80 03.4N, 1 24.5E
0300	9/10	small floes, open water to south	80 03.8N, 1 20.3E
0400		**v/l underway**	80 04.0N, 01 17.7E
0423		**MET STN 69** HTW 200m off pack ice edge	80 03.8N, 1 15.3E
0500	9/10	small floes pack ice to north edge runs 070, 250 deg	80 03.8N, 1 14.5E
0600	9/10	small floes pack ice to north edge runs 070, 250 deg	
0700	9/10	small floes pack ice to north edge runs 070, 250 deg	
0800	9/10	small floes pack ice to north edge runs 060, 240 deg	80 01.9N, 1 07.5E
0805		TB	
1056		**v/l underway**	
1114		**MET STN 70** HTW 400m downwind of ice edge 055,235	79 59.87N, 1 02.62E
1300		ice edge 040,220	79 59.8N, 01 00.1E
1428		TB. ice edge 020, 200	
1500			79 59.6N, 0 59.3E
1530		ice edge curved, distance downwind not accurate	
1725		**v/l underway**	
1756		**MET STN 71** HTW 800m downwind of ice edge	79 57.8N, 0 59.4E
1800		ice edge 030,210 deg	
1822		CTD to 2800 m depth	
2035		CTD inboard. ice edge 030,210 deg	
2100		TB	79 56.4N, 1 05.24E
2355		**v/l underway**	
14/08/99 jday226			
0012		**MET STN 72** beam-on alongside ice edge. Edge curved and scattered small ice downwind	
0100		TB	79 55.3N, 00 59.3E
0200		ice edge even less defined	
0300	9/10 pack to NW	open pack for 1 mile to SE, then open water	
0400		HTW	79 55.2N, 00 59.1E
0600			79 55.2N, 01 00.3E
0700		**v/l underway**	79 55.0N, 01 02.1E

Day, time.	Ice conc.	Station notes	Position
0718 *wind 330 4 m/s*		**MET STN 73** HTW	79 5.1N, 01 01.0E
0800	7/10	small floes, ice edge 020,200 deg	79 54.8N, 01 01.7E
1440	9/10	**MET STN 74** HTW	79 52.5N, 00 54.2E
1500	9/10		
1600		heading 330	79 52.21N, 00 53.64E
1620	9/10	TB	
1650		cradle to bird table to clear ice from air pipe	79 51.9N, 00 54.3E
1700	8/10	small + big floes	
1734		work on bird table finished, cradle away.	
1835		HTW balloon stowed	
1900	8/10	**v/l underway** towards open water	79 50.7N, 00 56.8E
1950	3/10	ice edge 040,220 deg	79 47.2N, 01 04.5E
2000		open water, plus strips and patches ice	79 46.1N 01 03.8E
		END of MET PHASE, no more ice	

Table 5.2: The hourly visual observations made by the science party. The WMO system or "Egg Code" was used. Note: "7." is entered as "70" (for ease of post-processing). Sa, Sb and Sc are stage of development of the sea ice, and Fa, Fb, Fc represent the form of the sea ice, or the floe size. Ice concentration is expressed in tenths.

*1 Ship in open water, well defined Ice edge 400m to west of ship. Two distant bergs visible, each approx. 300m long.

*2 Ship in open water with ice edge in sight.

*3 Ship maintaining position, ice conditions not changing.

*4 Tether balloon in open water ice edge not visible

*5 Ship in open water 800m from ice edge

*6 Ship 500m into the ice.

*7 Ship in open water, ice edge in sight to west.

Jday	Date	Hour	Ice conc.	Sa	Sb	Sc	Fa	Fb	Fc	Comments
214	2/8/99	18								
214	2/8/99	19								
214	2/8/99	20								
214	2/8/99	21								
214	2/8/99	22	0							
214	2/8/99	23	0							
215	3/8/99	0	0							
215	3/8/99	1	1							
215	3/8/99	2	4							
215	3/8/99	3	4							
215	3/8/99	4	3							
215	3/8/99	5	3							
215	3/8/99	6	3							
215	3/8/99	7	2							
215	3/8/99	8	3							
215	3/8/99	9	2							
215	3/8/99	10	2							
215	3/8/99	11	0							
215	3/8/99	12	0							
215	3/8/99	13	1	6	9		3			
215	3/8/99	14	1	6			3			
215	3/8/99	15	1	6			3			
215	3/8/99	16	2	6			2	3		
215	3/8/99	17	4	6			2	3		
215	3/8/99	18	4	6			3			
215	3/8/99	19	5	6	70	90	3			

CONTENTS

Jday	Date	Hour	Ice conc.	Sa	Sb	Sc	Fa	Fb	Fc	Comments
215	3/8/99	20	5	40			3			
215	3/8/99	21	8	70			3			
215	3/8/99	22	8	40			4			
215	3/8/99	23	9	90			5			
216	4/8/99	0	5	70			4			
216	4/8/99	1	5	70			4			
216	4/8/99	2	5	70			4			
216	4/8/99	3	5	70			4			
216	4/8/99	4	5	70			4			
216	4/8/99	5	4	70			4			
216	4/8/99	6	3	80			5			
216	4/8/99	7	4	70			4			
216	4/8/99	8	4	70			4			
216	4/8/99	9	6	70			4			
216	4/8/99	10	6	70			4			
216	4/8/99	11	7	80			4			
216	4/8/99	12	4	80			4			
216	4/8/99	13	1	70	6		3			
216	4/8/99	14	/	/	/	/	/	/	/	
216	4/8/99	15	9	70	6	40	4			
216	4/8/99	16	6	70	40		4			
216	4/8/99	17	9	70	80	40	4			
216	4/8/99	18	5	40			4			
216	4/8/99	19	6	40	70		4			
216	4/8/99	20	/	/	/	/	/	/	/	
216	4/8/99	21	6	70			5			
216	4/8/99	22	7	70			5			
216	4/8/99	23	7	70			5			
217	5/8/99	0	7	70			5			
217	5/8/99	1	7	70			5			
217	5/8/99	2	7	70			5			
217	5/8/99	3	7	70			5			
217	5/8/99	4	8	70			5	4		
217	5/8/99	5	8	80			4			
217	5/8/99	6	7	80			4			
217	5/8/99	7	6	80			4			
217	5/8/99	8	4	40			2			Fog
217	5/8/99	9	9	40			5			
217	5/8/99	10	9	40			5			
217	5/8/99	11	/	/	/	/	/	/	/	
217	5/8/99	12	8	80	70		5			
217	5/8/99	13	2	40			3			fog
217	5/8/99	14	3	40			3	4		
217	5/8/99	15	6	40	70	80	3	4		
217	5/8/99	16	8	70	80		4			
217	5/8/99	17	8	70			5			
217	5/8/99	18	9	70			5			
217	5/8/99	19	9	70			5			

CONTENTS

Jday	Date	Hour	Ice conc.	Sa	Sb	Sc	Fa	Fb	Fc	Comments
217	5/8/99	20	9	70			5			
217	5/8/99	21	9	90			5			
217	5/8/99	22	9	90			5			
217	5/8/99	23	9	90			5			
218	6/8/99	0	9	90			5			
218	6/8/99	1	9	90			5			
218	6/8/99	2	9	90			5			
218	6/8/99	3	9	90			5			
218	6/8/99	4	9	90			5			
218	6/8/99	5	9	90			5			
218	6/8/99	6	9	90			5			
218	6/8/99	7	4	90			3			
218	6/8/99	8	1	70			2			
218	6/8/99	9	5	80			4			
218	6/8/99	10	5	80			5			
218	6/8/99	11	5	80			5			
218	6/8/99	12	8	80			4			
218	6/8/99	13	6	80			5			
218	6/8/99	14	5	80			4			
218	6/8/99	15	6	80			5			
218	6/8/99	16	5	80			3			
218	6/8/99	17	8	80	40		4	5		
218	6/8/99	18	8	80			3	4		Fog
218	6/8/99	19	/	/	/	/	/	/	/	
218	6/8/99	20	3	70	40		5	3		
218	6/8/99	21	3	70	40		5	3		
218	6/8/99	22	4	70	40		5	3		
218	6/8/99	23	3	70	40		5	3		
219	7/8/99	0	3	70	40		5	3		
219	7/8/99	1	3	70	40		5	3		
219	7/8/99	2	3	70	40		5	3		
219	7/8/99	3	3	70	40		5	3		
219	7/8/99	4	3	70	40		5	3		
219	7/8/99	5	4	70			3	4		
219	7/8/99	6	4	70			5	3		
219	7/8/99	7	8	70			5			
219	7/8/99	8	6	70			4			
219	7/8/99	9	4	70			3			
219	7/8/99	10	3	70			3			
219	7/8/99	11	5	70			3			
219	7/8/99	12	6	60			3			
219	7/8/99	13	4	40			3			
219	7/8/99	14	9	40			3			
219	7/8/99	15	5	40			3			
219	7/8/99	16	1	40			3			
219	7/8/99	17	1	40			2			
219	7/8/99	18	1	40			2			
219	7/8/99	19	1	40			2			

CONTENTS

Jday	Date	Hour	Ice conc.	Sa	Sb	Sc	Fa	Fb	Fc	Comments
219	7/8/99	20	1	40			2			
219	7/8/99	21	1	40			2			
219	7/8/99	22	1	40			2			steam North
221	9/8/99	9	5	7	10		2			
221	9/8/99	10	5	7	10		2			
221	9/8/99	11	5	7	10		2			
221	9/8/99	12	5	7	10		2			
221	9/8/99	13	6	7	10		2	3		
221	9/8/99	14	6	7	10		2	3		
221	9/8/99	15	6	7	10		2	3		
221	9/8/99	16	9	7	10		2			
221	9/8/99	17	9	10			2			
221	9/8/99	18	10	9			1	2		
221	9/8/99	19	10	10			1	2		
221	9/8/99	20	9	10			2			
221	9/8/99	21	9	10			2			
221	9/8/99	22	9	10			2			
221	9/8/99	23	9	10			2			
222	10/8/99	0	9	10			2			
222	10/8/99	1	9	10			2			
222	10/8/99	2	9	10			2			
222	10/8/99	3	9	10			2			
222	10/8/99	4	9	10			2			
222	10/8/99	5	9	10			2			
222	10/8/99	6	9	10			2			
222	10/8/99	7	9	10			2			
222	10/8/99	8	1	6			1			
222	10/8/99	9	1	6			1			
222	10/8/99	10	1	6			1			
222	10/8/99	11	3	6			1			
222	10/8/99	12	3	6			1			
222	10/8/99	13	3	6			1			
222	10/8/99	14	8	6			1			
222	10/8/99	15	3	6			1			
222	10/8/99	16	3	6			1			
222	10/8/99	17	3	6			1			
222	10/8/99	18	3	6			1			
222	10/8/99	19	3	6			1			
222	10/8/99	20	/	/	/	/	/	/	/	*1
222	10/8/99	21	/	/	/	/	/	/	/	
222	10/8/99	22	/	/	/	/	/	/	/	
222	10/8/99	23	/	/	/	/	/	/	/	
223	11/8/99	0	/	/	/	/	/	/	/	
223	11/8/99	1	/	/	/	/	/	/	/	
223	11/8/99	2	/	/	/	/	/	/	/	
223	11/8/99	3	/	/	/	/	/	/	/	
223	11/8/99	4	/	/	/	/	/	/	/	

CONTENTS

Jday	Date	Hour	Ice conc.	Sa	Sb	Sc	Fa	Fb	Fc	Comments
223	11/8/99	5	/	/	/	/	/	/	/	
223	11/8/99	6	/	/	/	/	/	/	/	
223	11/8/99	7	/	/	/	/	/	/	/	
223	11/8/99	8	/	/	/	/	/	/	/	
223	11/8/99	9	/	/	/	/	/	/	/	
223	11/8/99	10	2	6			1	2		
223	11/8/99	11	2	6			1	2		
223	11/8/99	12	5	6			1	2		
223	11/8/99	13	4	6			1	2		
223	11/8/99	14	3	6			1	2		
223	11/8/99	15	4	6			1	2		
223	11/8/99	16	5	6			1	2		
223	11/8/99	17	9	10			3			
223	11/8/99	18	8	10			3			
223	11/8/99	19	8	10			3			
223	11/8/99	20	8	10			2			
223	11/8/99	21	0							*2
223	11/8/99	22	/							
223	11/8/99	23	/							
224	12/8/99	0	5	10			2			At ice edge
224	12/8/99	1	5	10			2			At ice edge
224	12/8/99	2	6	10			2			At ice edge
224	12/8/99	3	6	10			2			
224	12/8/99	4	6	10			2			
224	12/8/99	5	4	10			2			
224	12/8/99	6	4	10			2			
224	12/8/99	7	3	10			2			
224	12/8/99	8	3	10			2			
224	12/8/99	9	3	10			2			
224	12/8/99	10	/							
224	12/8/99	11	/							
224	12/8/99	12	5	10			2	1		
224	12/8/99	13	6	10			2	1		
224	12/8/99	14	5	10			2	1		
224	12/8/99	15	5	10			2	1		
224	12/8/99	16	/	/	/	/	/	/	/	
224	12/8/99	17	9	10			2	1		
224	12/8/99	18	9	10			2	1		
224	12/8/99	19	8	10			2	1		
224	12/8/99	20	8	10			2	1		
224	12/8/99	21	8	90	10		3	2	1	
224	12/8/99	22	8	90	10		3	2	1	
224	12/8/99	23	8	90	10		3	2	1	
225	13/8/99	0	8	90	10		3	2	1	
225	13/8/99	1	8	90	10		3	2	1	*3
225	13/8/99	2	8	90	10		3	2	1	
225	13/8/99	3	8	90	10		3	2	1	
225	13/8/99	4	8	90	10		3	2	1	

Jday	Date	Hour	Ice conc.	Sa	Sb	Sc	Fa	Fb	Fc	Comments
225	13/8/99	5	3	10			2			
225	13/8/99	6	2	10			2			
225	13/8/99	7	2	10			2			
225	13/8/99	8	2	10			2			
225	13/8/99	9	2	10			2			
225	13/8/99	10	/							*4
225	13/8/99	11	/							
225	13/8/99	12	/							
225	13/8/99	13	/							
225	13/8/99	14	/							
225	13/8/99	15	/							
225	13/8/99	16	/							
225	13/8/99	17	/							
225	13/8/99	18	/							
225	13/8/99	19	/							
225	13/8/99	20	/							
225	13/8/99	21	0							*5
225	13/8/99	22	/							*5
225	13/8/99	23	/							*5
226	14/8/99	0	5	10			2			At ice edge
226	14/8/99	1	/							At ice edge
226	14/8/99	2	/							At ice edge
226	14/8/99	3	/							At ice edge
226	14/8/99	4	/							At ice edge
226	14/8/99	5	5	10			2			*6
226	14/8/99	6	5	10			2			*6
226	14/8/99	7	5	10			2			*6
226	14/8/99	8	7	10			3			*6
226	14/8/99	9	7	10			3			*6.
226	14/8/99	10	6	10			3			*6
226	14/8/99	11	/	/	/	/	/	/	/	*6
226	14/8/99	12	5	10			3			*6
226	14/8/99	13	5	10			3			*6
226	14/8/99	14	5	10			3			*6.
226	14/8/99	15	7	10	9		3			further in
226	14/8/99	16	8	90	10		3			
226	14/8/99	17	8	90	10		3			
226	14/8/99	18	8	90	10		3			
226	14/8/99	19	8	90	10		3			
226	14/8/99	20	0							*7
226	14/8/99	21	0							
226	14/8/99	22	0							Party Time!
226	14/8/99	23								

Table 5.3: The various visual ice observations made by the navigation officers. Cover A is the ice concentration (tenths) data entered on the hourly form provided to the bridge by the science party. Cover B is the ice concentration (tenths) data entered in the ship's scientific log (as in Table 5.1). The last five columns were taken from the 6-hourly Meteorological reports (Met Office, 1996), where ci is the concentration or arrangement of ice (NOT in tenths), Si is the stage of development, bi is land of ice origin, Di is the bearing of the principal ice edge and zi is the ice situation and trend over the previous 3 hours.

Jday	Date	Hour	Cover A	cover B	ci	Si	bi	Di	zi
215	3/8/99	18			2	9	0	9	2
215	3/8/99	21		5					
215	3/8/99	22		6					
215	3/8/99	23		8					
216	4/8/99	1		2					
216	4/8/99	2		2					
216	4/8/99	3		3					
216	4/8/99	4		3					
216	4/8/99	5		3					
216	4/8/99	8		3					
216	4/8/99	9		3					
216	4/8/99	10		3					
216	4/8/99	11		3					
216	4/8/99	12		3	6	6		2	0
216	4/8/99	17	8						
216	4/8/99	18	9						
216	4/8/99	20	9						
216	4/8/99	21	3						
216	4/8/99	22	3						
216	4/8/99	23	3						
217	5/8/99	0	3		3	7			5
217	5/8/99	2	3						
217	5/8/99	3	3						
217	5/8/99	5	7						
217	5/8/99	6	6		4	9	0	9	5
217	5/8/99	9	7	9.5					
217	5/8/99	10	10	9.5					
217	5/8/99	11	6	6					
217	5/8/99	12	6		3	8		6	2
217	5/8/99	13		2					
217	5/8/99	14		7					
217	5/8/99	15		8					
217	5/8/99	16		9					
217	5/8/99	17		9					
217	5/8/99	18		9					
217	5/8/99	19		9					
217	5/8/99	20	9	9					

Jday	Date	Hour	Cover A	cover B	ci	Si	bi	Di	zi
217	5/8/99	21	9	9					
217	5/8/99	22	9	9					
217	5/8/99	23	9	9					
218	6/8/99	0		9					
218	6/8/99	1		9					
218	6/8/99	2		9					
218	6/8/99	3		9					
218	6/8/99	4		9					
218	6/8/99	5		10					
218	6/8/99	6		8	5	8			0
218	6/8/99	7		8					
218	6/8/99	8	7	7					
218	6/8/99	9	5	5					
218	6/8/99	10	5	5					
218	6/8/99	11	3	3					
218	6/8/99	12	7	7					
218	6/8/99	13		9					
218	6/8/99	14		8					
218	6/8/99	15		5					
218	6/8/99	16		3					
218	6/8/99	17		4					
218	6/8/99	18		4					
218	6/8/99	19		4					
218	6/8/99	20		2					
218	6/8/99	21	4	2					
218	6/8/99	22	4	2					
218	6/8/99	23	3	2					
219	7/8/99	0			2	8		1	0
219	7/8/99	1		3					
219	7/8/99	2		3					
219	7/8/99	3		2					
219	7/8/99	4		3					
219	7/8/99	5		3					
219	7/8/99	6		4					
219	7/8/99	7		7					
219	7/8/99	8		8.5					
219	7/8/99	9	3	3					
219	7/8/99	10	3	3					
219	7/8/99	11	4	4					
219	7/8/99	12		4	3	8		1	0
219	7/8/99	13	4	4					
219	7/8/99	14	8	8					
219	7/8/99	15	4	4					
219	7/8/99	16		2					
219	7/8/99	17	1	1					
219	7/8/99	18	1	0	6	9	0	5	0
219	7/8/99	19	1	0					
219	7/8/99	20	1	0					

CONTENTS

Jday	Date	Hour	Cover A	cover B	ci	Si	bi	Di	zi
219	7/8/99	21	1	0					
219	7/8/99	22	1	0					
221	9/8/99	9	3	3					
221	9/8/99	10	3	3					
221	9/8/99	11	3						
221	9/8/99	12			2	4		1	0
221	9/8/99	18		10	7	8	0	4	3
221	9/8/99	21	9						
221	9/8/99	22	9						
221	9/8/99	23	9						
222	10/8/99	0			5	5		1	2
222	10/8/99	1	9	8.5					
222	10/8/99	2		9					
222	10/8/99	3		9					
222	10/8/99	5	9	9					
222	10/8/99	6		9	5	8	0	9	0
222	10/8/99	10	1						
222	10/8/99	11	1						
222	10/8/99	12			5	5		7	0
222	10/8/99	18			5	8	1	8	0
223	11/8/99	0			5	5		7	0
223	11/8/99	6			5	8	1	8	0
223	11/8/99	17		9					
223	11/8/99	18		8	5	6	1	5	2
223	11/8/99	19		6					
223	11/8/99	20		7					
224	12/8/99	5	8	5.5					
224	12/8/99	6		5.5	6	8	4	7	2
224	12/8/99	7		5.5					
224	12/8/99	8		5.5					
224	12/8/99	17		9					
224	12/8/99	18		9	5	8	0	5	2
224	12/8/99	19		8					
224	12/8/99	20		8					
225	13/8/99	0			5	7		1	5
225	13/8/99	1		9					
225	13/8/99	2	8	9					
225	13/8/99	3	8	9					
225	13/8/99	5	9	9					
225	13/8/99	6		9	5	8	6	7	0
225	13/8/99	7		9					
225	13/8/99	8		9					
225	13/8/99	12			4	6		1	0
225	13/8/99	18			5	8		7	0
226	14/8/99	0			4	6		1	0
226	14/8/99	3		9					
226	14/8/99	6			5	8		3	2
226	14/8/99	7	8						

Jday	Date	Hour	Cover A	cover B	ci	Si	bi	Di	zi
226	14/8/99	8	7	7					
226	14/8/99	9	9						
226	14/8/99	12			4	7		1	2
226	14/8/99	14		9					
226	14/8/99	15		9					
226	14/8/99	16		9					
226	14/8/99	17		8					
226	14/8/99	18	8	8	4	8		3	1
226	14/8/99	19		8					
226	14/8/99	20		3					
226	14/8/99	21		0					
226	14/8/99	22		0					
226	14/8/99	23		0					

Table 5.4: Calibrations for PIMMs Air & Sea Temperature Sensors

Sea Temp	=A+Bx+Cx2+Dx3	Air Temp	=A+Bx+Cx2
A	-1.88533	A	-5.313817
B	2.42426417	B	3.9328756
C	-2.4050424E-02	C	0.04854119
D	9.5747176E-03		

Table 5.5: PIMMs Deployments

No.	JDay	Time	Duration	Comments
1	214	11:35	1 hrs	Open water
2	217	19:45	4.5 hrs	in Ice
3	218	19:40	7 hrs	in open ice, small flows
4	221	09:00	7 hrs	
5	222	09:00	4.5 hrs	
6	224	06:35	4 hrs	Ice edge in thick Brash

Table 5.6: Comparison of the cumulative number of PIMMs Orbcomm messages sent to those received at SOC during the first hydro section.

Day	Sent	Received
207	-	39
208	-	67
209	84	86
210	95	98
211	-	104
212	150	116
213	162	121
214	195	-
215	209	-

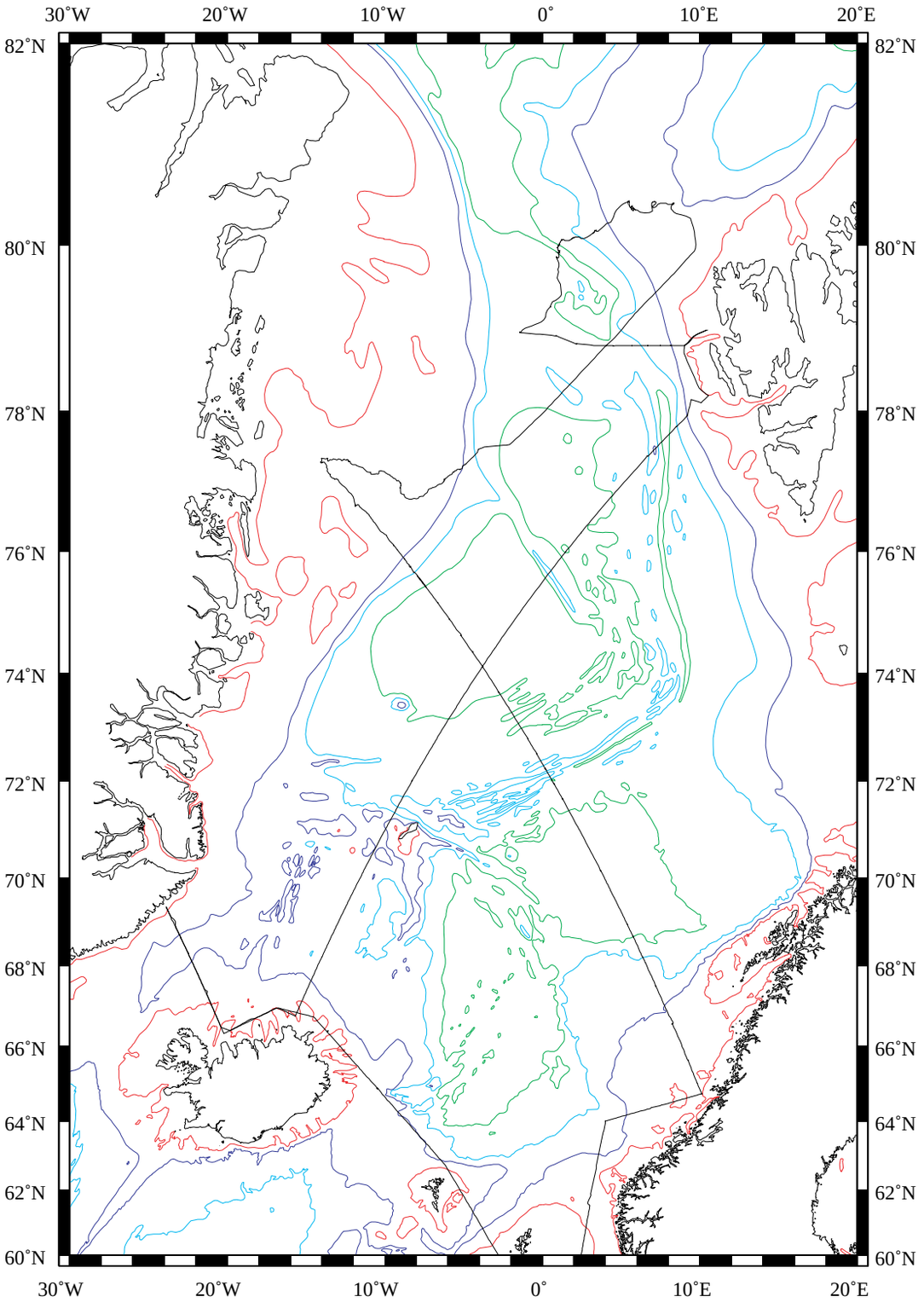

Figure 1.1: Cruise track. Depth contours are 200 m (red), 1000 m (dark blue), 2000 m (light blue), 3000 m (green), using Gebco bathymetry data.

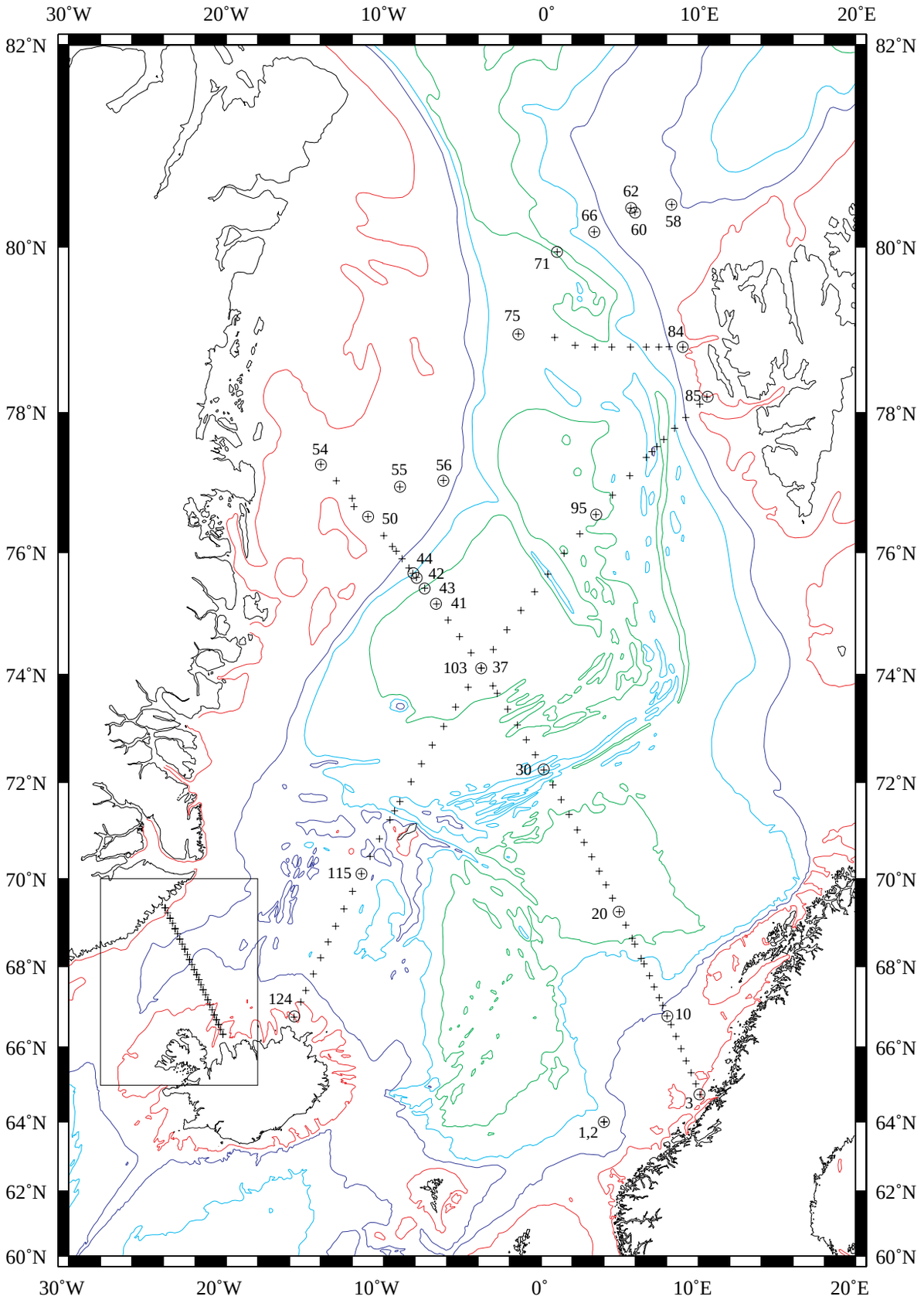

Figure 1.2: Station positions (+). Selected stations are numbered and identified by a circle. Denmark Strait stations (inset box) are shown in figure 1.3. Colour scale as in figure 1.1.

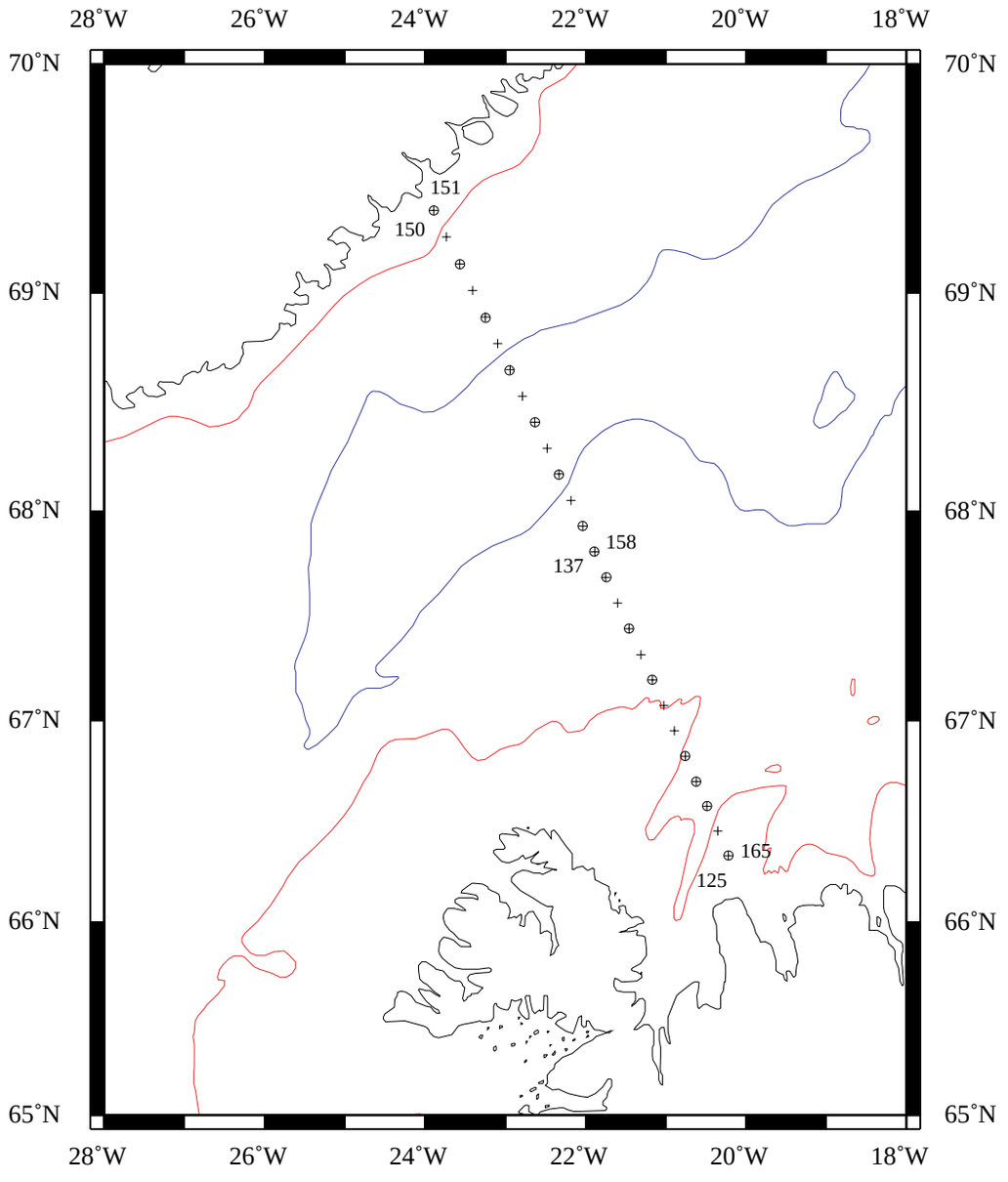

Figure 1.3: Denmark Strait stations. Outward stations (Iceland to Greenland) are indicated by plus signs and are numbered to the left of the track; repeat stations on the return are indicated by circles and are numbered to the right of the track. Colour scale as in figure 1.1.

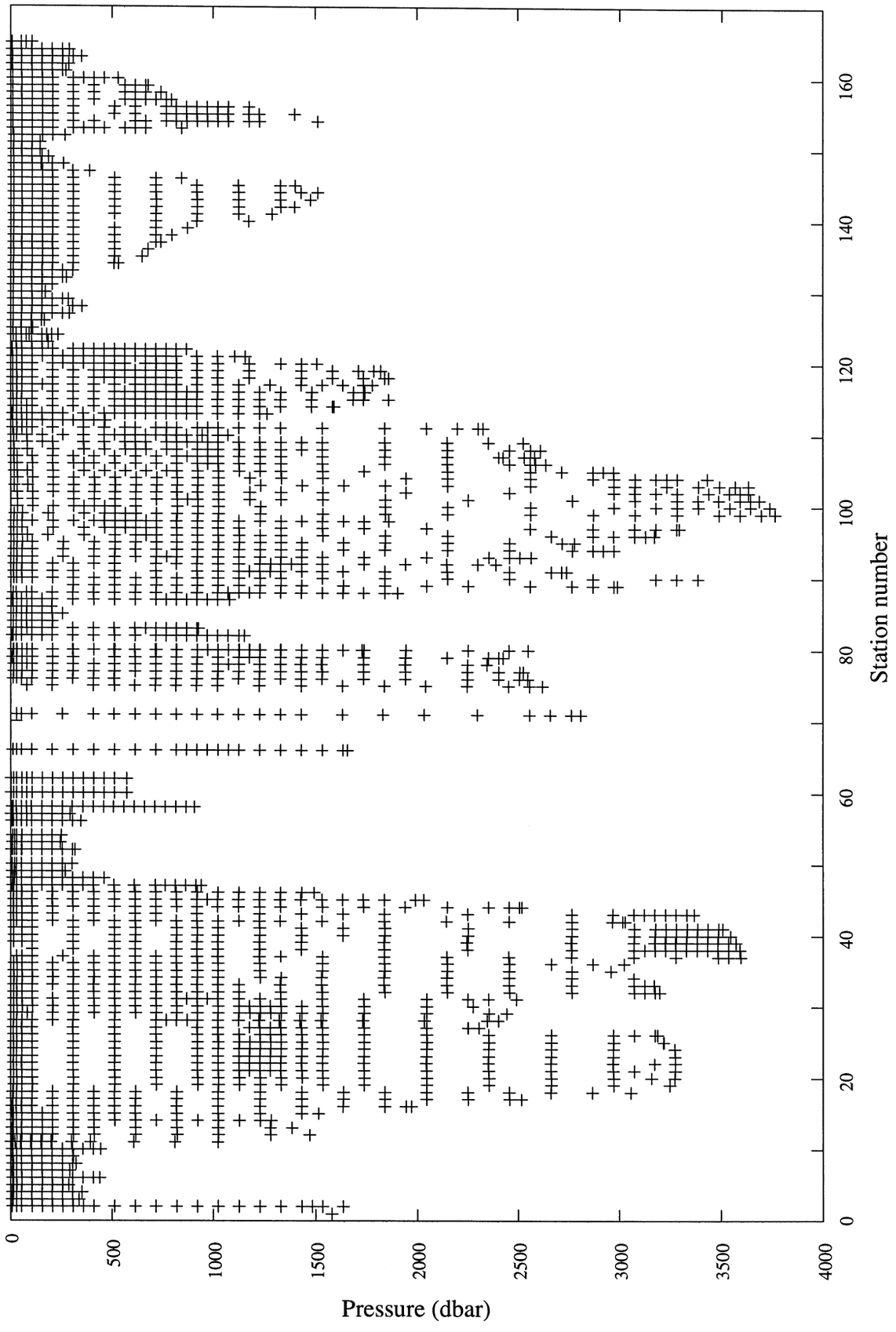

Figure 2.1: Bottle depths for each station during the cruise.

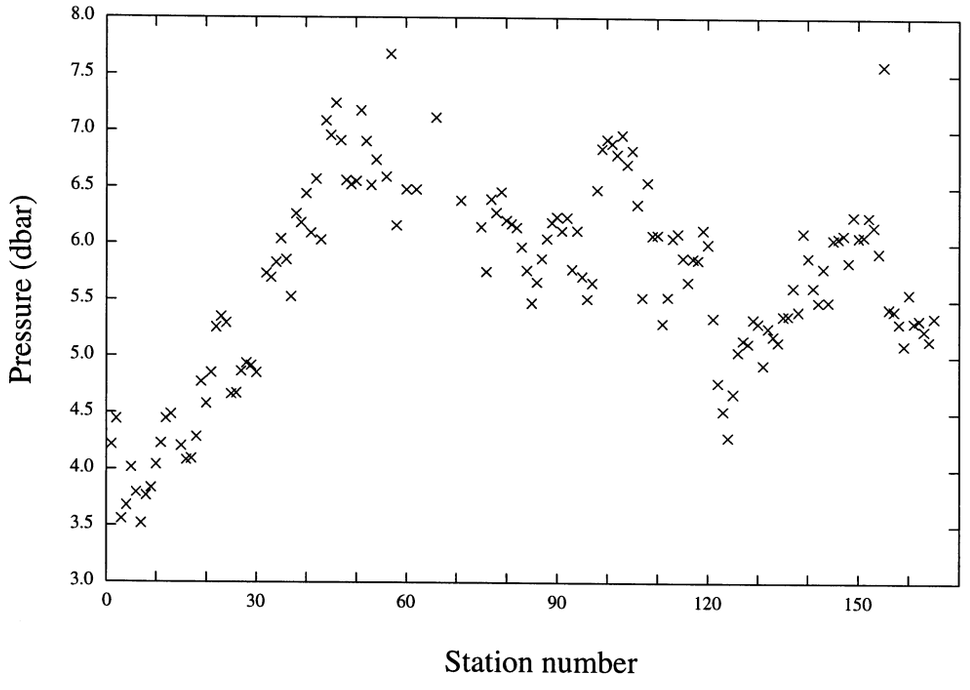

Figure 2.2: Uncorrected CTD deck pressures.

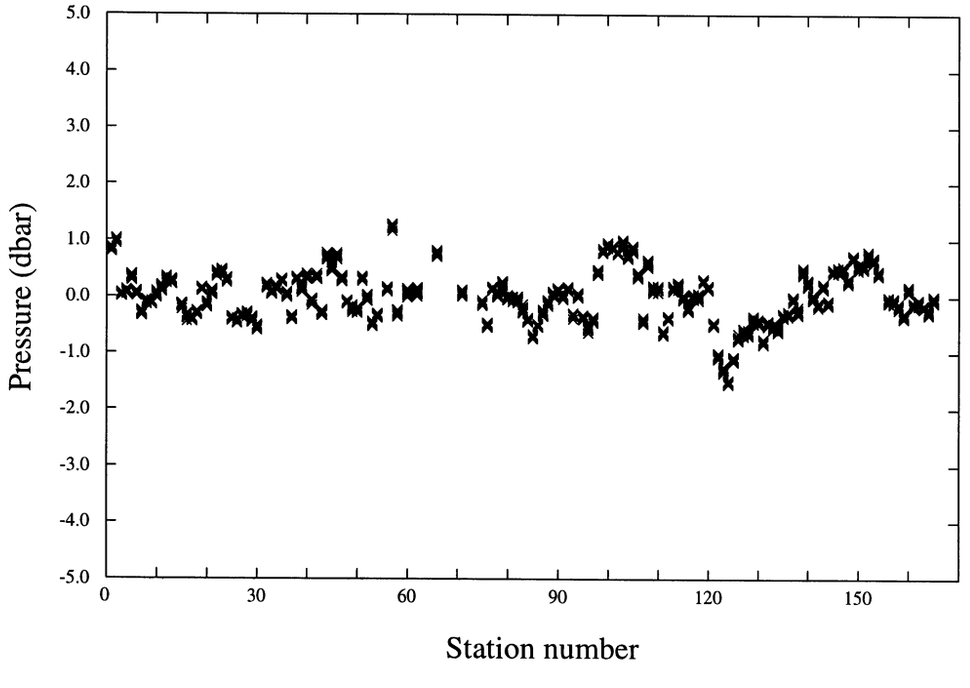

Figure 2.3: Corrected CTD deck pressures.

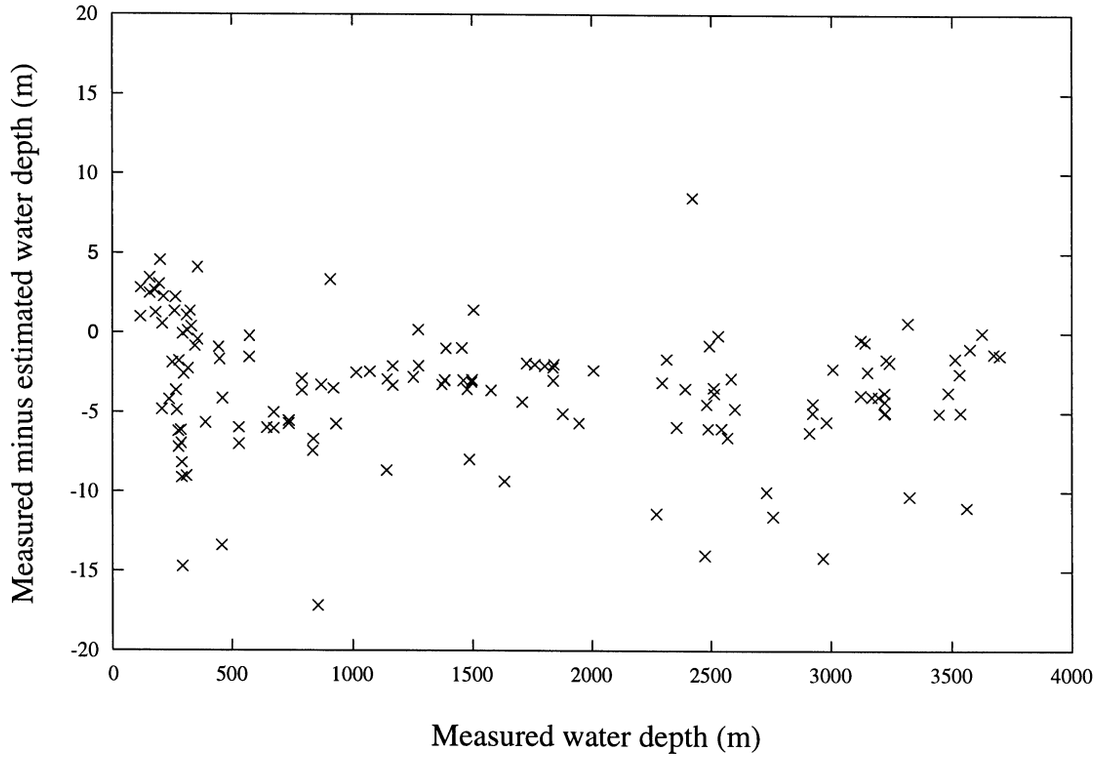

Figure 2.4: Difference between measured (echo sounder) and estimated (CTD plus altimeter) water depth.

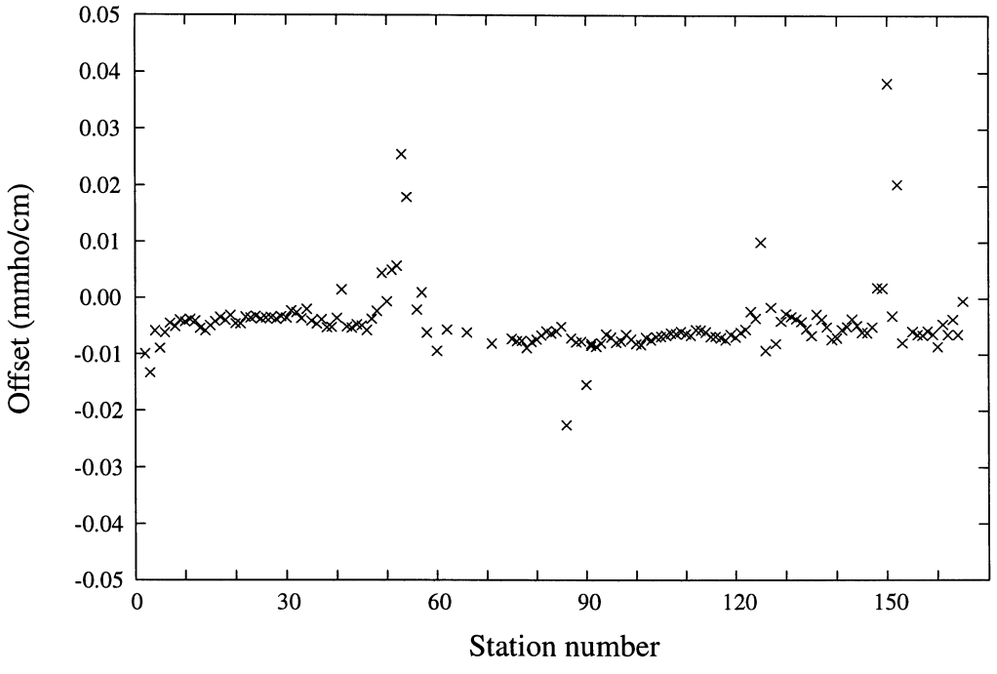

Figure 2.5: Mean conductivity difference (sample minus CTD) for each station for final calibration.

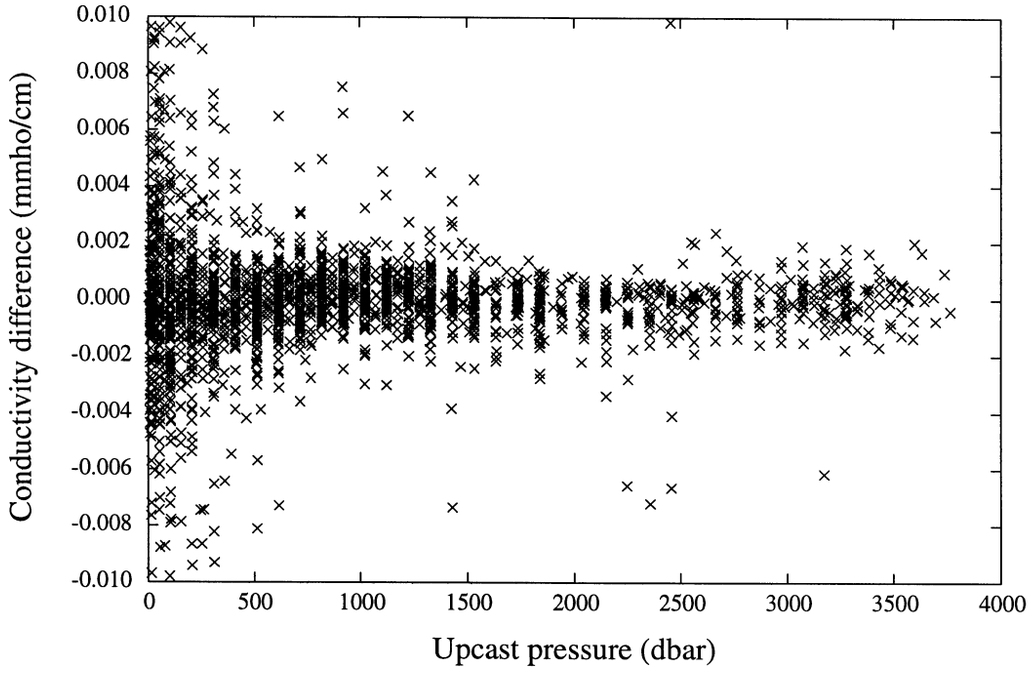

Figure 2.6: Conductivity difference for final calibrated CTD (sample minus CTD) versus upcast CTD pressure.

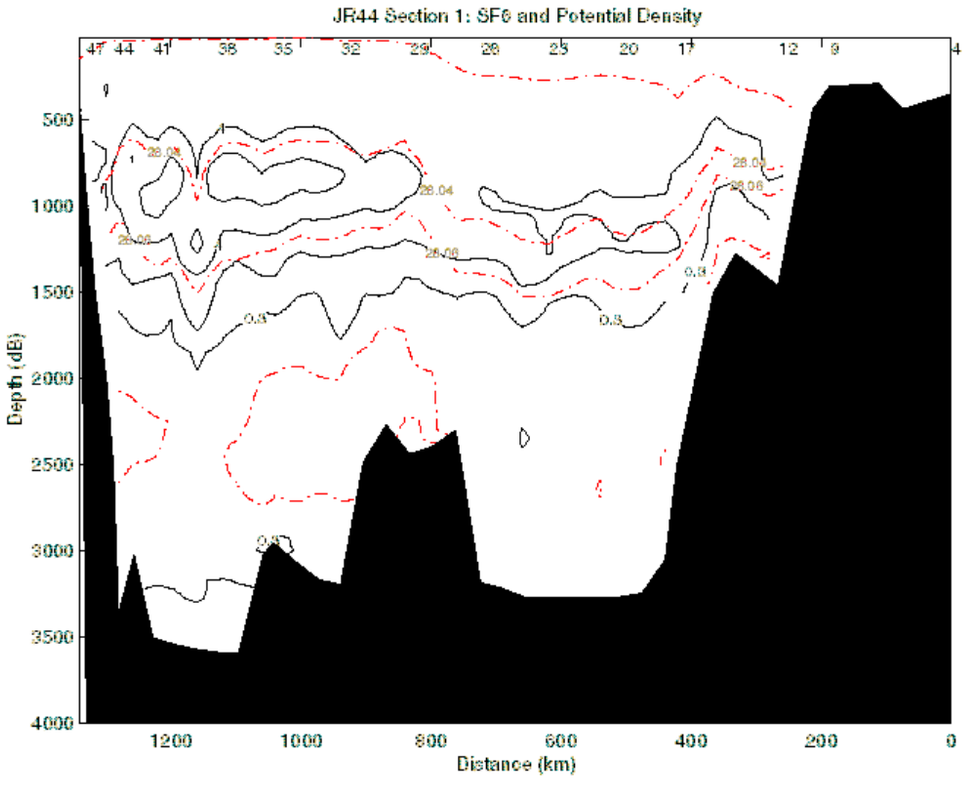

Figure 2.7: SF6 and σ_θ along leg 1 of JR44 across the Norwegian Basin and the Greenland Basin. SF6 contours are shown as black continuous lines; σ_θ contours are shown as dashed red lines every 0.01 kg/m^3 from 28.03 to 28.07. Station numbers are on the top of the figure. Note that density values are not final calibrated ones.

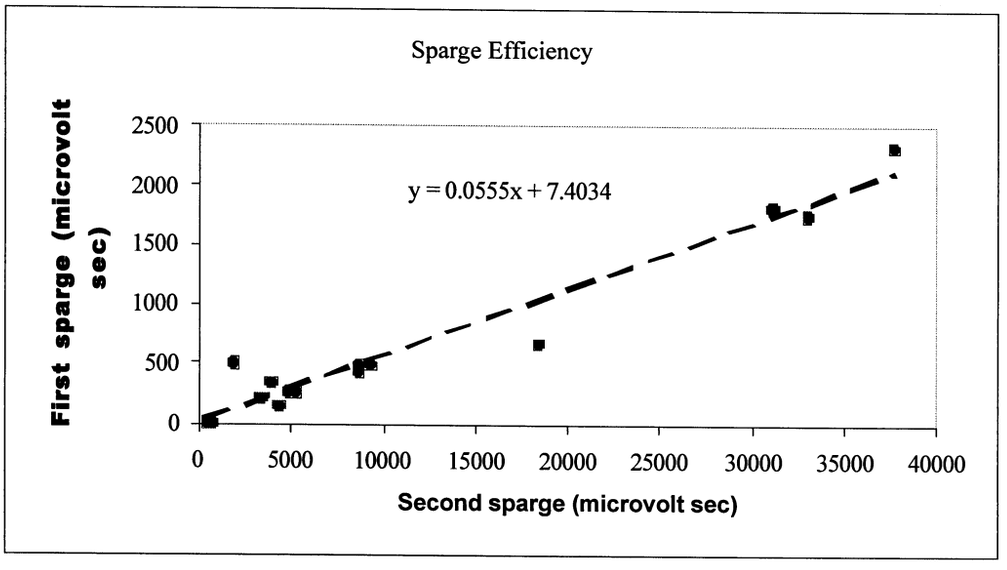

Figure 2.8: Sparge efficiency.

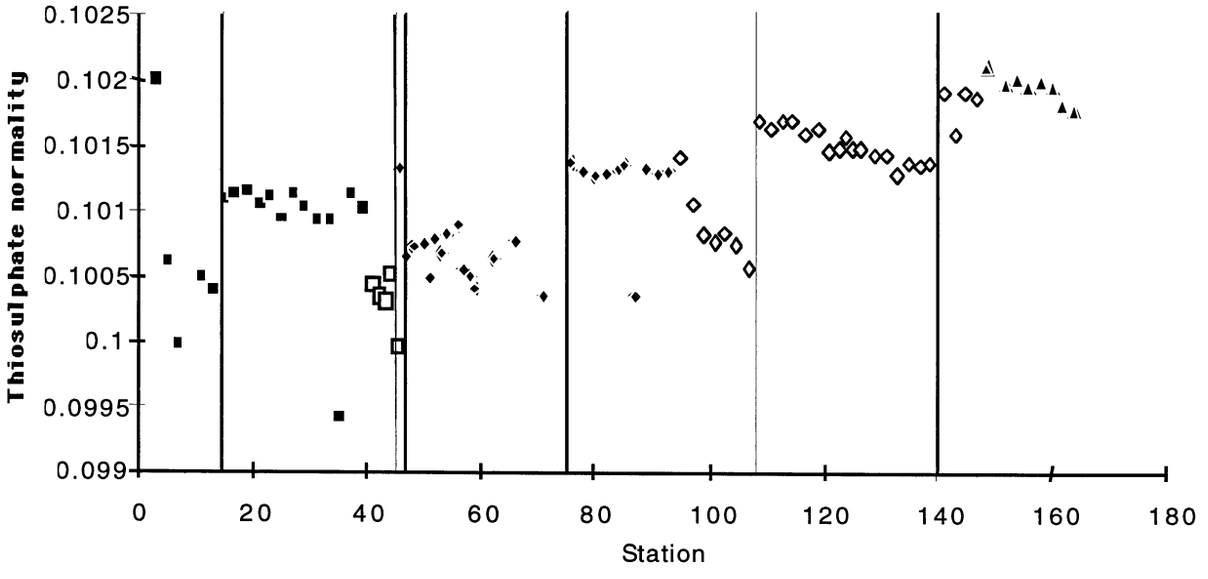

Figure 2.9: Variation of thiosulphate normality with each batch of thiosulphate and iodate. Key: different marker points: new thiosulphate batch used; lines: new iodate standard.

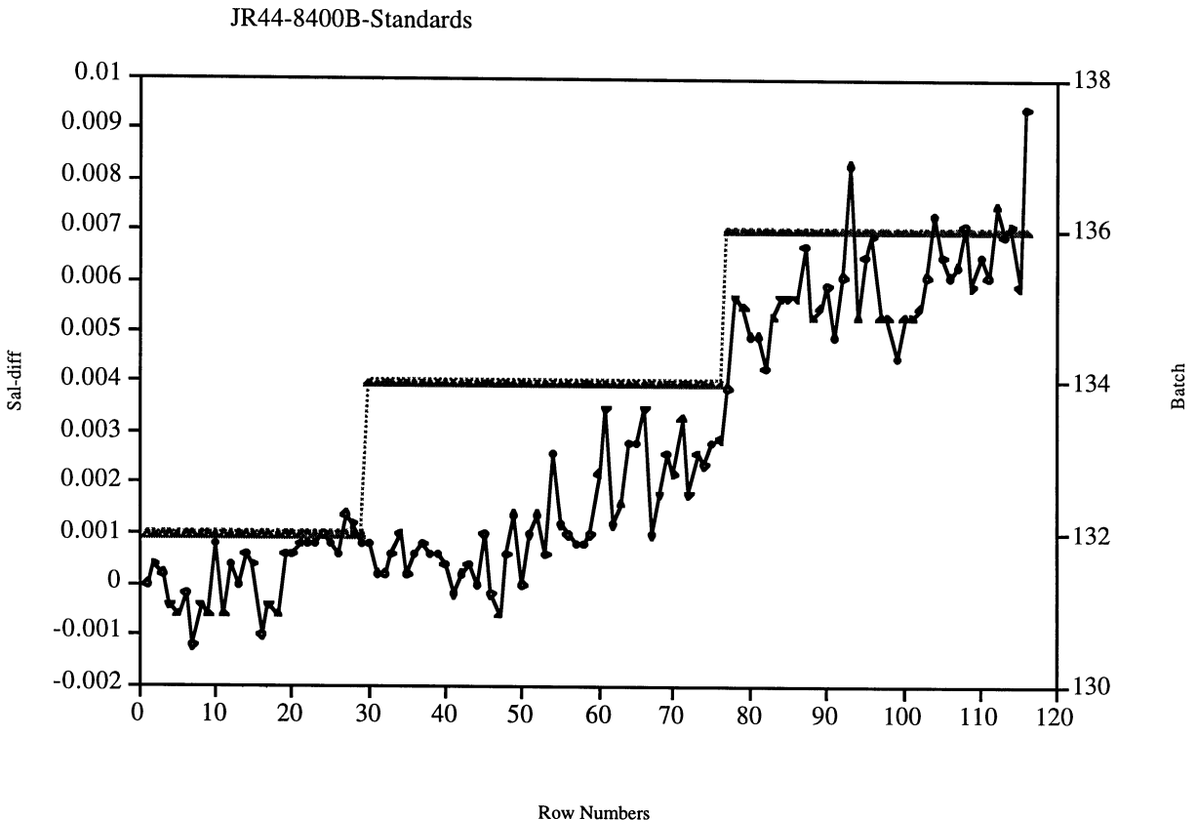

Figure 2.10: Guildline salinometer 8400B standardisation history. Three different standard seawater batches were used, P132, P134 and P136.

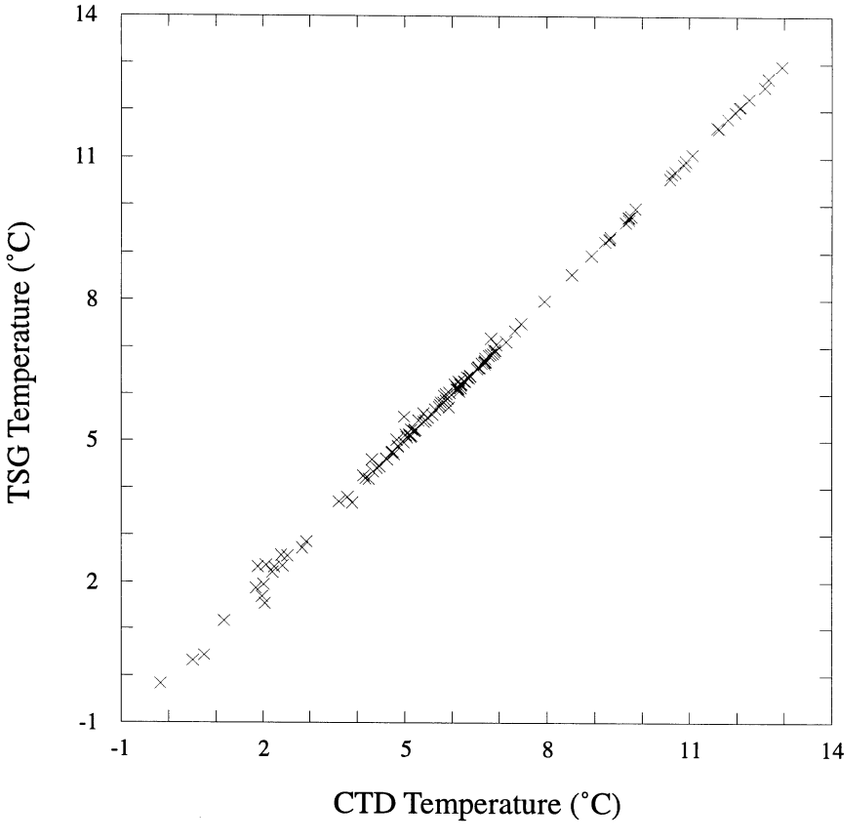

Figure 3.1: Thermosalinograph temperature versus CTD temperature at a depth of 7 m (7 dbar).

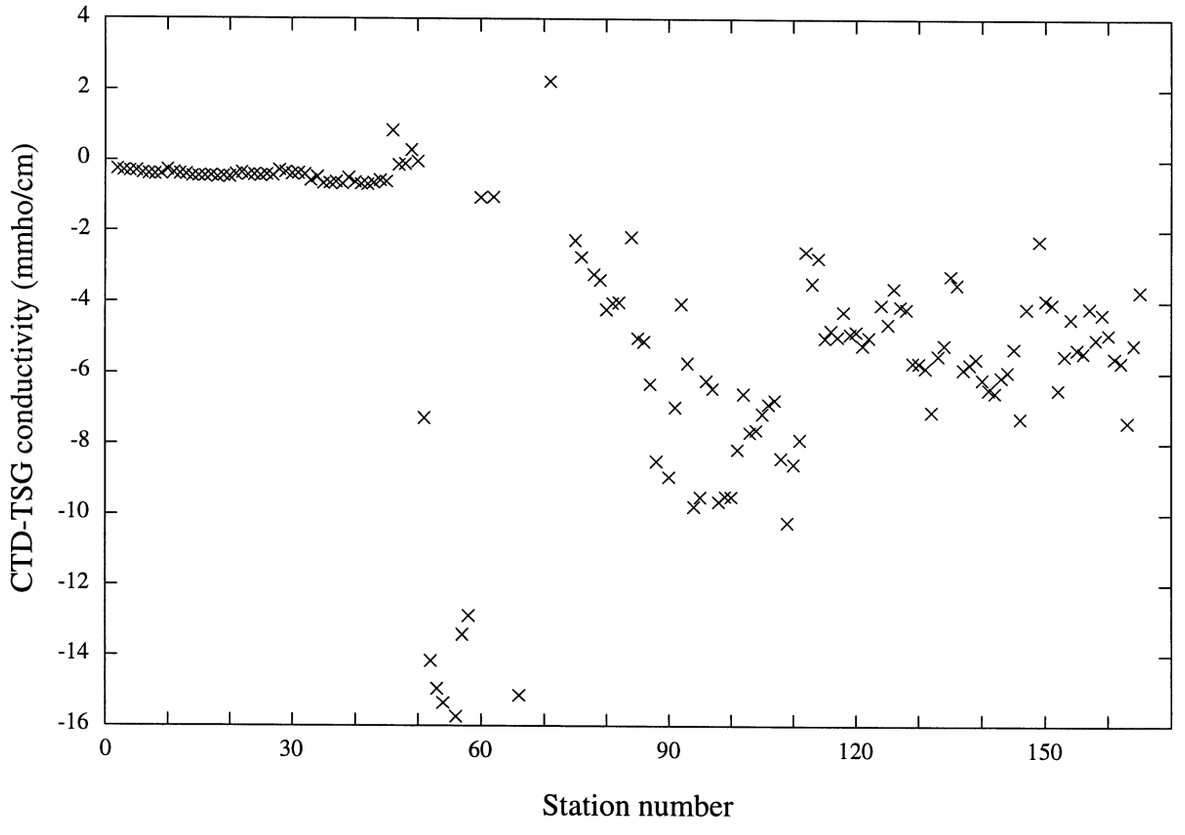

Figure 3.2: Difference between thermosalinograph conductivity and CTD conductivity at 7 m depth (7 dbar).

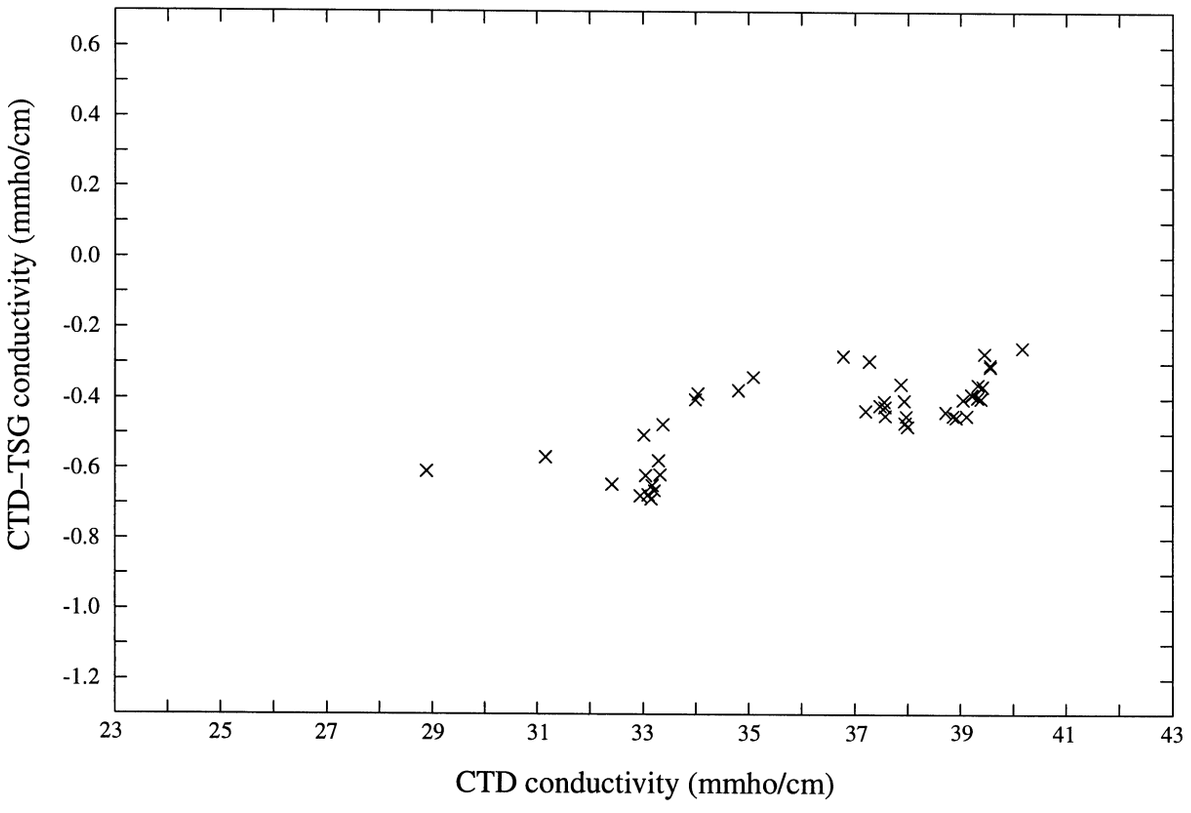

Figure 3.3: Difference between thermosalinograph conductivity and CTD conductivity as a function of CTD conductivity (at 7 m depth / 7 dbar) for stations 1–45.

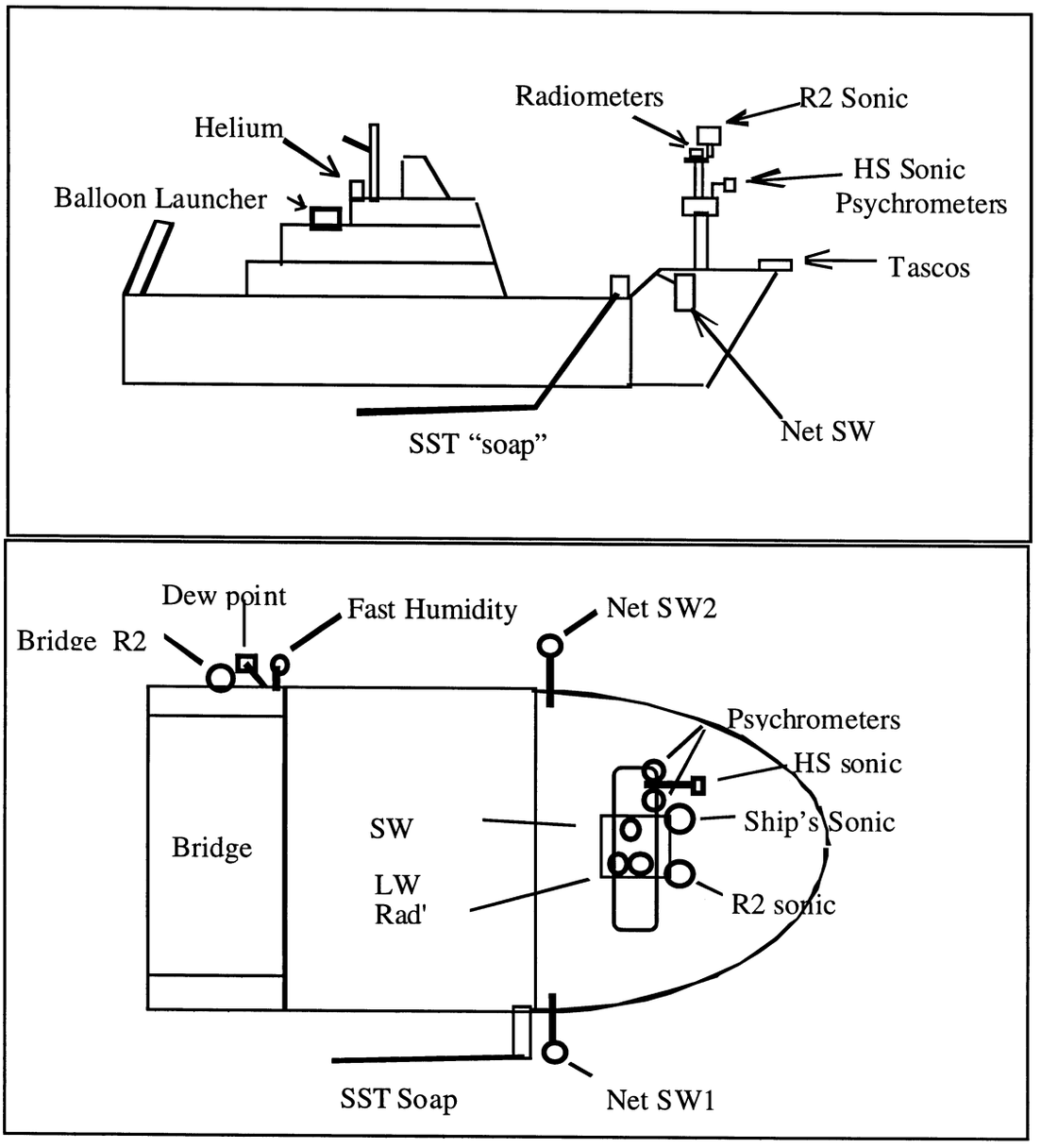

Figure 4.1: Schematics of the instrument locations; (top) a side view of the whole ship, and (bottom) a plan view of the forward half of the ship.

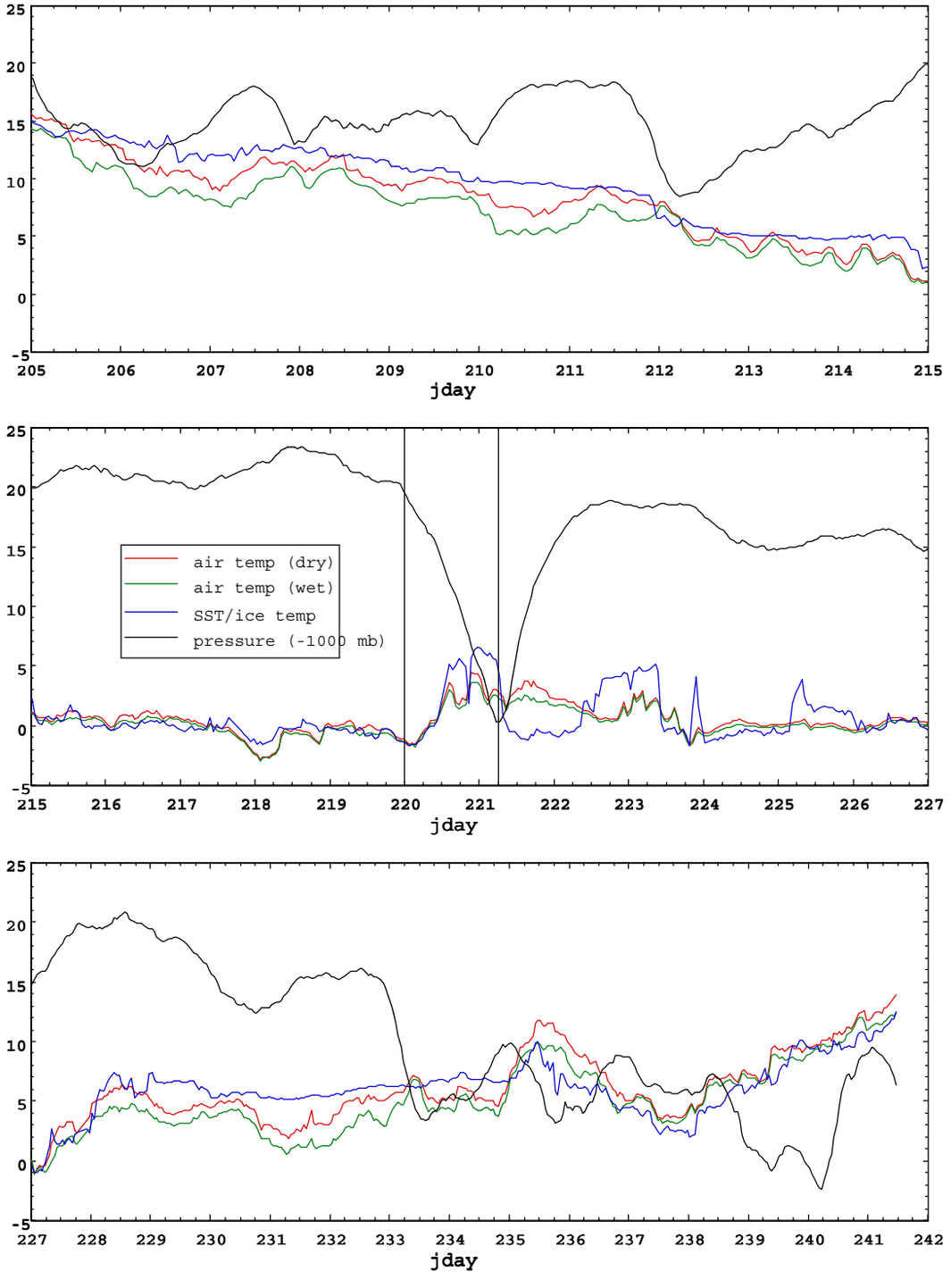

Figure 4.2: One-hour averages of air pressure and air and sea temperatures. The top and bottom plots shows data from the two hydrographic sections and the middle plot shows data during the period that the ship was in the MIZ, The dotted lines on the middle plot indicate the period during which the ship steamed further North in open water.

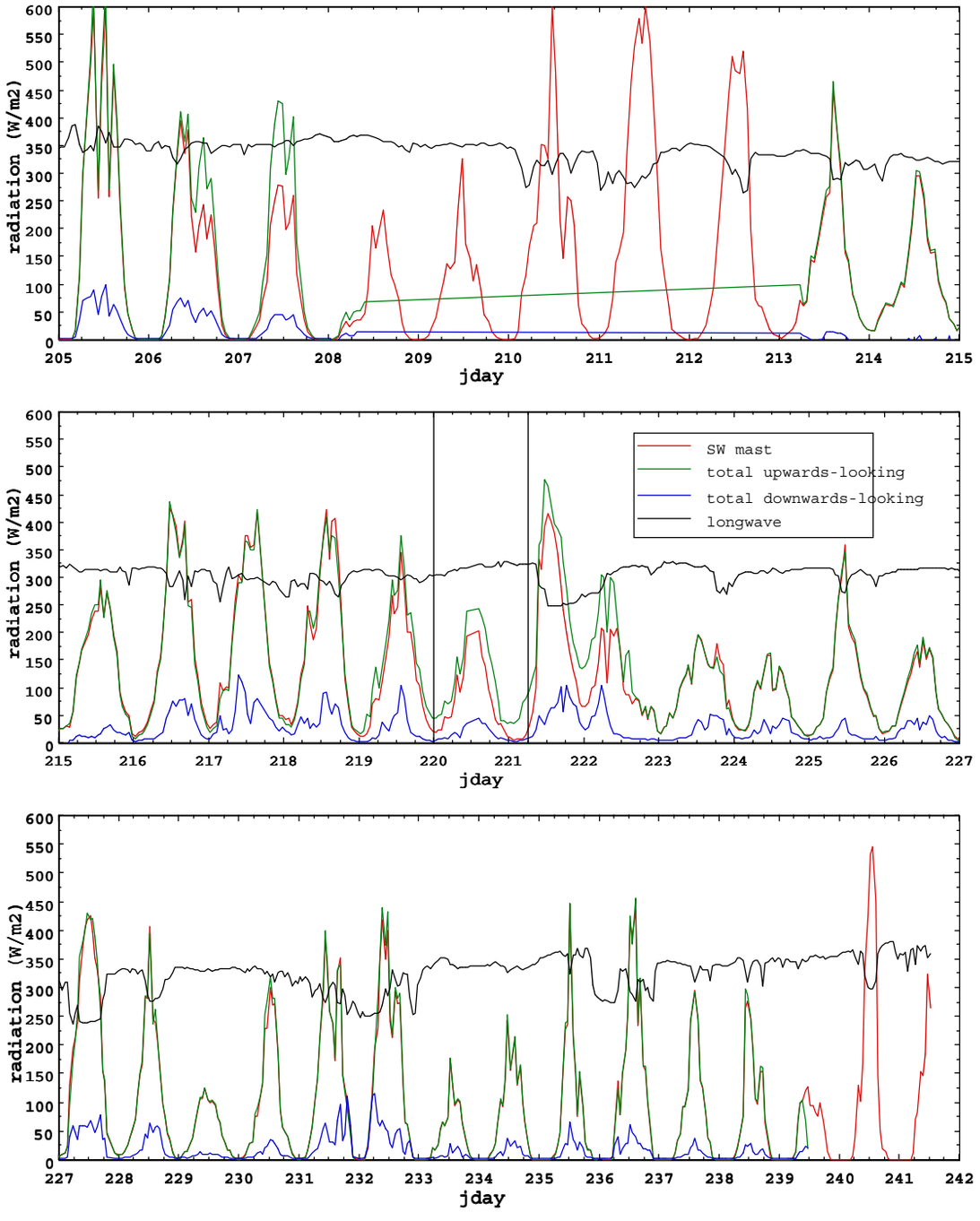

Figure 4.3: Time series of one-hour averages of the radiation. The upwards-looking shortwave sensor on the foremast is shown in red, and the total from the two upwards-looking 1/2 hemispheres is shown in green; the data show periods of disagreement between these which are discussed in the text.. The total from the downwards looking instruments are shown in blue. The 1/2 hemisphere sensors were switched off from day 208 to day 213. Incoming longwave radiation is shown in black. The dotted lines on the middle plot indicate the period during which the ship steamed further North in open water.

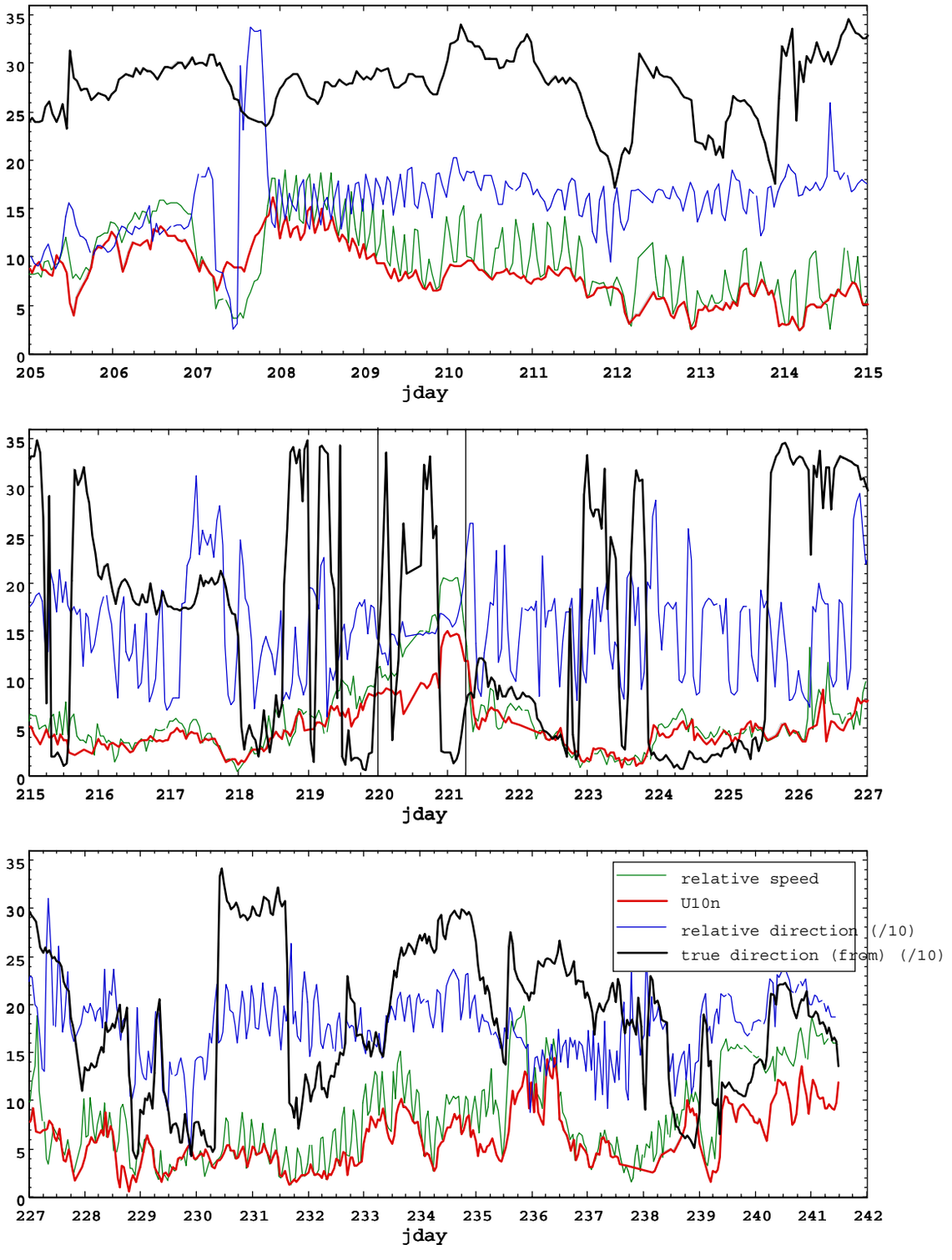

Figure 4.4: One hour averaged wind speed and direction from the R2 anemometer on the "bird table". The dashed lines indicate relative speed (m/s) and direction. The solid lines indicate true wind direction (from) and true wind speed corrected to a height of 10 m and neutral stability.

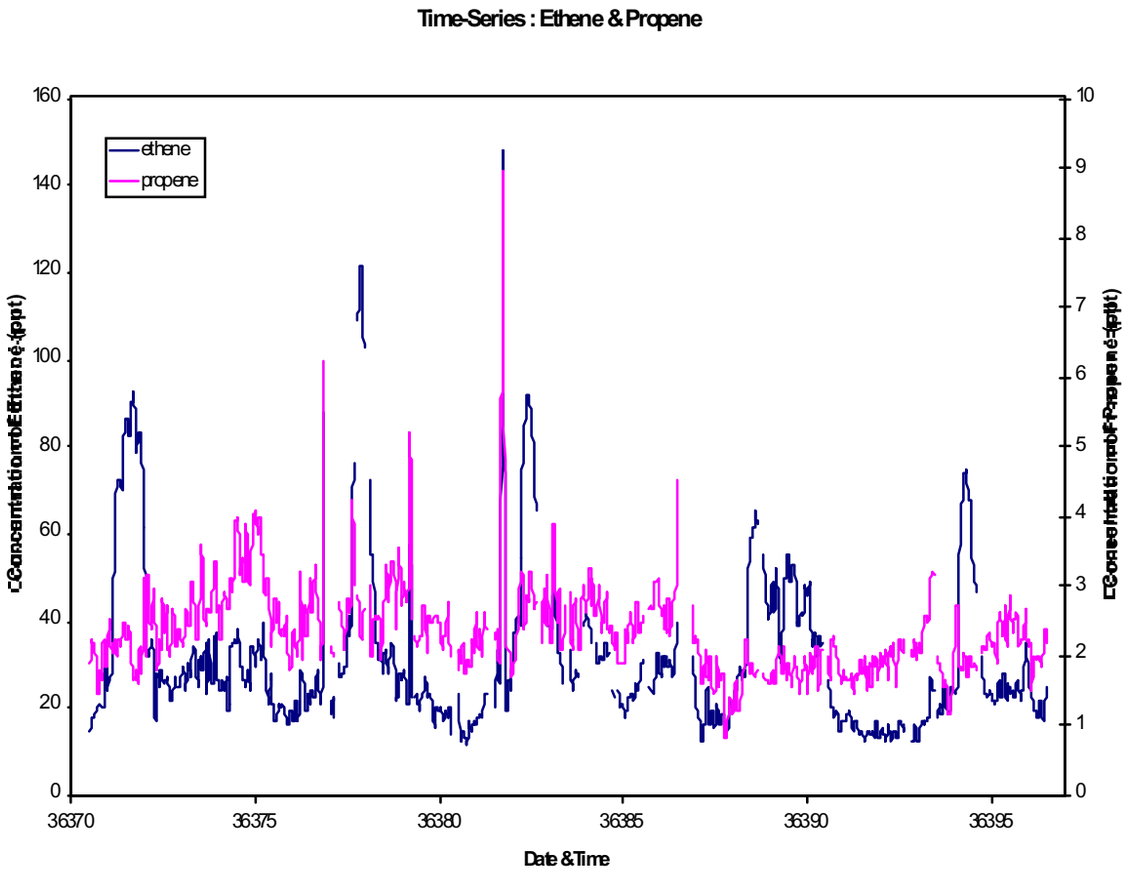

Figure 4.5: Time series of ethane and propane concentrations.

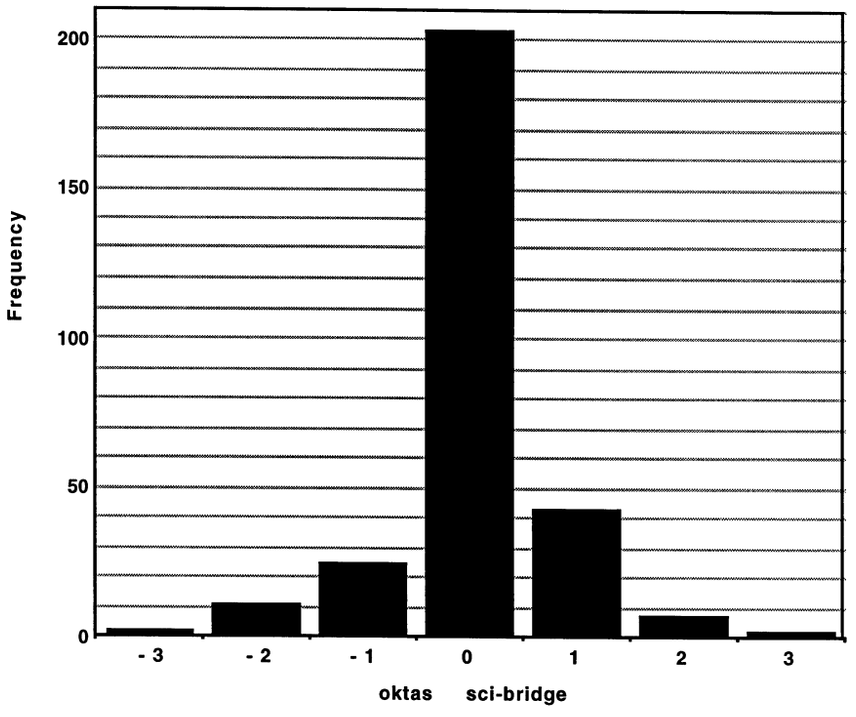

Figure 4.6: The difference between the visual observations of cloud cover made by the scientific and ship staff.

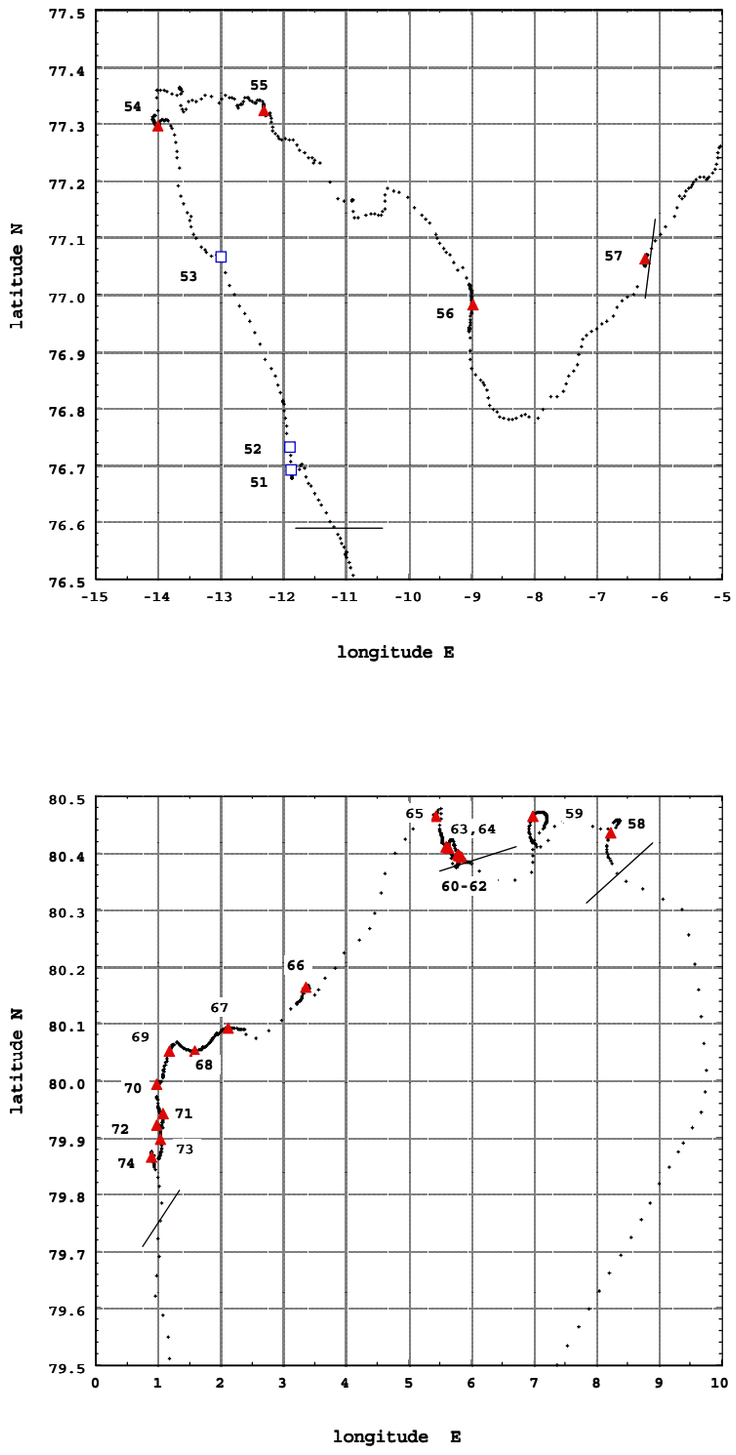

Figure 5.1: Ship track during Cat's Whiskers, showing the hydrographic stations in the MIZ (open circles), the stations occupied during the meteorology phase (solid triangle) and some ice-edge positions (lines), for a) the southern MIZ stations (top) and b) the northern MIZ stations bottom).

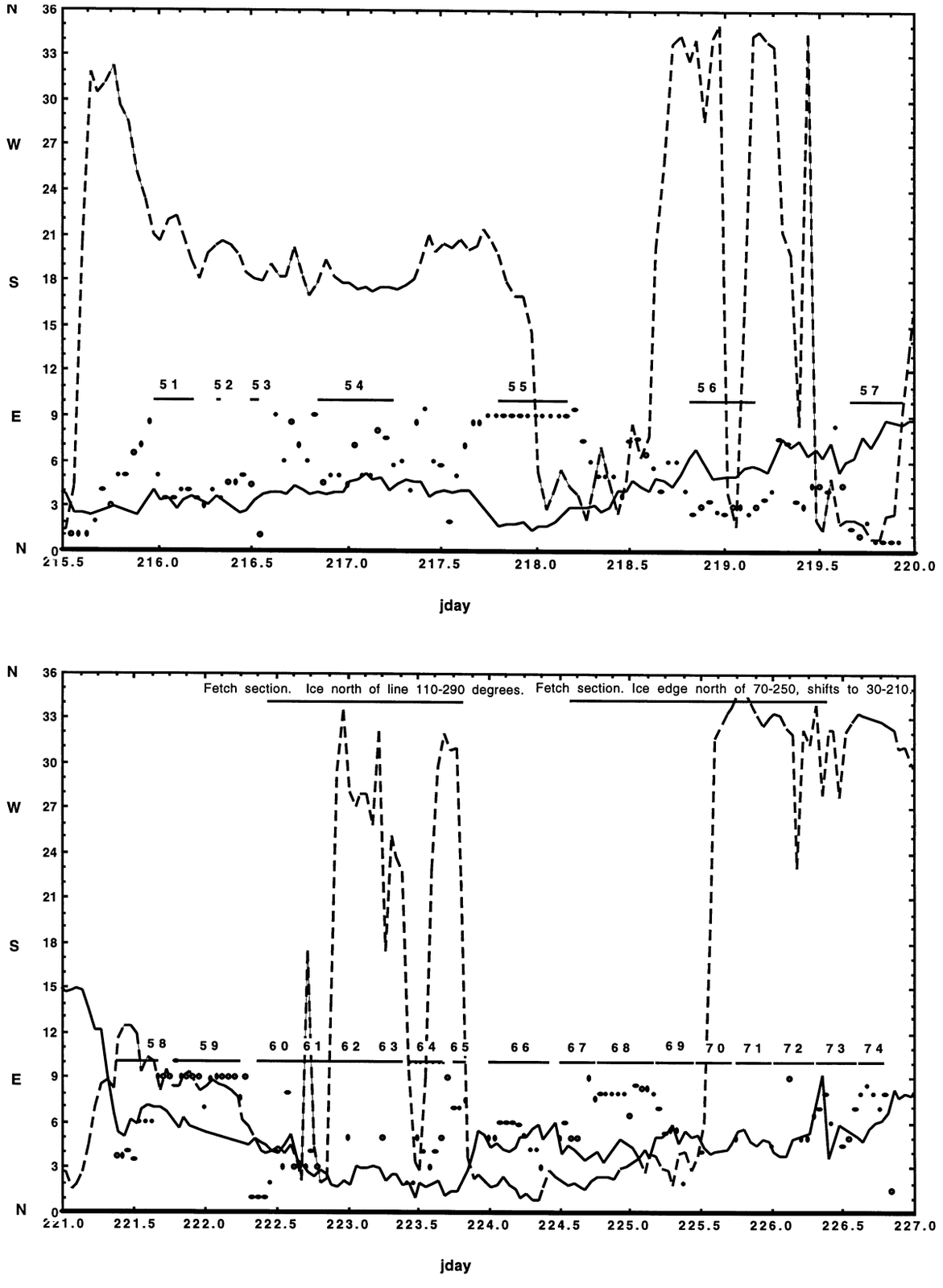

Figure 5.2: Time series of southern (top) and northern (bottom) MIZ stations, showing: true wind speed corrected to 10 m and neutral stability (solid line), and true wind direction (from) divided by 10 (dashed line). Also shown are the duration of each station (numbered lines) and an average of the various visual ice observations of ice concentration in tenths (open circles).

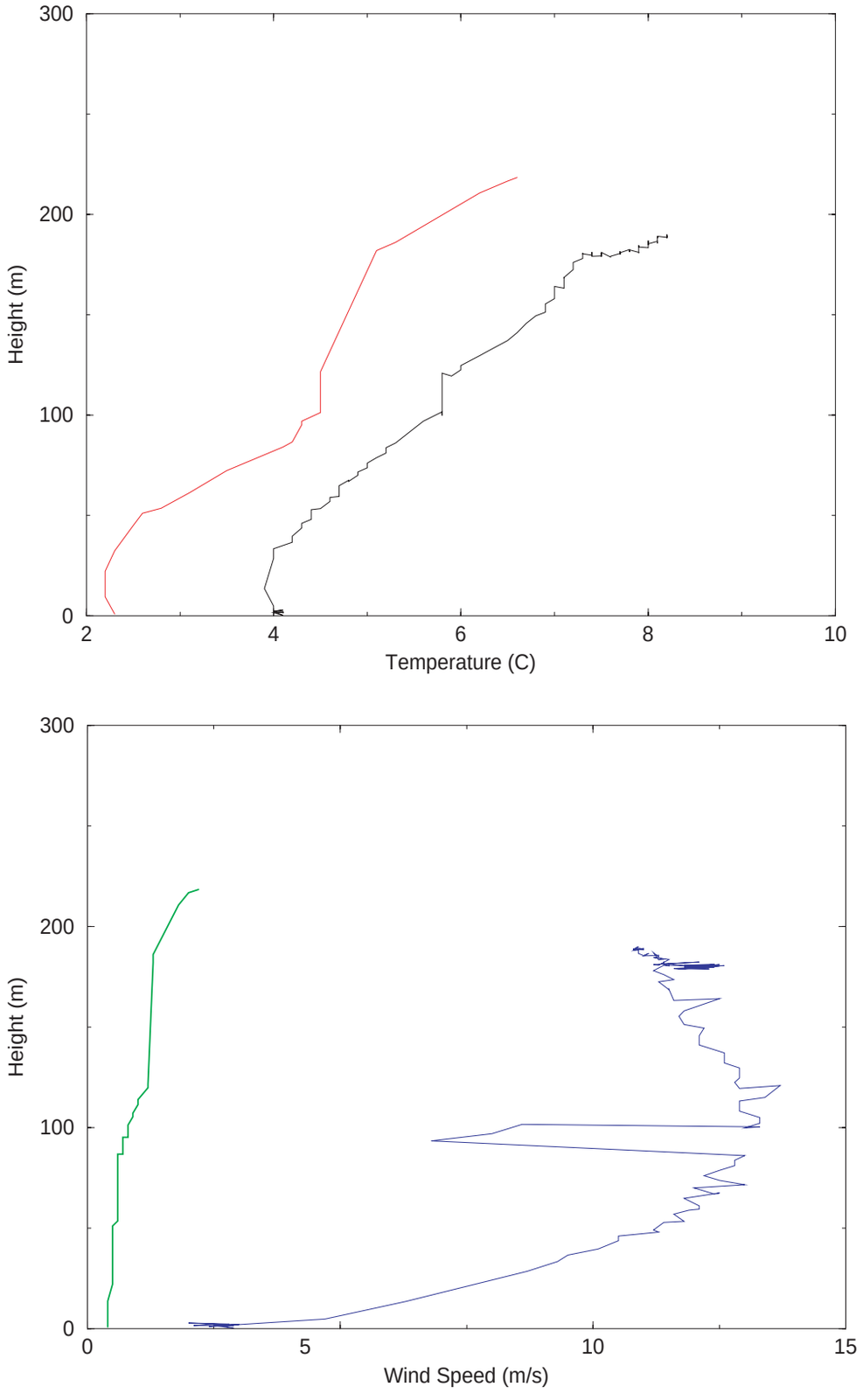

Figure 5.3: Radiosonde (23:00 GMT) and balloon sonde (21:30 GMT) profiles from the evening of day 221 (9 August). The upper plot shows temperature profiles (radiosonde faint line to the left) and the lower shows wind speed profiles (radiosonde to the left).

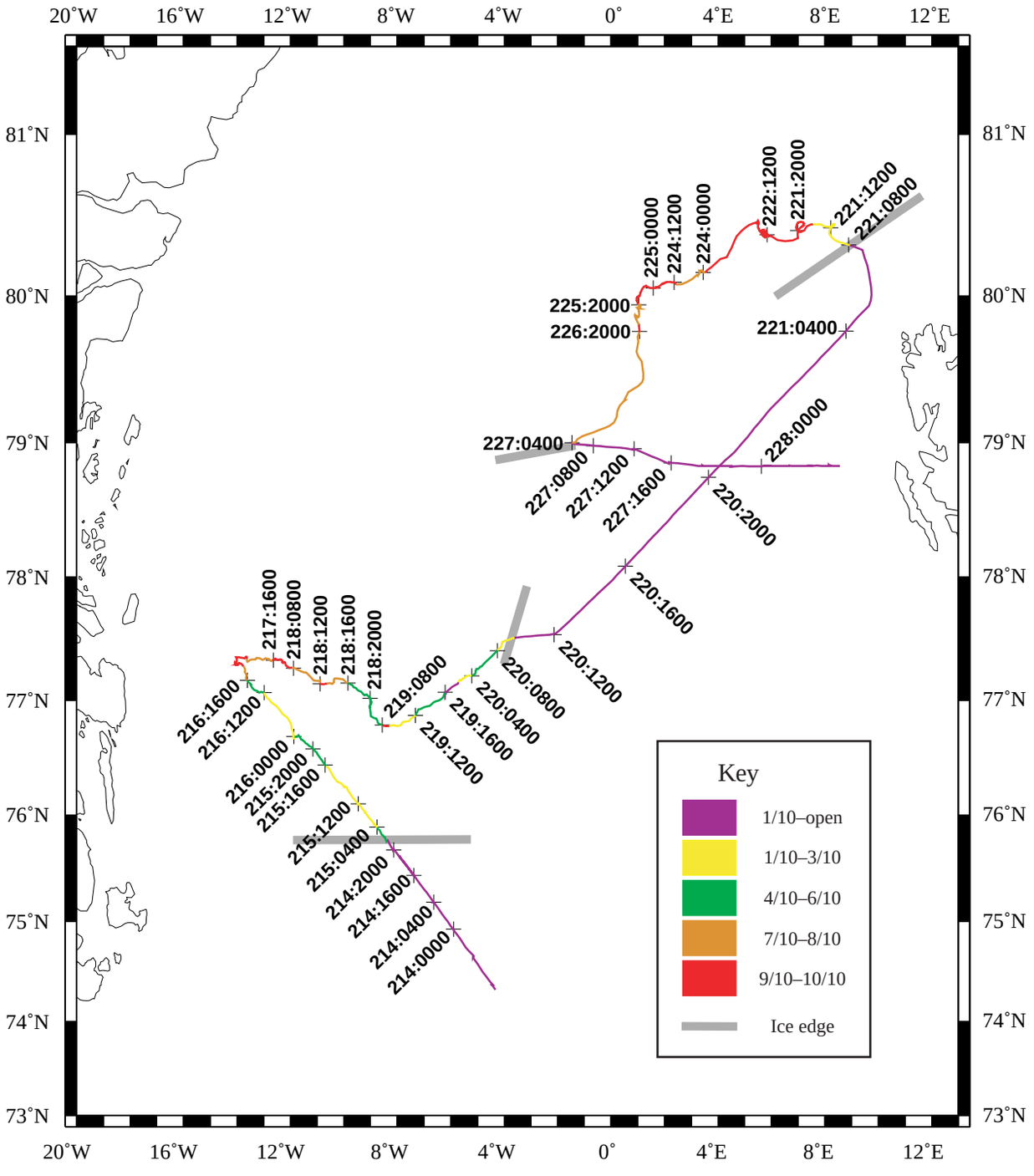

Figure 5.4: Visual observations of ice concentration, recorded in tenths, and positions and orientations of ice edge at entry and exit. Crosses show positions with Julian day number and time (hhmm) GMT.

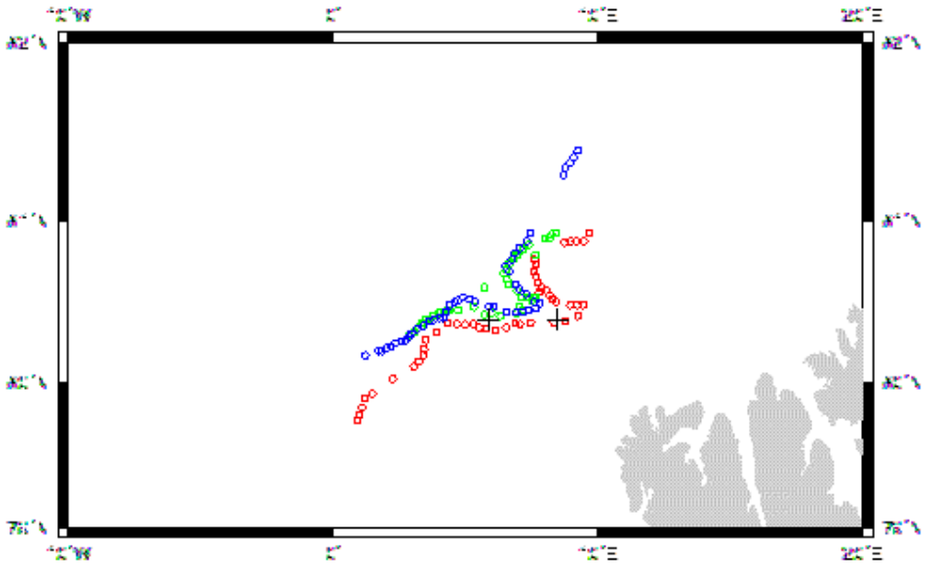

Figure 5.5: Ice edge observed in cloud-free AVHRR images on the 8th (red), 9th (green) and 11th(blue) of August. The ship-observed ice edge is shown as black crosses.

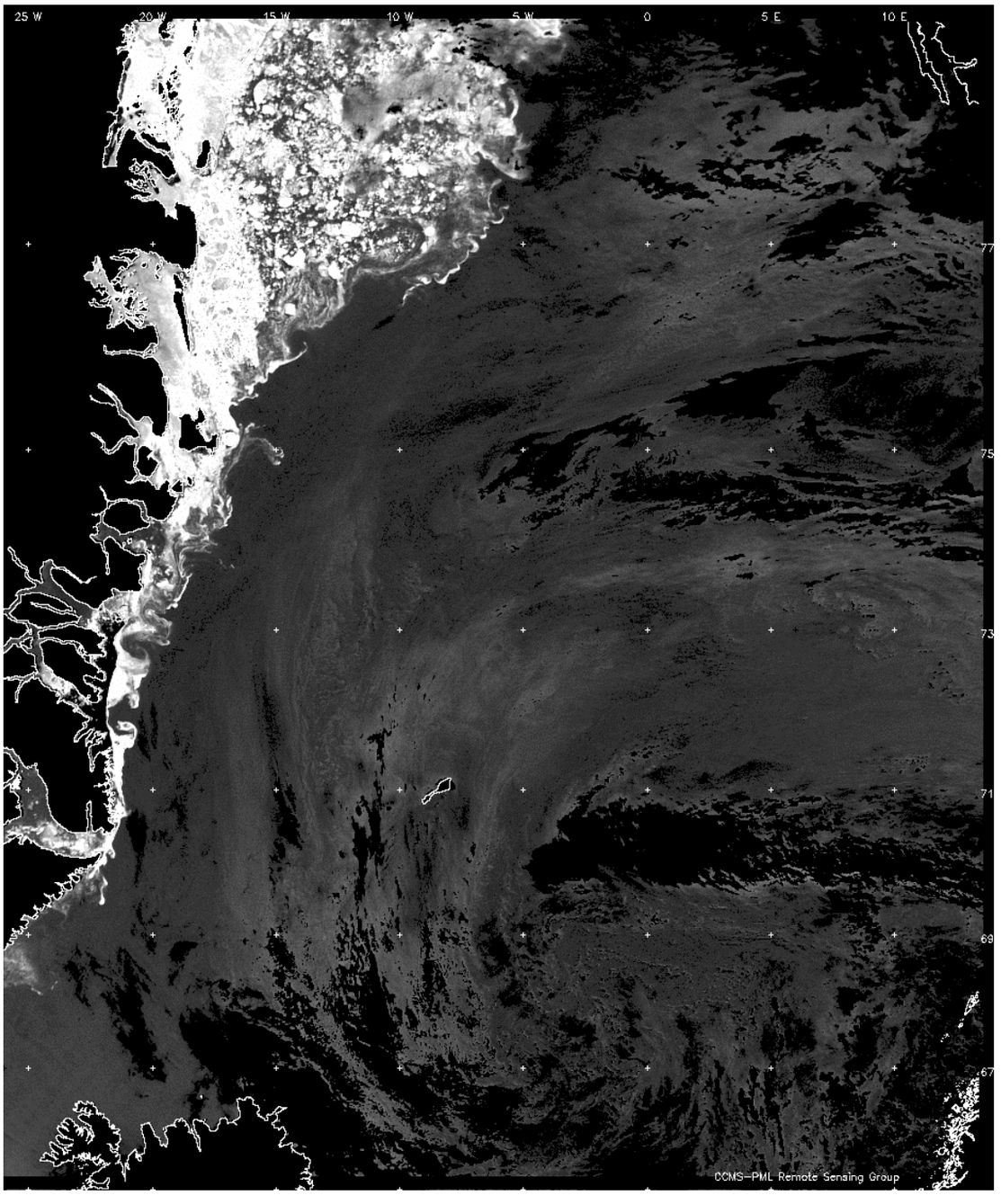

Figure 5.6: ERS-2 infra-red image of Nordic Seas, with cloud mask applied.

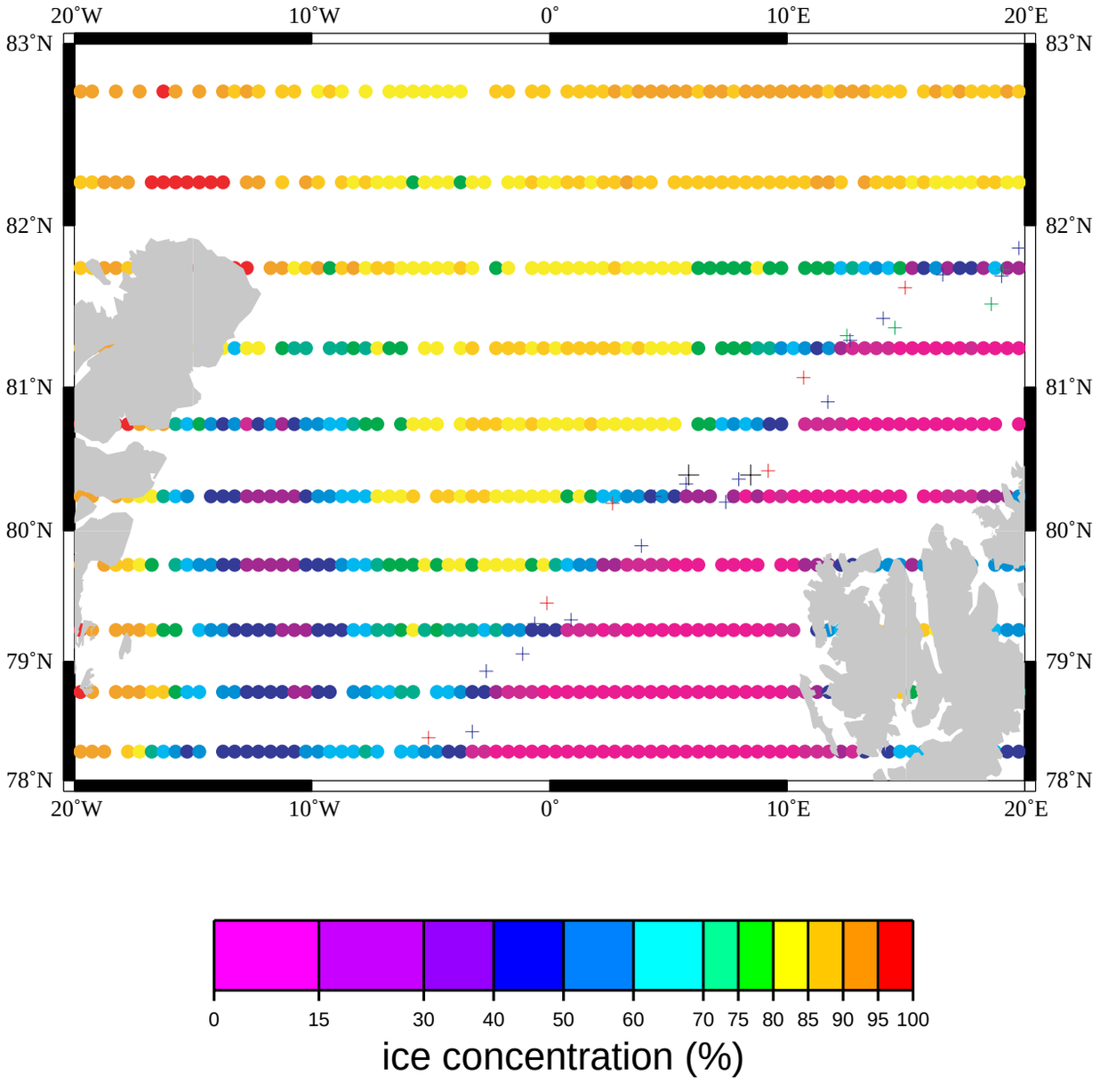

Figure 5.7: Passive microwave sea ice concentration from 5 August. Crosses show the ice edge position as reported by NAVTEX, on the 3rd (blue) and 10th (red) of August. Black crosses show the ship observed ice edge.

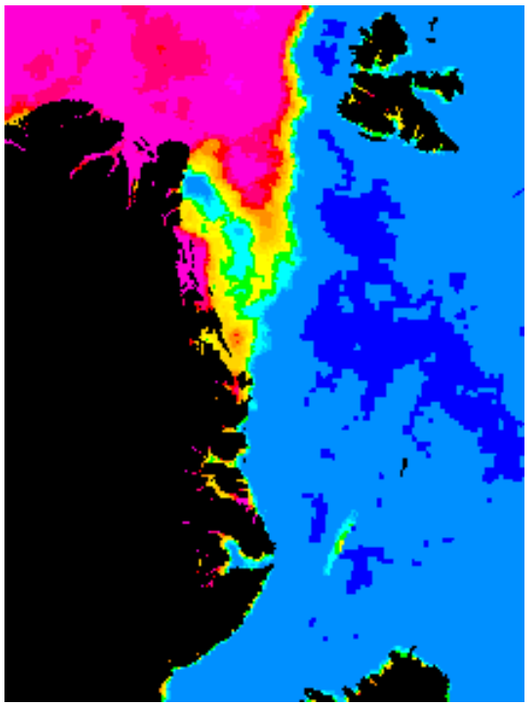

Figure 5.8: SSM/I data for 8 August 1999 obtained from the Danish Centre for Remote Sensing.

Plate 1: The JCR on station.

Plate 2: sea ice over Belgica Bank.

Plate 3: the bears.